DEVELOPMENT OF AN EFFECTIVE FUEL LEVEL SENSING TECHNOLOGY FOR PROPANE POWERED VEHICLES

Stephan W. Orzechowski

B.A.Sc. (Toronto)

A thesis submitted in conformity with
the requirements for the degree of

MASTER OF APPLIED SCIENCE

Graduate Department of Mechanical and Industrial Engineering
University of Toronto

ABSTRACT

The suitability of modern fuel level sensing technology is evaluated in the context of propane vehicles. This current technology is shown to be unsatisfactory due to problems with poor reliability and performance. In an effort to solve this problem, level sensing technologies suitable for static and dynamic applications are explored as possible alternatives. From the technologies discussed, the Helmholtz method is chosen as the best option due to its potential to disregard errors caused by the movement of the fuel inside the tank.

A study of the major factors affecting the implementation of the Helmholtz method is also presented. This study focuses on the acoustic properties of Helmholtz resonators as they apply to fluid level sensing. Experimental results demonstrate the ability of this method to detect volume change in a tank. These experiments also explore the effects of using speakers as excitation sources. The behavior of tanks with simple and complex geometric features are also examined.

ACKNOWLEDGEMENTS

I would like to first extend my deepest gratitude to my supervisor, Professor William Cleghorn. His patience and guidance has made this experience especially fruitful and memorable. Along with him, I would also like to extend a special thanks to the engineers at General Motors who made this project possible, especially Sam Luinstra and Dick Kauling. Also at General Motors, I would like to thank Richard Gibson and Larry Kwan for their assistance in obtaining the proper instrumentation. The financial support that General Motors of Canada provided for the project and to me personally is also gratefully acknowledged.

To my wife Tara, whom I married while working on this project, I extend the greatest of indebtedness. Her patience, her willingness to listen, and her delicious lunches will always be remembered. Finally, I also thank Tara's parents, Richard and Judith, for the great deal of support, patience and trust that they have afforded me during the past two years.

TABLE OF CONTENTS

LIST OF SYMBOLS

A	Amplitude of excitation source
c	Speed of sound
D	Diameter of neck
F	Driving force
K	Effective stiffness of resonator
k	Ratio of specific heats
L	Actual length of neck
L'	Effective length of neck
M	Effective mass of resonator
n	Wave number
R	Radius of neck
R_r	Radiation resistance
S	Cross sectional area of neck
V	Volume of resonator
x	Displacement of mass M in the neck
λ	Wavelength
ρ_o	Density of gas in the resonator
ω_o	Resonant frequency

LIST OF FIGURES

LIST OF TABLES

INTRODUCTION

Concerns of high pollution and limited energy resources have forced governments to create legislation that will encourage the development of alternative energy sources. This has been reflected in the automotive industry in many forms, including the development of alternative fuel technologies. With this goal in mind, many of the large automotive manufacturers have established research and development centers dedicated to solving the many technical issues involved in the use of alternative fuels.

One of these technical issues is that of on-board fuel level measurement. Until now, the development of this technology has been focused on gasoline tanks. Yet, even after many decades of refinement, the existing systems have failed to gain the confidence of the users. The main complaints are usually rooted in problems with the accuracy, linearity or stability of the gauges.

Most current automobiles are equipped with a float type sensor that detects the depth of the fuel at a particular point inside the tank. These sensors, though inaccurate, have proven to be adequate enough for use in gasoline vehicles. This can be explained by the ease that exists in finding a gasoline refueling station even in remote areas. Therefore, refueling while there is still a safe amount of fuel in the tank can compensate for any inaccuracies in the gauge readings. Unfortunately, the same refueling infrastructure does not yet exist for other fuels such as propane. This could potentially create a problem if automotive companies were to introduce alternative fuel vehicles into the market.

Unreliable fuel gauges could cause vehicles to become stranded in dangerous situations if they were to run out of fuel.

It is clear that there is a need to develop a more reliable and accurate method to measure fuel level, especially in alternative fuel vehicles. A great deal of information is available on different methods that have been developed to measure volume in applications ranging from industrial processing to rockets. The challenge is now to apply these concepts to the particular problem of alternative fuel vehicles.

OBJECTIVES

This project aims at developing a new system that can accurately detect the amount of fuel remaining inside an automotive fuel tank. The focus will be on liquefied fuels, and more particularly on propane. For this purpose, three objectives have been set.

The first is to perform a detailed background research on the different methods that have been developed over the years to measure fluid level. This research is not to be limited to automotive applications. In fact, a very important part of it is to discover technologies used in other areas that show promise in automotive fuel level measurement.

The second objective is to choose a potential candidate technology based on a thorough understanding of the choices available. This decision must also take into account all the safety regulations currently in place for propane equipment, as well as all the needs that are characteristic of an automotive component. Of special interest will be to find a method to improve the accuracy, linearity, and stability of the readings displayed on the fuel gage in the vehicle's instrument panel. It is hoped that the technology developed will also be transferable to any vehicle that uses other liquid fuels such as gasoline or alcohol.

The final objective is to study the basics of the chosen technology and to confirm its potential for use in alternative fuel vehicles. This study should demonstrate the particular advantages of the chosen technology, as well as uncover any potential difficulties.

CHAPTER 1 BACKGROUND

1.1. VOLUME SENSING

The first issue that must be considered in volume sensing is the physical quantity to be measured. Even though measuring volume directly is very difficult, it is possible to infer volume from other quantities such as the depth or pressure of the liquid. In automotive applications, the common approach to fuel volume measurement has been through level sensing, which can be used to infer volume if the geometry of the tank is known.

The main problem with this approach has to do with the changing conditions that the fluid may be exposed to while measurements are being taken. For instance, if the vehicle is not perfectly horizontal, the fuel will shift to accommodate the new direction of gravity with respect to the tank. Depending on the geometry of the tank, this may cause the level of the fuel to increase or decrease at the point where it is being measured, even though the actual amount of fuel has not changed. Therefore, when a vehicle is parked or is moving on a plane that is not horizontal, it is common for the fuel gauge to display an error caused by this effect. The location of the sensor may be used to compensate for this phenomenon by locating it near the axis of rotation of the fuel surface (see *Figure 1.1*). However, this can only work on regular shaped tanks, and does not account for all situations.

Level sensors may also be fooled by the motion of the vehicle. This includes acceleration, deceleration, and turning maneuvers. If the forces generated during these maneuvers are small enough, the fuel will just flow to one side of the tank and the surface of the fuel will

remain approximately flat (although it may not be horizontal). This will introduce an error similar to that caused by tilting of the vehicle. However, during harsher maneuvers, the fuel may gain enough energy to slosh in the tank. The non-uniform nature of slosh will cause level sensing to be extremely inaccurate.

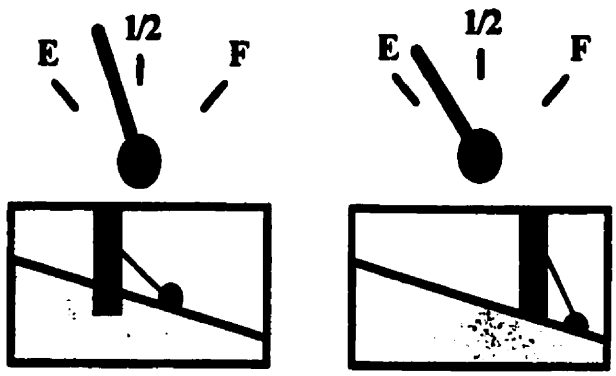

Figure 1.1: Effect of float location on the output reading [1]

It is possible to compensate for inaccuracies caused by the tilting of the surface of the fuel, as long this surface remains approximately flat. When using a single level sensor, a computer can be used to adjust the data gathered using several strategies. For instance, filtering routines can be used that take average readings over a period of time, and that can selectively eliminate readings that are known to be wrong (i.e. sudden peaks followed by sudden drops). In more sophisticated vehicles that are equipped with accelerometers, the acceleration data can be used to adjust the readings from the level sensor according to changes in the dynamics of the vehicle. Hardware filtering can also be added in the form of resistor/capacitor (R/C) filters located before the analogue to digital converter (see *Figure 1.2*) [2]. In addition, depending on the geometry of the sensor, a slosh barrier can also be added that will limit the speed in which the level of the fluid in the immediate vicinity of the sensor will raise and drop (see *Figure 1.3*) [3].

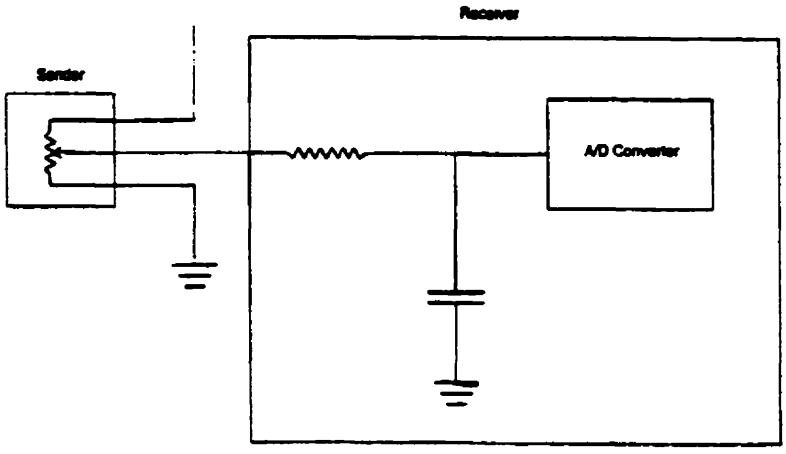

Figure 1.2: Low pass R/C filter used to dampen slosh and to filter EMI/RFI emissions [2]

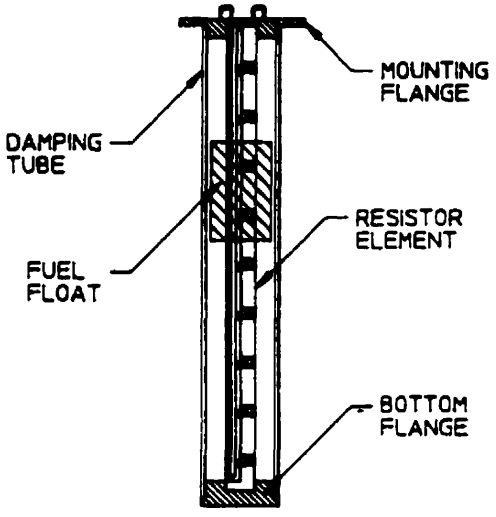

Figure 1.3: Damping tube used to reduce slosh effects [3].

Another strategy that may be used to compensate for tilting of the fuel surface is to employ multiple level sensors. In level sensing, the actual quantity that is of interest is the location of the top surface of the fluid. Having this information, it is possible to calculate the volume of the fluid below this plane. However, it is impossible to locate a plane in space using a single point obtained by a single sensor. In fact, the minimum number of points required to locate a plane in space is three. *Figure 1.4* shows how the inclination of the surface of the fuel can be

found by defining two angles of inclination with respect to the vehicle: front to rear, and left to right [4].

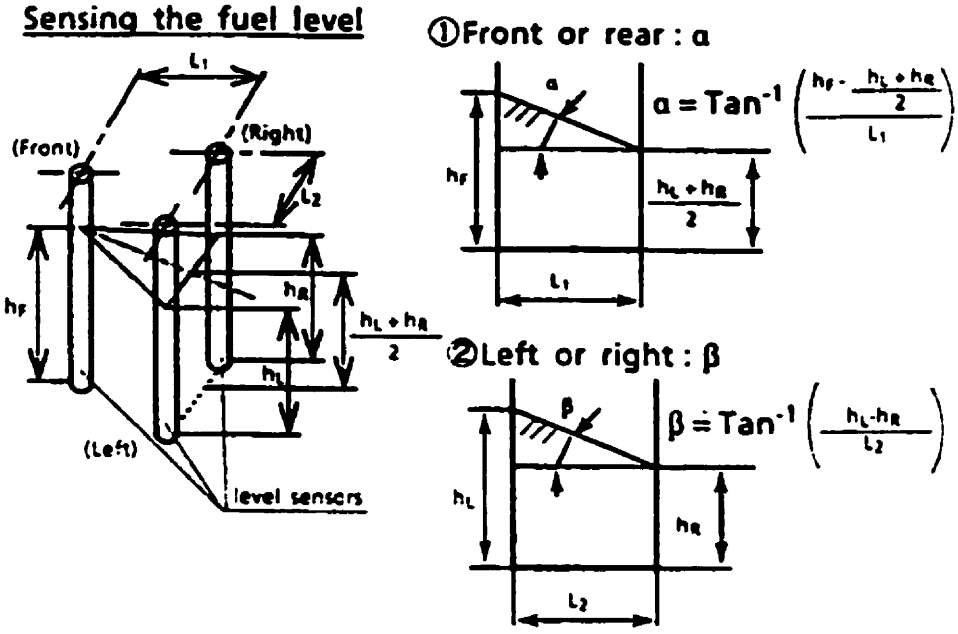

Figure 1.4: Method for locating the top surface of a fluid using three level sensors [4]

The main difficulty in using multiple level sensors is calculating volume accurately after the location of the surface of the fuel has been determined. This becomes particularly difficult as the geometric complexity of the tank increases. From a data processing point of view, the volume can be calculated using a known mathematical model that defines the geometry of the tank. Another approach is to use a look up table which already has the required information stored. Both of these approaches have been successfully applied, however they are both specific to tank geometry [4, 5, 6, 7, 8]. This means that if the shape of the tank is changed, the mathematical model or the look-up table must be modified accordingly. Another disadvantage of this approach is that the need for extra sensors and data processing hardware and software makes these systems very costly to implement.

In cases where sloshing becomes severe, level sensing is extremely inaccurate. Even multiple sensors become unable to give accurate readings. However, since sloshing usually occurs in short bursts, slosh barriers and R/C filters can be used to reduce most of this noise Time averaging routines can also help, as well as intelligent data processing routines.

1.2. System Considerations for Level Sensing

In addition to the problems just described, there are several other issues that must be considered in fuel level sensing. First, the linearity of the output signal is dependent on the interaction of the sensor with the fuel tank. If the tank has an irregular shape which causes the level of the fluid to drop in a non-linear fashion, the readings from the level sensor will not accurately reflect the change in volume of the fuel in the tank (see *Figure 1.5*) [1, 9]. In addition, depending on the method used to measure level, it may be very difficult to measure the end points accurately (i.e. full and empty) [1, 10]. For empty readings, either the sensor may not be able to reach the bottom (for example a float), or the bottom may become contaminated with residues which eventually interfere with the accuracy of the sensor. In the case of full tank readings, it is not uncommon that tanks are designed such that the fuel is allowed to reach points higher than the highest possible reading of the sensor (for example inside the filling spout) [1]. From the designer's perspective, this ensures that the gauge will always be able to reach full. However, this also means that the actual amount of fuel in a full tank will depend on the filling habits of the user and in the variability of the shut-off pressure on different filling pumps. As a result of these inconsistencies, the end points of level sensors in different vehicles can have a negative effect on the perception of linearity of the gauge [1, 10].

Other system issues that must be considered include the stack up of tolerances between the different components in the tank and the level sensor [1]. Also, the geometry of the tank may change with time due to deformations caused by material creep, and by variations on the internal pressure of the tank due to changes in atmospheric conditions [1, 11]. Variability of the manufacturing process can also cause different tanks to exhibit different stiffness and therefore to behave differently over time [11, 12]. The geometry of the tank may also cause pockets of fuel to form in areas that cannot be reached by the measuring probe.

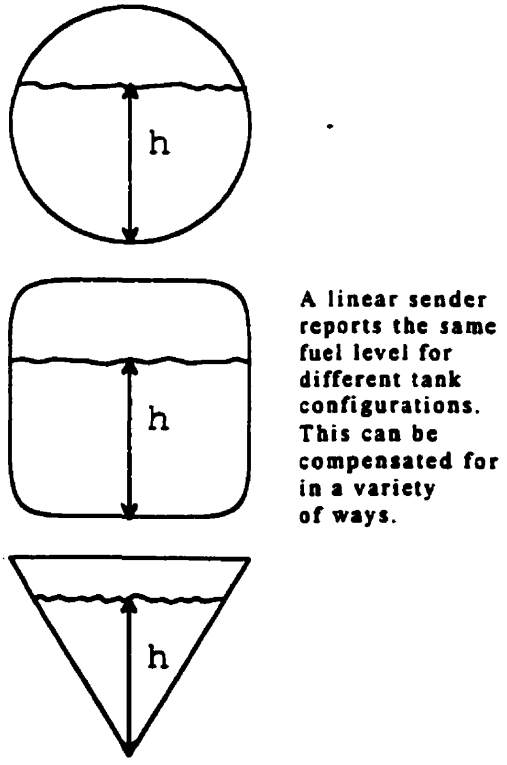

Figure 1.5: Effect of the cross sectional shape of the tank on the linearity of a level sensor [9]

1.3. CUSTOMER PERCEPTIONS

An added difficulty concerning fuel gauge design is the variability of the interpretations of fuel gauge behavior among different people. For instance, a fuel gauge that does not move during dynamic driving conditions may cause the customers to complain because they

believe that the gauge is broken [13]. In addition, the way linearity is perceived varies from one person to another. For example, some drivers increase the frequency with which they look at the gauge as the level of the fuel decreases [1]. As the gauge gets closer to the empty mark, these drivers tend to increase the frequency with which they look at the gauge. Therefore, the driver may think that the gauge is falling faster on the second half of the tank, when in fact this is an illusion caused by the fact that they have been looking at the gauge with shorter intervals.

In general, most complaints that customers have with regard to fuel gauges have to do with either their accuracy, their linearity, or their stability [1, 10, 14]. Yet, there is a great level of subjectivity when it comes to deciding on acceptable levels of error or variation in these three areas [1]. Therefore, accuracy, linearity and stability must be designed while considering how they will be perceived by different customers.

1.4. PROPANE

One alternative fuel that is of particular interest in this study is propane, due mainly to its increasing popularity. This makes it necessary to consider the properties and physical attributes of this fuel. Propane is stored as a liquid, and is usually pressurized between 150 and 300 psi. Propane tank manufacturers such as Sleegers Engineering design their propane tanks for a maximum pressure of 312 psi.

In terms of safety, it is necessary to look at the ignition characteristics of propane. This is particularly important when considering any sensors that will be mounted inside the tank and that require the use of electronic components. A value of particular relevance is the amount

of energy required to ignite propane. This value will govern the maximum current and voltage that can be present in any exposed conductors inside the tank. A comparison to gasoline shows that this value is comparable between both fuels [15, 16]. The main difference is that propane is stored with little or no oxygen inside the tank, which makes it less susceptible to accidental ignition [15]. Nevertheless, any sensor that requires electricity to be directed into the interior of the tank will need a firewall against voltage or current overload [17]. This is commonly done using what is known as a Zener diode barrier. These barriers use a Zener diode to limit the voltage, and a fuse to limit the current [17].

Another issue that must be taken into account is the composition of the fuel. Propane in particular is known for having a widely varying composition depending on the geographical location [18]. The composition may have an effect on the materials that can be used for a fluid level sensor, and the physical principle used to make this measurement. The amount of impurities is also significant since it may interfere with the long term operability of any component located inside the tank.

1.5. TECHNICAL SPECIFICATIONS

The design of this sensor must meet a minimum set of specifications set by the Canadian Standards Association, the ASME pressure vessel codes, and General Motors.

Table 1.1 summarizes the basic performance specifications that General Motors uses in the design of gasoline fuel level sensors. These requirements can be used as a basis for the design of a sensor for propane.

Aside from basic specifications, the sensor must be designed to meet safety, performance, and life expectancies set by regulatory agencies and by General Motors. For instance, the sensor should be able to function effectively for an extended period of time without maintenance and while being continuously exposed to the fuel. Another challenge is the temperature fluctuations experienced by vehicles during their service life. This has an effect on the properties of the fuel and of the materials used in the sensor. It may also cause inaccuracies in the sensor readings due to expansion and contraction of the sensor and the fuel.

Table 1.1: Summary of expected performance parameters for a gasoline fuel level sensor.

QUANTITY	RANGE
Accuracy	± 2%
Wear Resistance	100,000 cycles
Electrical resistor range	1Ω(empty), 44Ω(half), 88Ω(full)
Pressure resistance	1,45 psi (10 kPa)
Temperature Range	-40F to 125F (-40°C to 52°C)

Material selection is critical in this application. Certain plastics tend to absorb the fuel, which may cause them to swell. This problem is only aggravated by the high pressure used to store propane. If conductive plastics are used, fuel absorption will cause the electrical properties of the material to change with time. Some plastics may also be prone to degradation, and may contaminate the fuel. Metals are very prone to corrosion, especially if designs include galvanic couples. Conductive and resistive materials are prone to corrosion, degradation, and residue buildup that may affect their properties.

CHAPTER 2 CURRENT STATUS OF AUTOMOTIVE FUEL LEVEL SENSING TECHNOLOGY

An overview of technology currently used to measure fuel level in automotive applications is given in this chapter. Some companies who have developed new and unique systems are highlighted. It is important to note that all the technologies described in this chapter rely on level sensing.

2.1. GASOLINE ROTARY FLOAT ARMS

2.1.1 WORKING PRINCIPLES

A float arm sensor uses the vertical buoyancy forces of a float to locate the surface of the fuel. In order to translate the location of the float into an electronic signal that can be transmitted to the fuel gauge (or the electronic control module), the float is connected to a pivoting arm, which in turn carries a sliding electrode. The electrode rides on top of a variable resistor, which produces a change in resistance proportional to the location of the float.

Float arm sensors are by far the most common type of sensors used in automotive applications. Nevertheless, they have evolved very little over the past few decades, with the major developments concentrating on better materials and improved resistor performance, rather than on any modifications to the working principles.

2.1.2. CONSTRUCTION

Most vehicles now incorporate their fuel level sensors into the "fuel sender" assembly. This assembly carries other hardware such as the fuel pump, a filter, a canister, and the exit, return and venting lines for the fuel. Most vehicles carry only one level sensor. The only instance where more than one float sensor are used is in tanks with complex geometry that isolate pockets of fuel away from the main sensor.

The float is usually constructed from a closed cell foam designed to survive in direct contact with fuel without wearing or eroding. The connecting arm is typically made by bending a corrosion resistant steel wire. The arm is designed to carry a wiper which slides on top of a variable resistor.

The only significant change that this technology has seen in the past two decades has been a transition from wire wound resistors to thick film technology. Wire wound resistors are known for being very unreliable. The main problem stems from the wear experienced by the resistor as the wiper slides over it. With time, the wiper develops a sharp end which picks material away from the resistor wire [19]. In addition, the friction of the wiper causes fatigue in the wires due to continuous stretching and releasing actions [19, 20, 21]. A combination of these two problems results in common failure of these sensors due to wire breakage or shortage. In addition, loose windings can cause the wiper contact to become stuck [20].

Although wire wound technology is still being used, it is slowly being replaced by thick film resistor cards. Thick film resistor cards are manufactured by a screening process which deposits a resistor and a conductive element onto a ceramic surface [19]. This component is

later fired to improve bonding between all the layers. Laser trimming is used after firing to customize the resistance pattern. The manufacturing technique employed in thick film resistors offers the advantage that it allows customized resistance profiles to be easily manufactured into the card, allowing the output signal to be linearized with respect to the shape of the fuel tank (see *Figure 2.1*) [20].

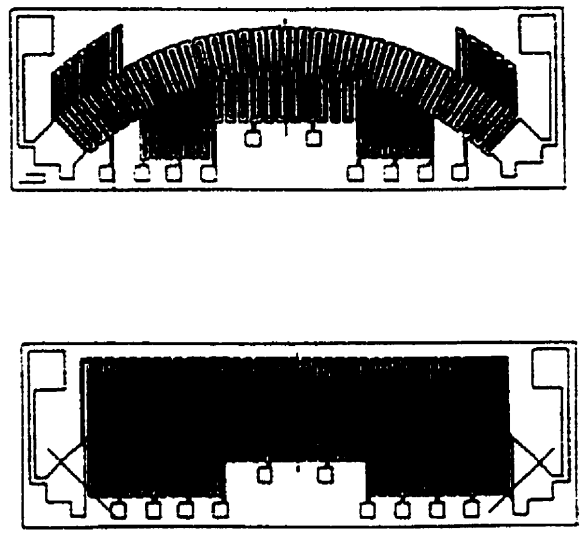

Figure 2.1: Typical resistor profiles made through the thick film process [20].

A new resistor technology that is now available in the market was developed by VDO in Germany [22]. It uses a magnet to attract the electrical contacts towards the resistor element. It mounts onto the fuel sender assembly in the same way as a regular thick film resistor. However, it does not rely on direct contact between a wiper and the resistor, which eliminates most of the wear. It is also encapsulated in a sealed chamber which keeps contamination and debris away from it. The main concerns with this design are the possibility of fatigue of the contact electrodes, and the suitability of an enclosed sealed chamber to high pressure applications such as propane. This design is illustrated in *Figure 2.2*.

Schematic:

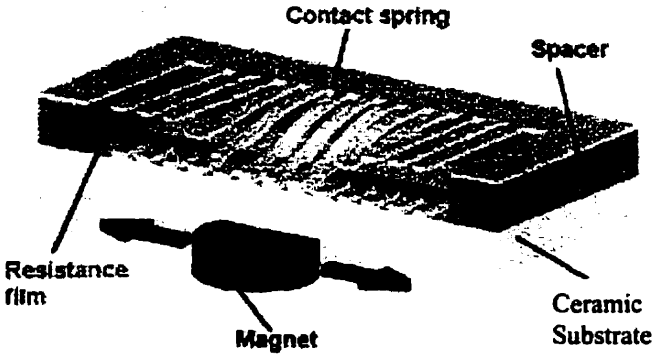

Figure 2.2: The VDO non-contact resistor design [22].

2.1.3. Advantages of Rotary Float Arm Sensors

The main advantage of rotary float arm sensors is by far their low cost. This technology has been in use for a long time, and therefore it is well developed. For the most part, these sensors have proven to be adequate in terms of reliability, and the use of sophisticated on-board signal processing software has greatly improved system performance.

Another advantage of rotary sensors is that a large float movement is translated into a small movement on the resistor. Although this causes a compromise on accuracy and resolution, it also requires a very small resistor which in turn reduces the cost significantly.

2.1.4. Disadvantages of Rotary Float Arm Sensors

Despite its success, there is a long list of deficiencies related to this technology.

- The fact that float sensors have moving parts make them prone to modes of failure related to fatigue and wear. This has an adverse effect on reliability.

- The movement of the float arm places special requirements for clearances [2, 14]. This means that these sensors are difficult to adapt to some tank shapes. They are also bulky in the sense that they need a large space to operate.

- Wire wound resistors can cause significant electrical noise [14].

- Even with thick film resistors, it remains difficult to linearize the sensor output over all possible conditions.

- It is very easy for the pivot arm to be damaged prior to, or during installation. This can potentially overthrow the calibration [23].

- Electrical contact may be lost if a dry film deposits on the surface of the resistor, if there is sulfuration of the resistive tracks, or if there is electrolytic corrosion [5].

- Any degradation of the float (or loss of buoyancy) will cause a progressive drift in the signal [5].

2.1.5. History of Reliability

Float arm sensors have reached a much improved record of reliability over the years. Wear of the resistor card remains the main problem, although material degradation and corrosion can also be a problem.

In general, float sensor technology has proven to be adequate for passenger and general purpose vehicles. However, other vehicles that travel considerably greater distances (such as

trucks and taxis) find this technology generally inadequate. The main reasons are the lack of durability and the difficulty in changing a sender unit.

2.2. PROPANE ROTARY FLOAT ARMS

2.2.1. WORKING PRINCIPLES

There are two basic types of rotary float arm sensors currently available in the market for propane vehicles. The first is a purely mechanical sensor used by most vehicles that have been converted to propane, such as taxis and police vehicles [23, 24, 25, 26]. These sensors have a float attached to a swivel arm. This arm transfers the motion to a rotating shaft using a bevel gear. At the end of the rotating shaft, and just behind the tank wall, there is a magnet which rotates as the float moves up and down. On the opposite side of the tank wall is a small gauge which follows the movement of the magnet and displays its location using a needle. This gauge may also have a resistor output compatible with common automotive fuel sensor outputs. Using this output, these sensors can be connected directly to the fuel gauge in the instrument panel of the vehicle.

Walbro, a supplier of fuel sender assemblies for gasoline vehicles, has also developed a new sender unit specifically designed for propane vehicles [27]. The main users of these units are automotive companies such as Chrysler. This unit is very similar to a conventional gasoline sender, and also uses the thick film technology previously described.

2.2.2. CONSTRUCTION

The components of the mechanical gauges that are inside the tank are usually all made from metal [25, 26]. The float is typically a sealed, hollow, aluminum chamber. The arm is also aluminum, so that the float can be welded to the arm. The rest of the internal assembly is made of steel alloys and aluminum. Some units have also been developed using some internal plastic components.

The materials used for the outer components of these sensors vary with the manufacturer [25, 26]. The outer housing is usually made of steel, but corrosion problems have prompted a few companies to switch to brass. The resistor unit (which is mounted on the tank with the use of two screws) is made of plastic and steel.

The sender unit designed by Walbro resembles a gasoline unit in most aspects [27]. The main differences are the mounting flange and the float. The mounting flange is made from cast aluminum and machined. All the fuel lines and valves are mounted on this flange. A feature of particular interest is the fitting used to pass the electrical wires through this flange. This fitting is manufactured by an American company named PAVE (see *Figure 2.3*) [15]. The float used by Walbro is made from a plastic material called Nitrophil which is also used in some gasoline sender units.

2.2.3. Advantages of Propane Float Sensors

The main advantage of current mechanical float sensors for propane is their low cost [24, 25, 26]. Also the addition of the wire output allows them to be interfaced to the gauge on the instrument panel. The aluminum floats used in these sensors have proven to be very reliable.

The unit manufactured by Walbro has the advantage that it combines most of the components necessary for a propane tank, such as safety valves and fuel lines, into a single unit [27]. This simplifies the design and assembly of the tanks significantly.

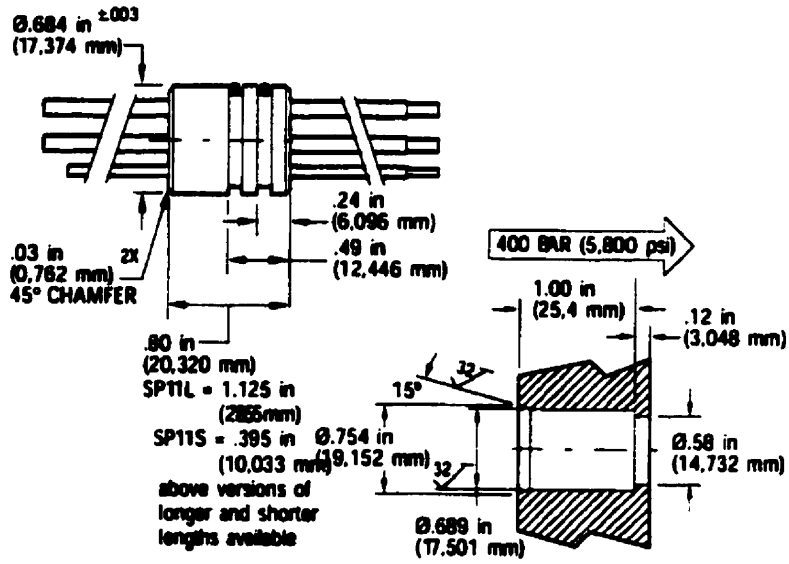

Figure 2.3: Compression fitting designed by PAVE for use in automotive propane tanks [28].

2.2.4. Disadvantages of Propane Float Sensors

Current propane sensors are plagued with many problems. The mechanical units are very inaccurate, and cannot be calibrated during installation [24, 25, 26]. Their construction makes them very prone to corrosion, for which they have a working life rated in months. The fact that there is a gauge mounted on the tank makes the sender unit prone to being broken by

flying rocks and other road debris. Sloshing in the tank also causes false readings, especially in older GM vehicles that lack proper electronic suppression. Another problem has been the movement towards non-standardized fuel gauges in the past few years, i.e. the movement away from the 0-90 ohm standard used by the most of the automotive industry.

The Walbro unit requires a large hole, and therefore does not fit most conversion tanks. Also, since it uses a float, it is also prone to inaccurate readings due to fuel sloshing.

2.2.5. History of Reliability

Mechanical float sensors have a very bad reputation [24, 25, 26]. Corrosion seems to be the main mode of failure. This can happen in the gearing inside (causing the sensor to stick), or on the outside where the gauge is exposed to the elements. The sender unit also tends to corrode, causing the gauge to stop functioning. In general, these sensor units are not expected to last more than a few months.

The unit developed by Walbro also has several problems. In particular, the float has been reported to sink if exposed to greatly varying weather conditions [18]. In addition, impurities in the fuel cause the resistor card to experience excessive wear by abrasion. These two problems have made this sensor very unreliable.

2.3. Linear Float Sensors

2.3.1. Working Principles

Linear float sensors work on a similar principle as rotary arm sensors. They differ in that there is no rotating float arm. Instead the float slides up and down along a vertical guide.

The float carries a double wiper which allows a conductive strip on one side of the vertical guide to contact a resistor strip on the other side [2, 3, 14]. This can be used to produce either a 3 wire potentiometer, or a 2 wire resistor (see *Figure 2.4*) [14].

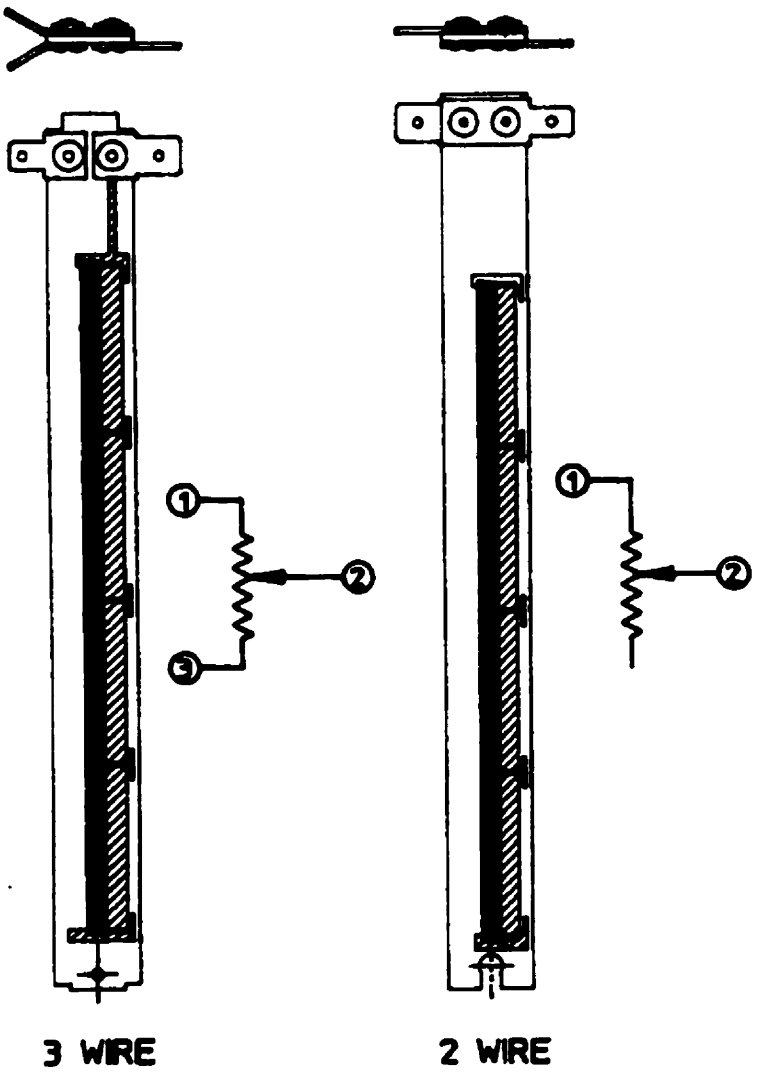

Figure 2.4: Two and three wire circuit designs used for vertical float sensors [14]

2.3.2. CONSTRUCTION

Currently, there are two basic types of construction used for linear float sensors: Metallic and Plastic

2.3.2.1. Metallic Construction:

This construction was developed by Spectrol Electronics [3, 14]. The conductor strip consists of a steel substrate with a low alkali porcelain coating (see *Figure 2.5*). The 0.2 mm coating prevents damage to this path from electrolytic action in the fuel.

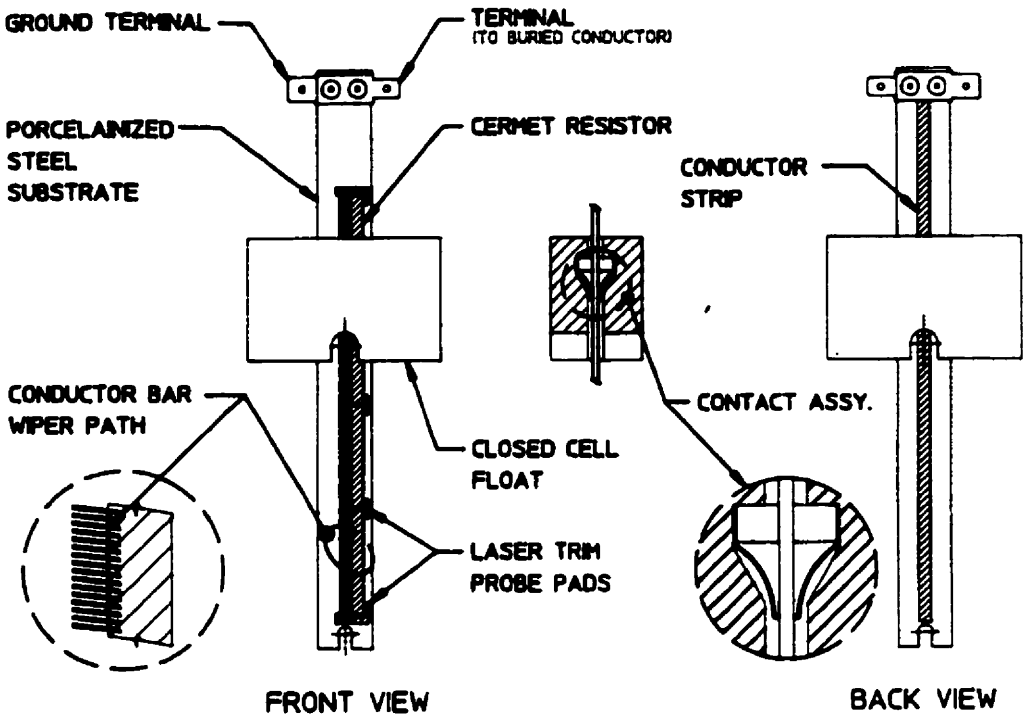

Figure 2.5: Cermet vertical float sensor designed by Spectrol Technologies [14].

The resistor strip is a thick film type, and can be tailored to the shape of the tank in order to improve linearity. The float used in this design is made from a closed cell foam.

2.3.2.2. Plastic Construction:

This construction was developed by Rochester gauges (see *Figure 2.6*) [2]. It follows the same working principle as the Spectrol design, but varies in the materials used for its

construction. The central support shaft is extruded from aluminum, acetal, or nylon. The float is acetal, and carries the two wipers. The resistive and conductive strips are made from a specially formulated conductive plastic. The entire assembly is held together under compression by a stainless steel shaft and two nuts.

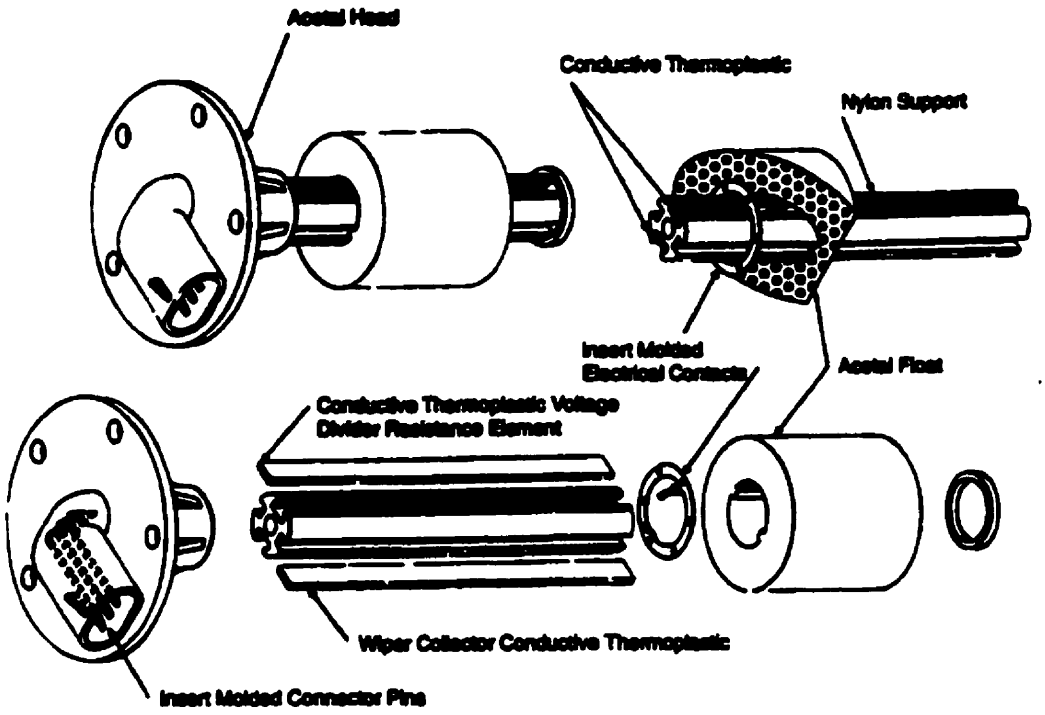

Figure 2.6: Vertical float sensor developed by Rochester Gauges [2].

2.3.3. ADVANTAGES OF LINEAR FLOAT SENSORS

These sensors are characterized by having very good resolution [21]. The wear issues are different with these sensors than with the rotary arm type since the wiper has to move larger distances, but the resistor surface is not worn by the wiper as much. Their symmetry makes them easier to design and build, and the fact that they are vertical allows easy installation of an anti-slosh barrier. They also have lesser space requirements for the moving parts.

The linear design allows the sensor to be easily tailored to tank depths up to a few meters [3]. This design also offers a reduced chance that the float will bind somewhere in the tank. The variable voltage or variable resistor output can be easily interfaced with modern automotive computers. The plastic sensors have the advantage of being resistant to corrosion and of being lighter.

2.3.4. Disadvantages of Linear Float Sensors

The main reason linear sensors have not yet found widespread use has to do with their greater cost. In particular, the need for a resistor that will span the entire length of the sensor adds considerably to their price. Also, the longer travel of the float can cause greater wear on the wiper contact.

Linear float sensors also have the same problems concerning the accuracy in the end points (full and empty) as their rotary counterparts. The plastic sensors may not corrode, but they have other problems that can cause their performance to deteriorate with time. For example, the conductive plastics may absorb fuel causing the resistance of the material to change over time.

2.3.5. History of Reliability

There is no data on the reliability of existing linear sensor designs. However, it is expected that similar problems will be found with these sensors as with rotary sensors.

Only two companies were found during the research who manufacture linear sensors in North America [2, 3, 14]. To date, neither has been able to introduce their sensors for use in mass

produced passenger vehicles. Spectrol Electronics has had some success in implementing their sensor in trucks and off road vehicles. However, wear in the sensor remains a problem.

2.4. Capacitive Sensors

2.4.1. Working Principles

A capacitive level sensor determines the depth of a fluid by measuring changes in the capacitance across two electrodes immersed vertically in the fluid [4, 5, 6, 7, 8, 29, 30]. Since the fluid acts as a dielectric, changes in its depth translate into a measurable change in the permitivity of the void between the electrodes (see *Figure 2.7*). This change can be measured using proper instrumentation and signal processing equipment. An oscillator is used to excite the capacitor with a series of pulses at a known frequency. The frequency of response of the capacitor will depend on the void permitivity, and therefore, on fluid level. From this, fluid level can be correlated directly to the frequency of response of the capacitor.

The calibration of a capacitive sensor is affected by changes in the dielectric qualities of the fluid, which in turn depend on the fuel grade, pressure, temperature, and other factors. This effect must be compensated by measuring the specific inductive capacitive of the fluid in order to maintain a reliable calibration [4]. This can be done by having a second capacitor of known geometry that is fully immersed in the fluid. This capacitor acts as a reference against which the measuring capacitor can be compared.

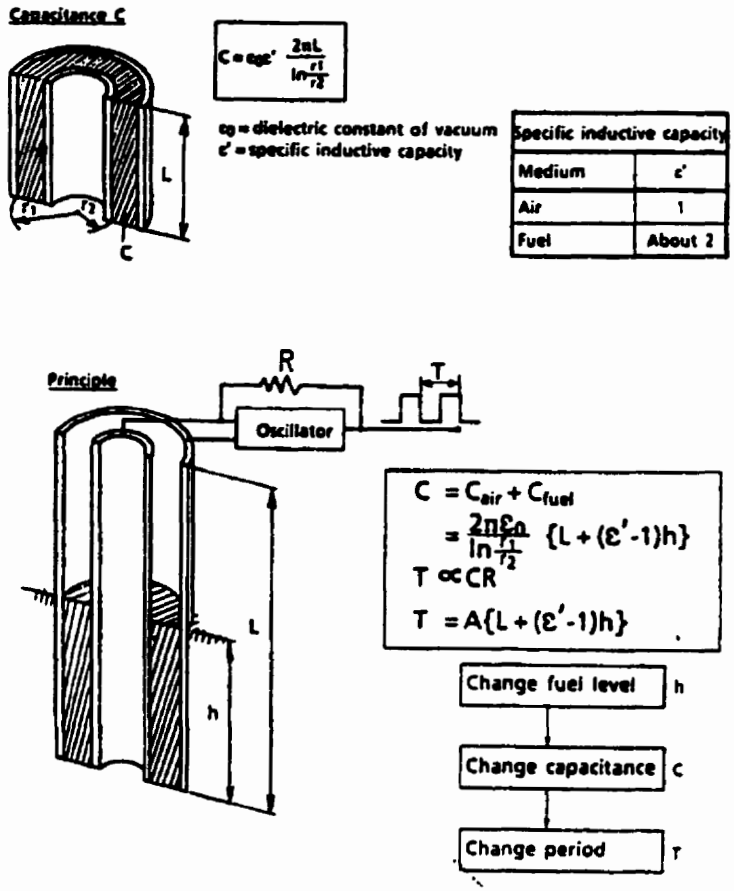

Figure 2.7: The capacitive sensor principle [4].

2.4.2. CONSTRUCTION

A capacitive sensor has no moving parts. The actual sensor consists of two electrodes that can be made from two concentric cylinders or from two flat plates placed in a parallel arrangement. The concentric cylinder style has the advantage of having better structural strength, and therefore can be easily adapted to deep tanks [4]. The parallel plate style requires supports along their length, which may create dead zones wherever the supports are located. One sensor was found in the literature that has a planar electrode and uses the metallic support frame as the second electrode [5]. In some static applications (i.e. storage tanks) the tank shell itself is used as one of the electrodes [17].

The two electrodes must be kept electrically insulated from each other with the use of spacers. The reference capacitor can be built into the main capacitor or can be separate. In a cylindrical sensor, the reference capacitor can be mounted inside the inner tube. This way the inner electrode of the main sensor can also be used as the outer electrode of the reference sensor. In flat plate sensors, the reference electrode may also share one of the main electrodes.

The electronic module makes an integral part of a capacitive sensor. This is because in order to read the signal, a system is required that can provide excitation, multiplexing, timing, and signal processing. The entire electronics module can be built into the mounting cap in the sensor. It is also possible to share some of the processing with the on-board computer of the vehicle, and leaving only the basic data acquisition functions on the sensor cap.

2.4.3. Advantages of Capacitive Sensors

One of the main advantages of capacitive sensors is that they have no moving parts. This removes the possibility of failure due to fatigue or wear. Also, there is a minimal number of parts that need to be inserted inside the fuel tank, improving reliability, and simplifying the material selection process. These sensors are also characterized for being accurate within a few percentage points of full scale [5].

The concentric cylinder design creates an anti-slosh barrier automatically. They also have no dead zones, and the calibration sensor can be easily added in the center (by using the middle electrode for the main sensor and for the calibration sensor) [4]. The depth of the tank is not

an issue since the sensors can be cut to length. They also require less space to operate since no clearance is required for a rotating arm or a sliding float.

2.4.4. Disadvantages of Capacitive Sensors

Most fuel sensor suppliers rate cost as the main disincentive for using capacitive sensors in automotive applications [31, 32, 33, 34]. Even though the sensor itself is very simple and cheap, the electronics and software that are required to run it can be very expensive.

Although wear and fatigue are not a problem, electrolytic accumulation, or sludge accumulation on the electrodes can deteriorate the accuracy of the sensor with time. In addition, the sensor can only be mounted vertically, and requires a direct line of sight to the bottom of the tank.

A potential problem for applying this sensor to propane applications is the changing in dielectric properties of the fuel with geographic location [18]. In particular, Hydrogen Sulfide can be a problem since it causes the propane to become conductive. Conductive fluids require special consideration when designing a capacitive sensor in order to prevent short circuiting between the electrodes.

2.4.5. History of Reliability

Capacitive sensors have been used mainly in the aircraft industry with a good track record. There are only a few known manufacturers of these sensors for automotive applications. Datcon developed a sensor using parallel electrodes an a cylindrical slosh barrier (see *Figure*

2.8) [35]. This sensor is used mostly in trucks and in off road applications (i.e. construction equipment).

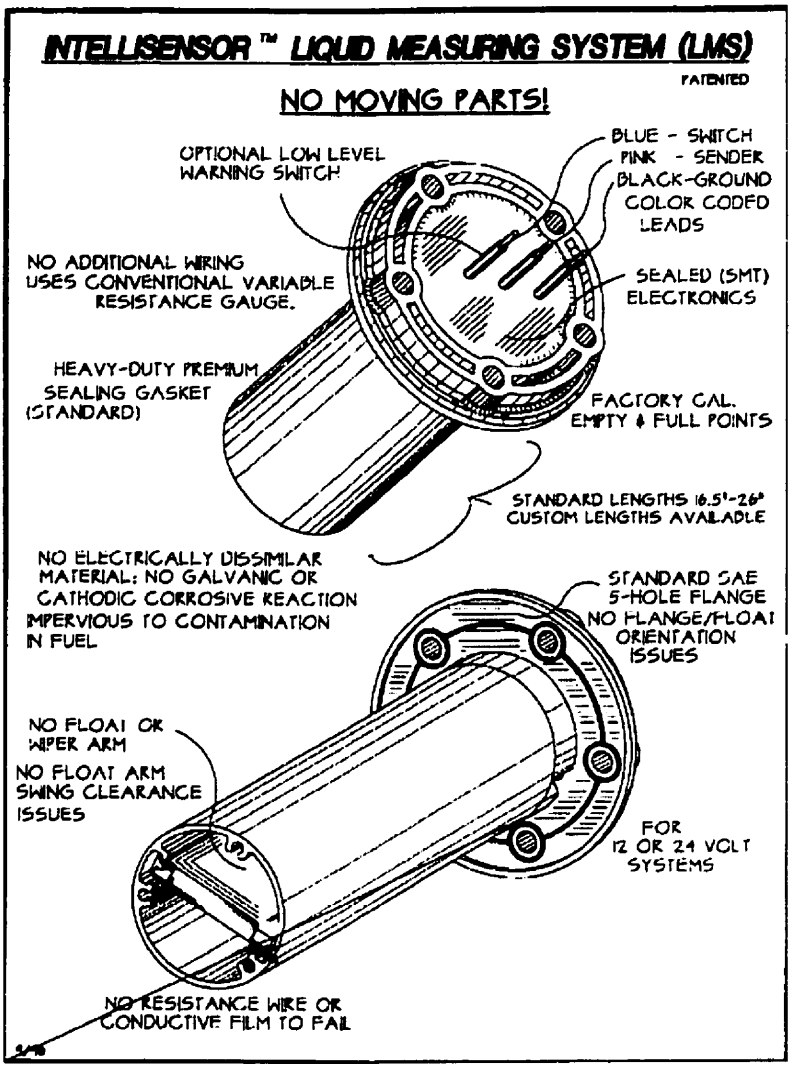

Figure 2.8: Automotive capacitive sensor distributed by Datcon [35].

Toyota developed a sensor consisting of a bundle of three capacitive sensors and a reference sensor (see *Figure 2.9*) [4]. Having three sensors allows the system to calculate the real location and inclination of the surface of the fuel, and can therefore compensate for tilting of the vehicle. Experiments with this sensor demonstrated an increase in accuracy on sloped surfaces and in dynamic driving conditions as compared to a single sensor (see *Figure 2.10*).

This sensor went into production in the early 1990's, but no long term performance data are available.

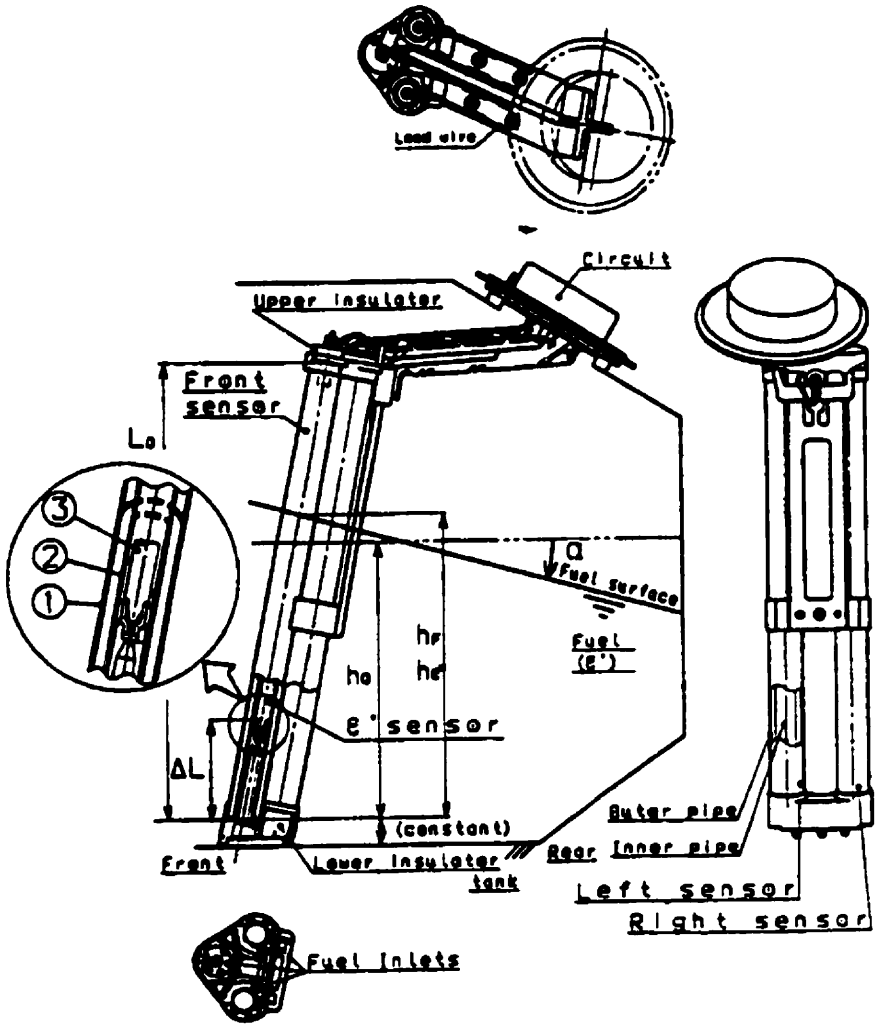

Figure 2.9: Multiple sensor designed by Toyota using the capacitive technique [4].

Magneti Marelli of Italy also developed a capacitive sensor, but interviews with representatives of the company were ineffectual in uncovering any details regarding plans for its production [33]. This sensor uses a planar electrode made by etching a coppered circuit on one side [5]. The metallic frame that supports the sensor is used as the opposite electrode (see *Figure 2.11*). The copper electrode is divided into the main sensor and the reference

sensor. The main sensor is etched to follow the shape of the tank, and therefore to linearize the output. This approach differs from the sensor developed by Toyota in that the latter uses software to linearize the output. Magneti Marelli also claims to have developed a multi sensor array similar to Toyota's, however no specific literature was found on this sensor [5].

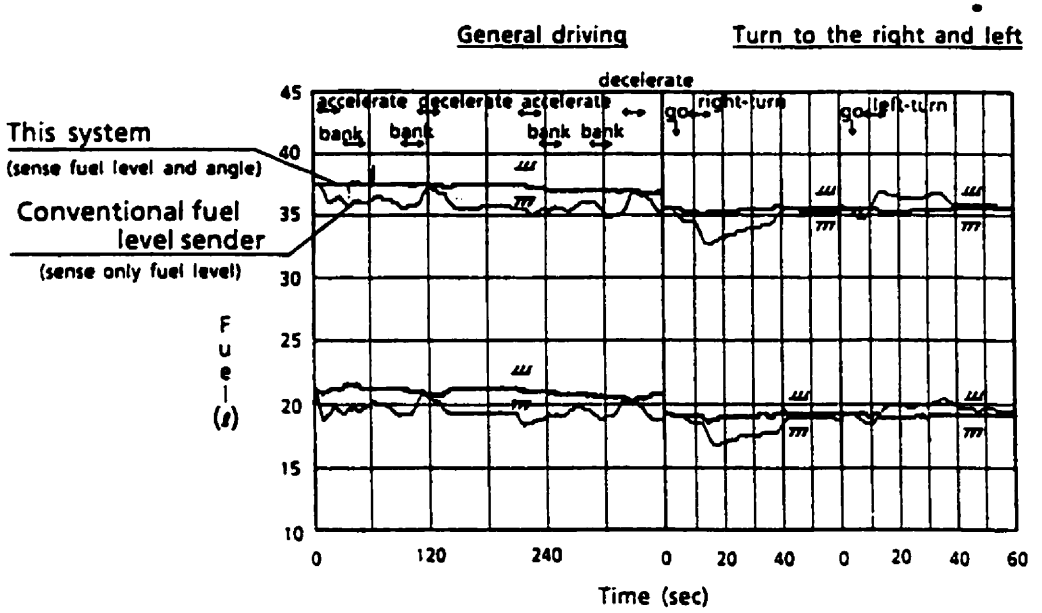

Figure 2.10: Results obtained by Toyota during dynamic testing of their multiple sensor design [4].

As mentioned before, capacitive sensing technology still requires some development. Some particular aspects that need further investigation include the selection of materials compatible with modern fuels, methods to reduce residue buildup, and the effect of conductive elements present in the fuel. The method used to add a reference sensor also needs some further development since some dead zones still exist, particularly in the lower end of the scale. With regard to the multi sensor approach taken by Toyota, the mathematical modeling that they have used for this system remains inadequate since it is only an approximation that does not take into account the shape of the tank. This requires further attention in order to meet the needs of modern conformal plastic tanks.

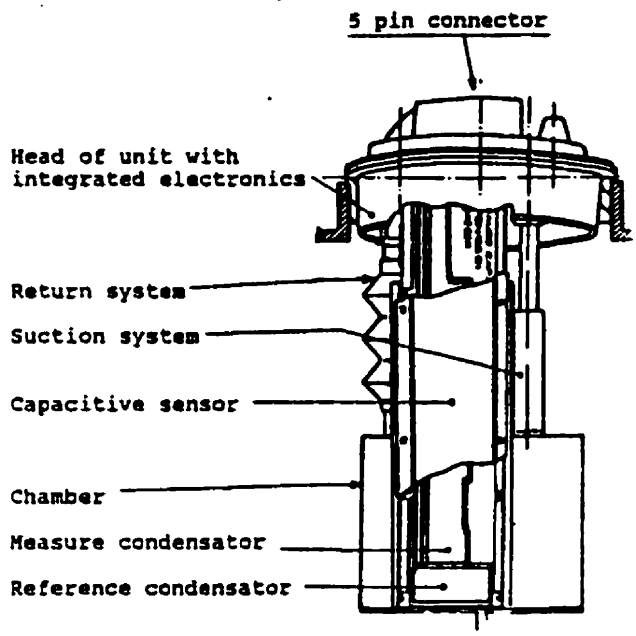

Figure 2.11: Capacitive sensor designed by Magneti Marelli [5].

CHAPTER 3 OTHER FLUID LEVEL SENSING TECHNOLOGY

The summary presented in chapter 2 only includes technologies that have been successfully applied to automotive fuel level sensing applications. Nevertheless, there are several other fluid level and fluid volume sensing technologies that could potentially be incorporated into automotive fuel tanks. This section summarizes some of these techniques.

3.1. ULTRASONIC SENSORS

3.1.1. WORKING PRINCIPLES

The principle of ultrasonic range sensing is very similar to that of sonar [36, 37, 38, 39, 40]. This method measures the time that it takes for a sonic pulse to travel to a target and come back [41]. This time is usually known as the Time of Flight, or TOF (see *Figure 3.1*). By knowing the speed of sound in the medium and the time of travel, it is possible to deduce the distance traveled. To do this, all that is required is an excitation source that can produce a sonic pulse, and a device that is sensitive enough to detect the returning signal. The same device can be used as the transmitter and the receiver, in which case it is known as a transceiver.

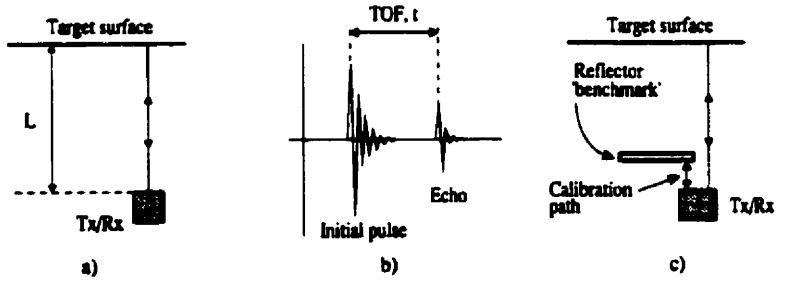

Figure 3.1: a) Basic setup of an ultrasonic distance sensor; b) Time of Flight (TOF) definition; c) Method for measuring speed of sound using a benchmark reflector [41]

This principle can be applied to fluid level sensing in a variety of ways. In their most basic configuration, ultrasonic sensors send a sonic pulse towards the surface of the liquid. This can be done from above (the dry side), or from below (the wet side) [42]. The signal travels through the vessel, bounces off the fluid surface, and returns to a receiver. The main problem with this approach is that, since there is no method to guide the pulse, the signal is prone to inaccuracies [39, 43]. For instance, echoes from objects interfering in the path of travel are a major problem. So are vibrations and noise from external sources that work to confuse the signal processing system.

Problems of this type were very severe when this technology was first applied. However, improvements in sensor construction and signal processing have made this technology very reliable. Modern sensors can be taught the conditions common to a particular application so that they can ignore interferences [38].

Some sensors have been designed so that the sonic pulses travel through a guide tube [39, 43]. This tube reduces the attenuation effects that sound waves suffer in a gas, and collimates the signal (see *Figure 3.2*). In addition, it reduces the effect from reflection signals coming from other features in the vessel.

A matter of particular concern with ultrasonic sensors is the fact that variations in the conditions of the transmitting medium will cause changes in the speed of sound. In order to compensate for this, some sensors use temperature and pressure compensation by measuring these quantities separately [38, 44]. Other sensors use a benchmark reading at a known

distance to continuously monitor the absolute value of the speed of sound (see *Figures 3.1c* and *3.2*) [39, 43].

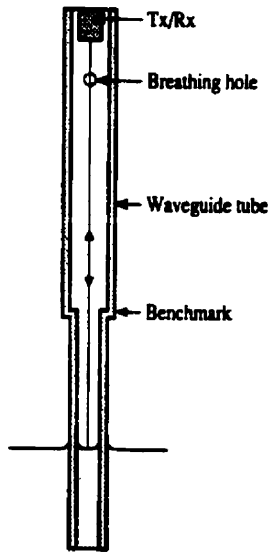

Figure 3.2: Waveguide tube used for ultrasonic level sensors [43]

3.1.2. CONSTRUCTION

In general, the most critical component in an ultrasonic sensor is the sound wave generator/receiver. This component is usually manufactured from a piezoelectric material and can be made as one single component, or as two separate parts. Combining the transmission and receiving functions reduces the overall cost of the unit, but gives the sensors a dead band [41]. A dead band is the time during which the transmitter is still vibrating after sending a pulse, and during which it is not ready to read the incoming signal. This effect is illustrated in *Figure 3.3*.

Having a dead band creates a limitation as to how close the surface being sensed can be located. The dead band can be reduced by using electronic damping of the transceiver,

although this has a negative effect on the complexity and the cost of the system [45]. It is also possible to physically cut the transceiver in half, and use one half for transmission and the other half for receiving [41]. This eliminates the dead band, but it increases the complexity of the sensor.

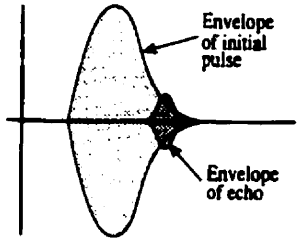

Figure 3.3: Overlap of the generated and returning signal in the dead band of the transceiver [41].

If a tube is used to guide the signal, it should be manufactured from a material that attenuates sound transmission. The size of the tube is not very critical, and diameters between 8 and 25 mm have been used successfully [39]. The tube itself can also be bent around the tank as desired, although some limitations do exist on the maximum radius of any bend. The length of the tube is also not critical, and lengths of more that 10 meters have been used successfully.

3.1.3. Advantages of Ultrasonic Sensors

The fact that sonic sensors do not need to contact the fluid makes them very safe when used in flammable liquids [38, 39]. This is true even if a sonic tube is used. In addition, the fact that all the electronics can located away from the fluid makes it possible to use these sensors in corrosive or otherwise detrimental environments.

The fact that the only moving part is the transmitter/receiver gives this sensors good reliability. This also reduces the amount of space that they need to operate. And since the tube size and geometry are flexible, they can be easily adapted to almost any shape of tank.

3.1.4. Disadvantages of Ultrasonic Sensors

The main detractor of ultrasonic sensors is their high cost. In terms of performance, having a combined transmitter/receiver give these sensors a dead band, and thus a restriction on the mounting location of the sensor. Also, noise problems can potentially become very significant in vehicle applications where external vibrations continuously affect the car. Unfortunately, little work has yet been done to confirm whether this is a problem or not.

Another potential problem is the frequency range used to create the sonic pulses. The term used to describe ultrasonic sensors is very misleading because the actual frequency range used can often fall within the audible range [43]. This is often necessary when using a gas as the transmitting medium because of the attenuation effects that the signal may suffer.

3.2. Vibratory Rod Principle

3.2.1 Working Principles

This sensor also works by measuring vibrations, except that in this case a solid rod is used as the medium for wave propagation [10]. The basic idea is to vibrate a solid metal rod at a known frequency and amplitude, and to measure the changes in the frequency response of the rod as it is immersed in the fluid. Essentially, the fluid acts as a damper which affects the vibration of the rod depending on the depth of immersion.

3.2.2. CONSTRUCTION

No evidence was found that these sensors have been used in production vehicles. One paper published by Robert Bosch GmbH describes a prototype of a sensor of this type which was used to measure gasoline level in a car [10]. The basic construction of this sensor consisted of a straight rod with a wave generation source (an electromagnet) and a piezoelectric bending transducer mounted on the dry end (see *Figure 3.4*). The electromagnet was used to generate bending waves along the rod at a fixed wavelength, and the characteristic oscillation frequency was measured using the piezoelectric transducer. This frequency was known to vary as a function of immersion depth, as long as the phase was kept constant.

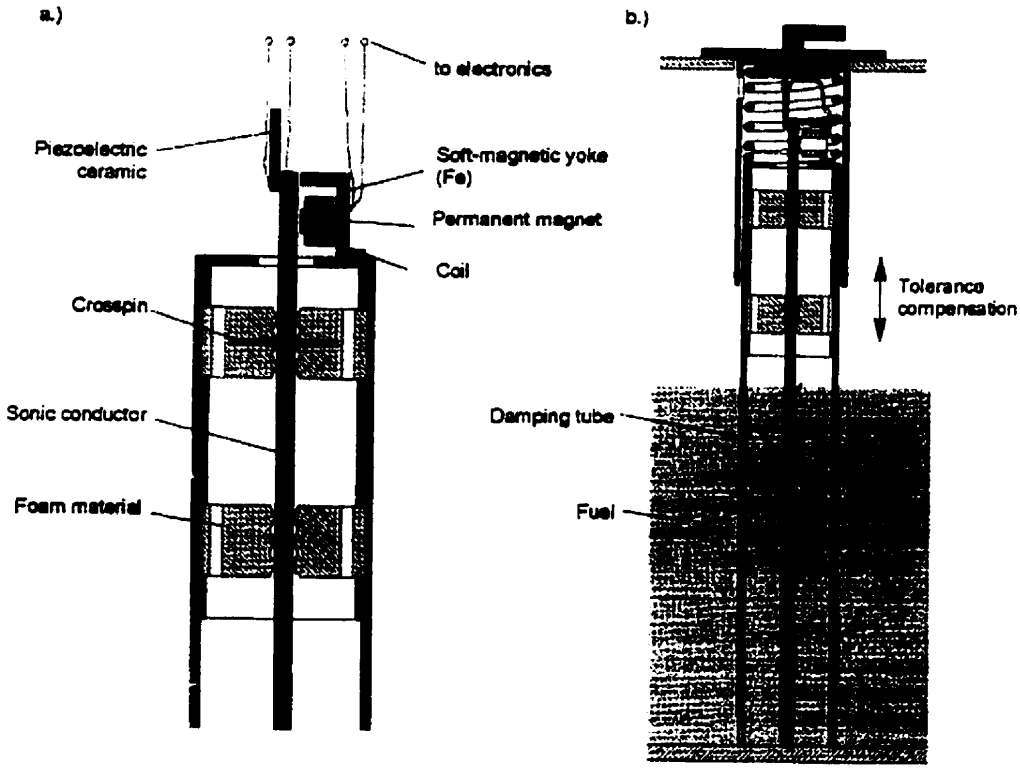

Figure 3.4: The vibrating rod sensor [10].

In its physical embodiment, the prototype sensor was built using a spring loaded telescopic slosh barrier (which adapts to changes in the shape and tolerances of the tank). The rod was held in place using special attachments designed not to interfere with the vibrations. Testing of this device showed that it could maintain good accuracy during a period of one year while immersed in a car's gasoline tank.

3.2.3. Advantages of Vibratory Rod Sensor

These sensors can be easily interfaced with on-board electronics. Accuracy is very good, and they are not as prone to being affected by external noise as ultrasonic sensors are. Their construction allows them to be bent around the tank, as long a minimum radius is observed. The profile of the rod itself can also be changed to fit the tank in order to linearize the output signal as a function of tank shape.

3.2.4. Disadvantages of Vibratory Rod Sensor

One of the main limitations of this technology is the material selection which must be done under strict requirements for acoustical properties. This severely limits the number of materials that can be used, which is a problem for components which are expected to have a long life inside a fuel tank.

The cost of manufacturing these sensors is also a potential problem due to their high complexity as compared to a float arm sensor. Also, an expensive electronics module is necessary to drive this unit.

Another problem is that changing the fluid measured may require sensor recalibration. This is also a problem if the damping characteristics of the fuel (i.e. density) change severely with time.

Finally, compared to ultrasonic sensors, the modes of vibration that must be accounted for in a vibrating solid rod are very complex (compression, flexural, torsional, and radial). This makes the signal acquisition and processing much more complex than in ultrasonic sensors.

3.3. Optical Sensors

There are many ways that optics have been applied to level sensing. Both continuous and discrete sensors have been developed, although most optical sensors available in the market today are only point sensors (ON/OFF) [17, 46, 47, 48, 49, 50].

The most common type of point sensors use a prism onto which a beam of light is directed [17]. If there is no fluid on the other side of the prism, the light will reflect back to an optical sensor (see *Figure 3.5*). However, if there is fluid on the other side, the light will be absorbed instead of bouncing back to the optical sensor. The light beam could be directed to the prism from a remote location using fiber optics, or it could be directed from an LED placed directly behind the prism. These sensors are very useful for process applications where all that is required is a signal when a tank is full or empty (see *Figure 3.6*); however, they fall short when continuous signals are critical. It is possible to arrange these sensors in an array that can measure level discretely, but this is rarely done because of cost and practical considerations.

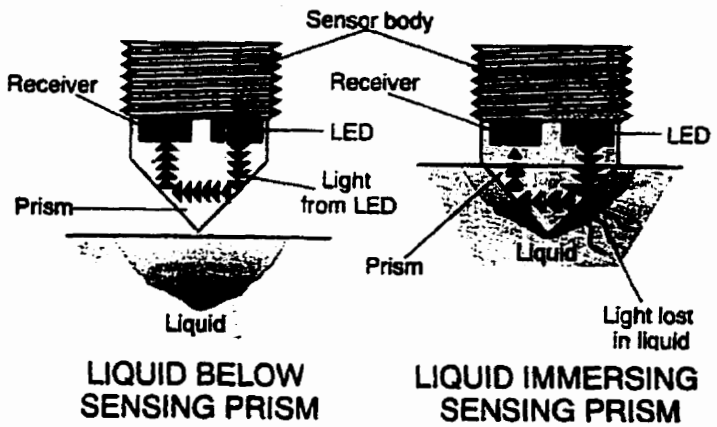

Figure 3.5: Prismatic sensor principle [17].

A similar type of sensor has been developed which uses a bent optical fiber with its protective cladding removed [48]. There is a transmitter on one end, and a receiver on the other end. If the bent section is immersed in a fluid, the fiber stops transmitting light to the receiver. Conversely, if the fiber is removed from the fluid, it allows light to be transmitted through. These sensors are not very common because they are more complex than the prism sensors, and do the same job.

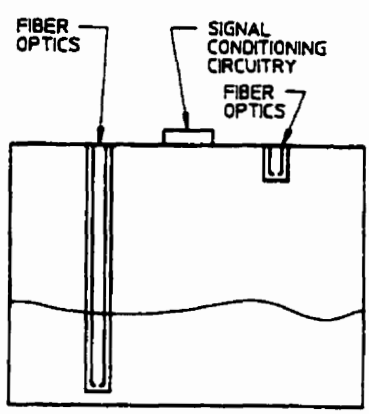

Figure 3.6: Prismatic sensors can be used to detect high or low volume conditions [3].

A few continuous measuring techniques have also been developed using optics. Most of these techniques have been developed in university and research labs, and none have yet

reached the market [46, 47]. There are still many problems with most of them. Some require very expensive, high quality optical fibers; others are very sensitive to the optical properties of the fluid. In general, they are all very sensitive to any deposits that may form on the optical components during long term immersion in a fuel tank.

Sandia National Labs in Texas has developed a hybrid sensor which measures hydrostatic pressure using optics (see *Figure 3.7*) [51]. It uses a corrugated diaphragm that is located horizontally near the bottom of the tank. The diaphragm is exposed to the fluid pressure on one side, and to the pressure above the liquid on the other side by using a tube that extends from the bottom to the top. The motion of the diaphragm is detected by using a transmitting fiber that sends a light beam towards the center of the diaphragm. Several receiving fibers surrounding the transmitting fiber detect the reflected light. All the fibers can be made of plastic (although this limits their length), and the system uses an LED for transmission and a PIN diode for detection. A computer analyzes the signal and detects the location of the diaphragm which changes according to the depth of the fluid.

The diaphragm is corrugated in order to increase its total displacement, and in order to linearize the output. Some problems still exist with the coefficient of thermal expansion of the diaphragm that creates an error with changing temperature. Another potential problem is the formation of a coating on the optical components since they are still exposed to the gaseous phase of the fuel.

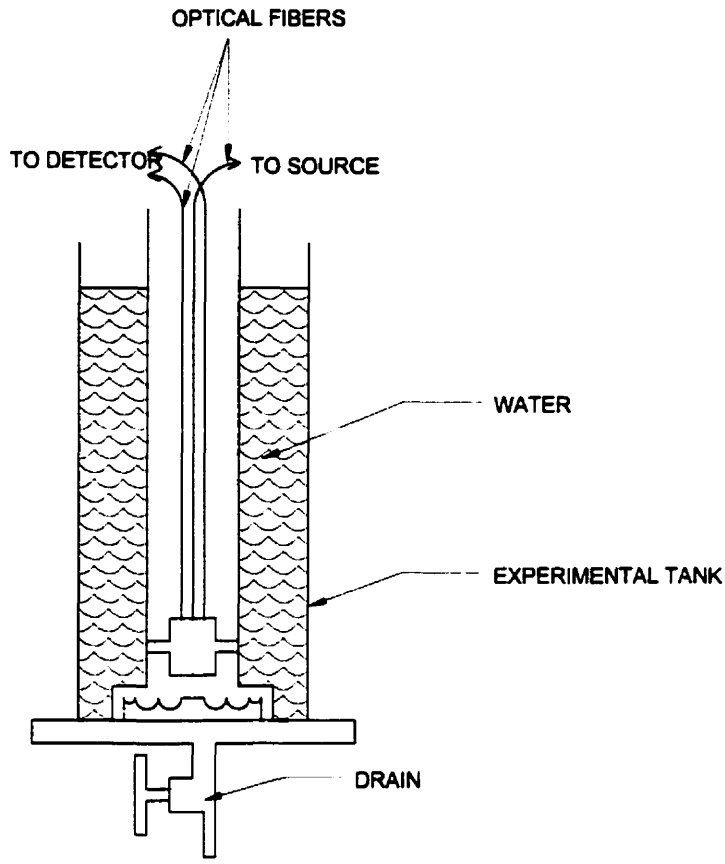

Figure 3.7: Optical sensor designed by Sandia National Labs [51].

A Japanese research team has developed a continuous optical sensor that works in a similar fashion to an ultrasonic sensor [47]. It uses an LED to generate a light beam which is directed at the surface of the fluid. The light beam travels to the surface and bounces back to a receiving fiber. A computer calculates the time of travel and deduces the distance to the fluid. This sensor has only been tested using oil as the measured fluid, and little data exists regarding its performance.

3.4. THERMAL SENSORS

Thermal sensors consist of a series of thermistors arranged discretely along the length of an insulated rod (see *Figure 3.8*) [3]. The idea behind thermal sensors is that when the

thermistors are exposed to an electrical current, their temperature increases [3, 10]. However, if they are immersed a fluid, their temperature will drop causing a measurable change in the resistance. This change can be detected using sophisticated electronics in order to sense changes in level. There is little literature available on this technology, but it appears that manufacturing and signal processing difficulties have placed a limitation on their development.

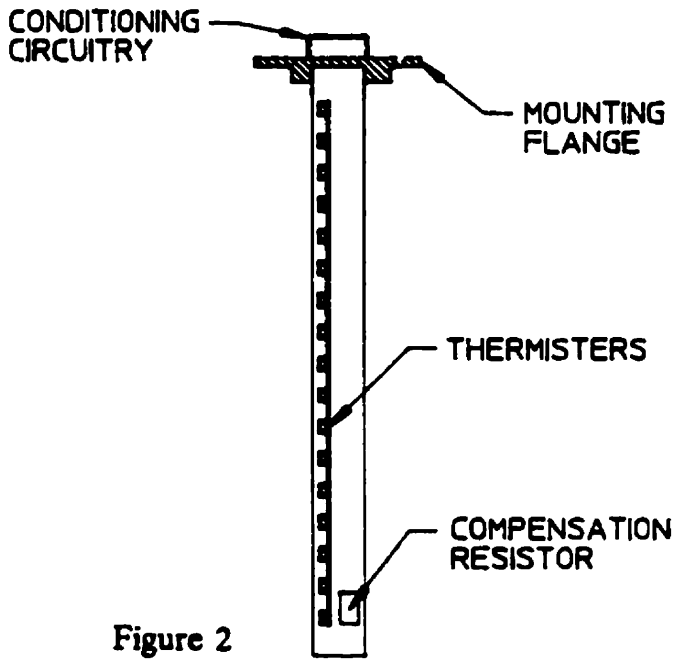

Figure 3.8: Thermal sensor [3]

3.5. HYDROSTATIC SENSORS

Hydrostatic sensing uses pressure sensors to calculate the depth of a liquid using basic fluid equations (see *Figure 3.9*) [52]. The total volume is then calculated from the depth of the liquid and the tank geometry. This method works well, but has several short comings. First, it requires a multitude of sensors to measure at least two pressure points (above the fluid and at the bottom of the tank), and at least the fluid temperature (to compensate for expansion).

Also, the motion of the fluid inside the tank adds fluctuations to the pressure readings that may be difficult to interpret. However, the main problem currently is to find suitable pressure sensors that have good accuracy, but that are also available at a reasonable cost. As an advantage, other properties such as density and mass can also be measure using this technique, which makes it very useful if more information about the fluid is desired (see *Figure 3.9*).

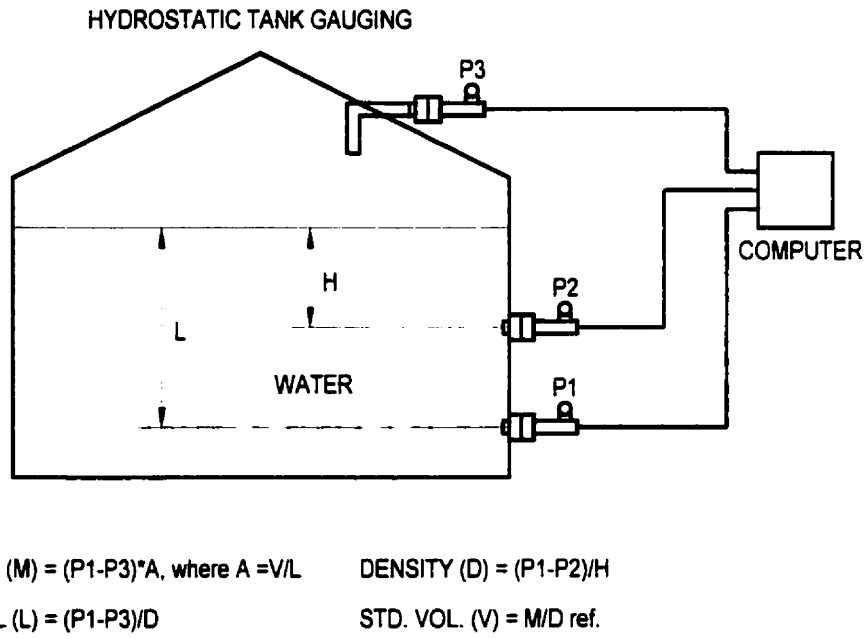

Figure 3.9: Hydrostatic measuring technique used to calculate mass, level, density, and standard volume [52].

3.6. PNEUMATIC SENSORS

Another method that can be used to determine the amount of fluid in a closed tank is to first measure the volume of the gas above the fluid, and then subtract this volume from the total volume of the tank. This approach is often referred to as pneumatic sensing. Three distinct techniques have been developed which take advantage of the ideal gas law to measure the volume of gas in the tank [53, 54, 55, 56, 57, 58, 59, 60, 61, 62, 63, 64].

The first method was developed in Japan [53, 54, 55]. The idea is to have two separate chambers, one of a known volume, and a second of unknown volume. The first chamber is illustrated in *Figure 3.10* as the smaller chamber contained within the tank. The second chamber is the air space inside the tank above the fluid. Both chambers are connected through a small hole which allows the gas quality to equalize between the two.

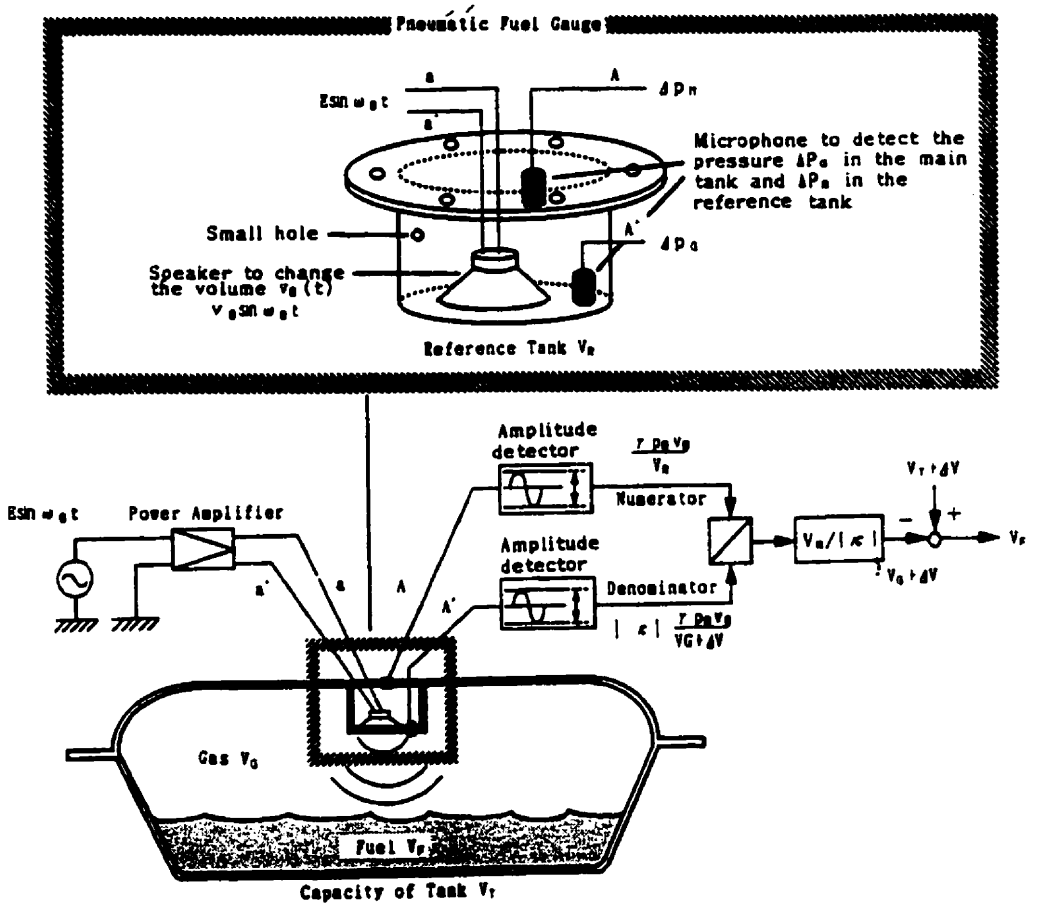

Figure 3.10: Pneumatic volume sensing [53].

A diaphragm is located in the wall shared by both chambers (a speaker in this case) which can be used to displace the air and cause a pressure change. There are also two microphones which can detect changes in pressure in each chamber caused by the diaphragm. The diaphragm is driven by a sine wave generator at a frequency which is matched experimentally

to the tank. The driving frequency is critical because certain frequencies can lead to standing waves inside the tank that will cause erroneous results.

By using the ideal gas law, and more specifically Boyle's law, the change in pressure caused by the diaphragm can be used to deduce the volume of the gas chamber above the fluid since the volume of the smaller chamber is already known. By subtracting the amount of gas from the total volume of the tank, it is possible to calculate the amount of liquid inside the tank.

Some features that are significant with this method are as follows:

- The optimal driving frequency of the diaphragm is dependant on the tank geometry.
- The calibration of the system is also dependant on the tank shape. This means that a new calibration curve must be develop experimentally for each new tank design.
- The use of pneumatic sensing means that the attitude (tilt) of the tank has no effect on the output. In addition, slosh inside the tank has little effect on the readings from the sensor.
- The use of two microphones compensates automatically for changes in the quality of the gas due to temperature and/or pressure changes.

This method has been implemented successfully into a gasoline vehicle, but only experimentally. No evidence was found that this sensor has yet been used commercially. For this reason, the long term robustness of this sensor is at this time unknown.

A second pneumatic method uses a principle known as the Helmholtz resonator [56, 57, 58, 59, 60, 61, 62]. A Helmholtz resonator is an acoustic equivalent of a simple mass and spring

system. It consists of a closed chamber with a tube attached to it through an opening (see *Figure 3.11*). The volume of air inside this tube is considered to be a mass, whereas the air inside the chamber is considered to be a spring. If the air volume inside the tube is excited using piston or a diaphragm, it is possible to cause the chamber to resonate with the same frequency as an equivalent mass-spring system.

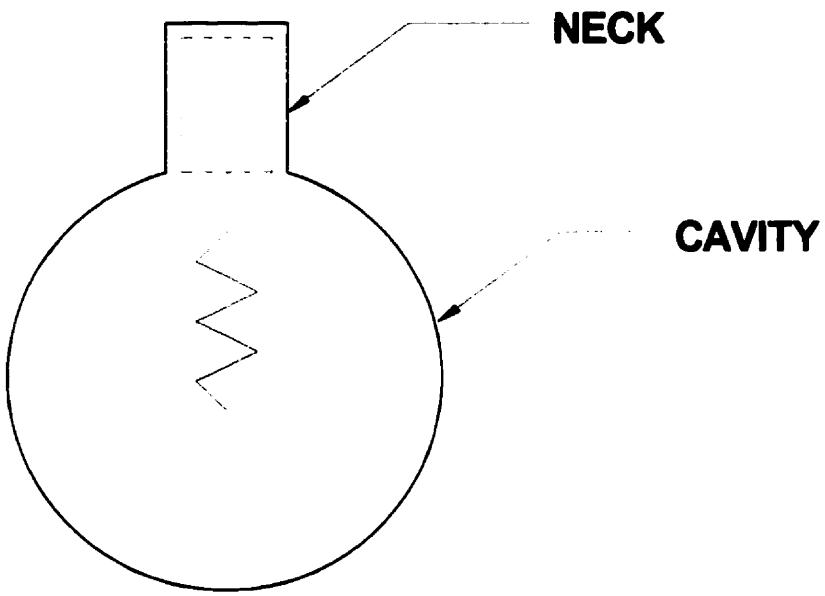

Figure 3.11: Helmholtz resonator.

Since the equivalent spring constant of the air inside the chamber is directly dependent on its volume, the Helmholtz frequency of the system is also dependent on the volume of air. Knowing this, it is possible to determine how much fluid is inside the chamber by measuring the natural frequency of the system. This can be done using a piston or diaphragm to excite the air, and a microphone to measure the response.

A third pneumatic measuring method involves using the fuel tank leakage detection system that already exists in many vehicles [63, 64]. The idea is to use the vacuum present in the engine manifold to create a change in pressure within the tank. The time that it takes to

change the internal pressure in the tank by a known amount is measured, while the gas is evacuated at a known flow rate. Having this information, it is then possible to calculate the volume of the gas inside the tank by using Boyles's law.

There is little information regarding this technology. Robert Bosch GmbH produced a prototype and holds a patent for a device that works on this principle [63]. The main concern with respect to its applicability to propane tanks is the high pressures that exist inside the tank.

CHAPTER 4 SELECTION OF A FEASABLE FUEL SENSING METHODOLOGY FOR THE PROPANE ENVIRONMENT

The next phase in this thesis consisted on using the information in chapters 1, 2 and 3 as the basis for the selection of a feasible fuel level sensing method suitable for propane tanks. As a first step in making this selection, the following functional requirements were chosen as critical for this application:

- Safety
- Longevity
- Linearity
- Accuracy
- Stability

Meeting requirements for linearity is not a difficult issue since on-board computers can be used to compensate for this problem. Furthermore, safety and longevity can be achieved with proper design and material selection. However, the requirements of accuracy and stability can only be met if the proper sensing method is used. From all the technologies described in chapters 2 and 3, three possible sensing methods can be extracted:

The first consists of point level sensing, which simply measures the depth of the fluid at particular point in the tank. It is important to point out that most of the technologies discussed in chapters 2 and 3 are simply alternative methods of doing this. The signals generated by these sensors generally add no information as compared to simple float sensors, although certain techniques may be better suited for particular environments and applications. Still, as was discussed in chapter 1, single point level sensors are incapable of providing enough information to compensate for the motion of the fuel in the tank of a vehicle.

The second method combines several level sensors to overcome this limitation. This in turn can be used to calculate the volume of fuel more accurately. Published information shows the improvement in the quality of the level readings if multiple sensors are used [4]. However, as was discussed in chapter 1, even multiple sensors are not able to compensate for severe fuel slosh in the tank.

The last method available consists of pneumatic sensing. To date, this technology has not been applied commercially, but published studies show the potential improvements that this technique can bring to in-vehicle fuel level sensing [53, 54, 55]. In particular, it has been shown that pneumatic methods are insensitive to most inaccuracies created by the motion of the fuel in the tank.

After careful consideration of these options, it became clear that the first method is unable to give accurate and stable readings in all circumstances. And even though the second method has shown better potential, this technology has been thoroughly investigated for many years and further research will not overcome its basic limitations.

Based on this, a decision was reached to pursue a pneumatic based method for this project. This decision was made based on the fact that pneumatic methods offer the greatest potential to fulfill all the functional requirements. In addition, this sensing technique has not been studied in as much detail as conventional level sensing methods, which provides more leeway for meaningful research.

CHAPTER 5 APPROACH AND METHODOLOGY

5.1. VOLUME MEASUREMENT

As was described in chapter 4, the approach chosen to develop a new propane fuel level sensor was the pneumatic principle. Using this approach, the quantity that is actually being measured is the volume of gas or vapor present in the tank. Since it is assumed that the tank is of fixed volume, the volume of liquid can be easily inferred by subtracting the volume of gas from the total volume of the tank. Of the different pneumatic methods described in section 3.6, the Helmholtz principle was chosen because it requires the simplest instrumentation.

5.2. THE HELMHOLTZ RESONATOR

A Helmholtz resonator is an acoustic equivalent of a simple spring-mass system [65]. As such, it shares some of the same characteristics of its mechanical equivalent, such as inertia, damping, and resonance. The actual Helmholtz resonator consists of a closed cavity that has rigid walls and a single opening (see *Figure 5.1*). On this opening is a neck connecting the interior of the cavity to the outside. For the purpose of modeling the resonator, the gas trapped inside the neck is considered to be a solid, incompressible block or mass which can move in and out. In contrast, the gas inside the cavity is considered to be a compressible gas which behaves like a spring when compressed. The viscous losses caused by the movement of gas in the neck, in addition to acoustic emanations from the mouth also add a damping element to the system [65].

Just as in a mechanical spring-mass system, if the mass in the neck of the resonator is somehow excited, there will be a given frequency where resonance will occur. This resonance (known as the Helmholtz resonance) will depend on the effective mass M of the gas trapped in the neck, and the effective stiffness K of the gas inside the cavity which acts as the spring (see *Figure 5.1*). Since the stiffness of the gas in the cavity is directly related to its volume, the resonant frequency of the resonator will depend directly on the volume of gas present in the cavity.

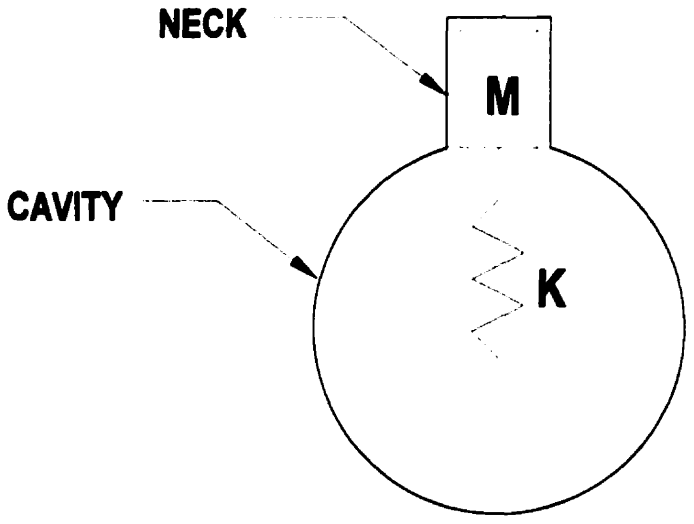

Figure 5.1: Idealized Helmholtz resonator.

This principle may be used to measure the amount of fluid stored in a tank by measuring the Helmholtz frequency of the tank for a given volume of fuel. This resonant frequency may then be related to a calculated or a previously known volume of gas. The volume of fuel may then be deduced from the total capacity of the tank (Note that this method will only work for liquefied fuels). One of the main attractions of this method is that the quantity being measured is only affected by the volume of the gas chamber, regardless of its shape [66]. Therefore, unlike typical fuel level sensing methods, the attitude of the tank, or even sloshing of the fuel inside the tank should have a negligible effect on the measurements.

5.3. THE HELMHOLTZ MODEL

The theory of the Helmholtz resonator has been extensively studied for well over a century. Helmholtz himself first modeled the system and developed equations describing its behavior [67]. However, since that time, it has become apparent that the original model has many limitations. Repeatedly, authors have reported discrepancies between calculated and experimental frequency values [67, 68, 69].

A Helmholtz resonator is usually described by an equation of the form [65]:

$$F = M\frac{d^2x}{dt^2} + R_r\frac{dx}{dt} + Kx \tag{5.3-1}$$

where F is the driving force, M is the effective mass of the resonator, R_r is the radiation resistance, K is the effective stiffness, and x is the displacement of the air plug in the neck. Note that this equation is analogous to a mechanical mass-spring-damper system with external excitation such as is depicted in *Figure 5.2*.

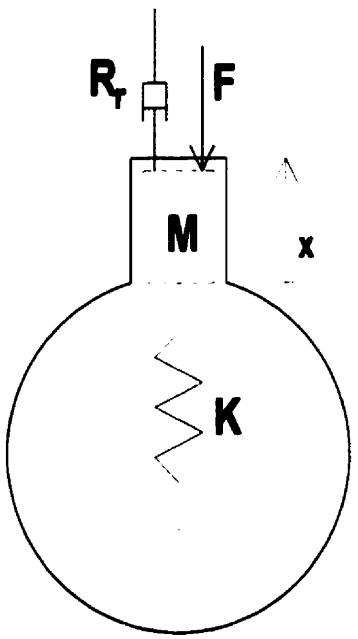

Figure 5.2: Helmholtz resonator with damping and external excitation.

The effective mass M refers to the mass of the air plug inside the neck of the resonator and may be calculated as follows [65]:

$$M = \rho_o S L' \tag{5.3-2}$$

where ρ_o is the density of the gas in the chamber, S is the cross sectional area of the neck, and L' is the effective length of the neck. The effective length of the neck is longer than the actual length of the neck because of radiation resistance at each end of the tube [65]. This means that a correction factor must be added to account for air surrounding the openings on both ends of the neck [56, 65]. For a round opening, this correction is usually $0.61R$, where R is the radius of the opening [56]. Since the neck has two open ends, the total correction is $1.22R$, meaning that the effective length L' of the air plug is:

$$L' = L + 1.22R \tag{5.3-3}$$

The radiation resistance R_r depends on whether the ends of the neck are flanged or not (see *Figure 5.3*).

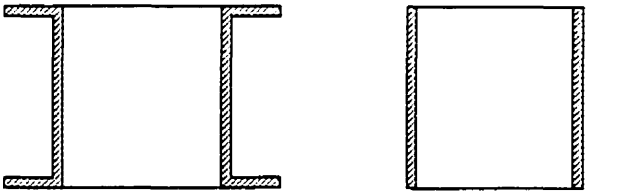

Figure 5.3: Difference between flanged and unflanged pipes.

Assuming that the wavelength of the excitation source is much larger than the radius of the neck R, the radiation resistance at the neck is given by [65]:

$$R_r = \rho_o c \frac{k^2 S^2}{2\pi} \qquad \text{for a flanged pipe, or} \tag{5.3-4}$$

$$R_r = \rho_o c \frac{k^2 S^2}{4\pi} \quad \text{for an unflanged pipe.} \tag{5.3-5}$$

Where c is the speed of sound in the gaseous medium and k is the ratio of specific heats.

The effective stiffness K of the system may be found by considering the pressure increase in the cavity for a given displacement x of the air in the neck (assuming that the displacement of the air is uniform across its cross section). The effective stiffness for a resonator with an open ended pipe is given by [56, 65]:

$$K = \rho_o c^2 \frac{S^2}{V} \tag{5.3-6}$$

where V is the volume of the cavity.

In equation (5.3-1) it is assumed that a harmonic driver is used to excite the system. The force F that this driver exerts on the system is a function of the cross sectional area S of the neck and the amplitude A of the incoming acoustic wave [65]:

$$F = SAe^{j\omega t} \tag{5.3-7}$$

The resonant frequency ω_o can be found from equation (5.3-1) and is given by [65]:

$$\omega_o = c\sqrt{\frac{S}{L'V}} \tag{5.3-8}$$

Note that the resonant frequency is dependent upon the inverse of the square root of the volume of the cavity.

5.4. Correlation Between Theory and Practice

At first sight, the equations just described seem to give the basis upon which to build a Helmholtz resonator. It should be possible to use equation (5.3-8) to determine the dimensions of the system in order to obtain a given desired response. Nevertheless, applying this theory into practice faces several obstacles. For instance, experience by many researchers has shown that the correlation between the predicted resonant frequency of a resonator and the volume of the cavity is not always reflected by experimental values [63, 68, 69]. Also, choosing a desirable frequency range is very difficult because this range must take into account environmental disturbances and the limitations of the existing equipment. In addition, other acoustical resonating modes not described by these equations may appear in the system and interfere with the spring-mass resonant mode.

With respect to the accuracy of the models, one source of error that is often discussed is the correction used to account for the radiation resistance on both open ends of the neck. The correction of 1.22 cited previously is a number given by a particular author, despite the fact that other numbers are also quoted. For instance, Kinsler and Frey consider this correction to be 1.7 for flanged openings, and 1.2 for unflanged openings [66]. Other authors such as Troke and Ingard consider this correction to be a function of the diameter of the neck [68, 70].

Another important source of error is the excitation source. A jet of air flowing over the top of the neck is often used to excite these resonators in laboratory experiments. The principle is the same as is used to drive many musical instruments, such as organ pipes. Nonetheless, the

stream of air from the jet may hit the opposite side of the neck creating edge effect resonant modes that may interfere with the spring-mass resonant mode [69].

Speakers are also commonly used as excitation sources by hermetically coupling them to the mouth of the resonator. Locating a speaker in the mouth means that the mass of the diaphragm and the coil must be added to the mass of the gas in the neck in order to find the total effective mass of the system [65]. The stiffness of the speaker cone must also be combined with the stiffness of the air in the cavity in order to find the total stiffness of the system. In addition, the effective length L' used to calculate the mass of the air plug inside the neck is affected by the presence of the speaker. The presence of the speaker will generally cause a net reduction in the effective length L'.

Another example of the limitations of the original model was given by Troke [68]. In his study, he extended the model developed by Helmholtz to include the viscous effects on the walls of the neck by using the boundary layer theory developed in the field of aircraft design. The correction made to his model seems to correlate better to his experimental results. However, all his experiments were done using small resonators (with dimensions less than about 50 cm.), and therefore the effectiveness of this model in larger resonators remains unproven.

Troke remodeled the system by making the assumption that a static layer of air always exists near the walls of the neck [68]. He also assumed that the viscous forces were larger away from the center of the neck. He then developed a model where the effective mass of air in the neck is smaller due to these effects. From this he developed the following equation:

$$\omega_o = c\frac{D}{\sqrt{(L+D)V}} \tag{5.4-1}$$

where D corresponds to the diameter of the neck. Note that this equation shows the same relationship between frequency and volume as equation (5.3-8).

5.5. Regression Analysis of the Models

Despite their differences, equations (5.3-8) and (5.4-1) show that the resonant frequency of a Helmholtz resonator is inversely proportional to the square root of the air volume in the chamber:

$$\omega_o \propto \frac{1}{\sqrt{V}} \tag{5.5-1}$$

Therefore, there must exist a constant of proportionality C such that:

$$\omega_o = CV^{-\frac{1}{2}} \tag{5.5-2}$$

This equation can be linearized by taking the natural logarithm on both sides:

$$\ln\omega_o = \ln C - \tfrac{1}{2}\ln V \tag{5.5-3}$$

Therefore, a plot of $\ln\omega_o$ vs. $\ln V$ will have a slope of -0.5, and intercept the vertical axis at $\ln C$. Equation (5.5-3) may be used to predict volume changes in a storage tank by measuring the resonant frequency as long as the constant C is known. This constant could be calculated from theory, or could be determined experimentally.

5.6. Acoustic Considerations

Equation (5.3-8) shows that the spring-mass resonant mode of a cavity is not dependent on its actual shape, but only on its volume. However, the shape of the cavity may have an effect on the emanation of other overtones which may have an effect on the spring-mass resonance

[65]. In order to understand the types of overtones that may occur, it is necessary to separate the system into its three main components: the neck, the cavity, and the excitation source.

The neck may be treated as an open ended pipe which is susceptible to one, two, or three dimensional standing waves along its length or across its diameter. Standing waves may occur as the wavelength of the excitation source reaches the same order as the dimensions of the pipe. The fundamental acoustical mode seen in these pipes is usually a quarter wave resonance mode along the length of the pipe. This fundamental is accompanied by evenly spaced higher order overtones. Other standing wave modes are also possible across the diameter of the pipe if this dimension is suitably matched to the wavelength.

The fundamental quarter wave resonance and all the overtones of an open ended tube may be found using the equation [68]:

$$f_n = n\left(\frac{c}{4L}\right) \tag{5.6-1}$$

Where n = 1 corresponds to the fundamental and n = 2,3,4,... corresponds to its overtones. Note that the quarter wave resonant frequency will drop with increasing neck length. Also, since the wavelength is a function of the speed of sound and the frequency, this equation is in effect just a relation between the wavelength and the length of the neck.

The fundamental of the quarter wave resonating mode generally occurs at a higher frequency than the Helmholtz mode [66]. However, it is possible to build a resonator where the Helmholtz mode closely matches one of the lower overtones in the neck. This can be very problematic if the system is to be used to measure volume, since the interaction between the

different modes may cause erratic and unpredictable behavior. Research conducted by Khosropour and Millet shows the effect of edge tone frequencies generated at the neck which pull the Helmholtz frequency in different directions as the velocity of the excitation source (in this case a jet of air) is increased [69]. This demonstrates the importance of keeping the different resonant modes far enough apart so that they do not interfere with one another.

Just as in the neck, the main cavity of a Helmholtz resonator may also develop standing waves [65]. For this reason, the geometry of the cavity and the relation between the dimensions of the cavity and the wavelength of the excitation source become critical. In automotive fuel tank design, this is particularly problematic, since the geometric design of the tank evolves around available space rather than acoustic considerations.

The choice of excitation source is also very important because of its interaction with the system. As was already mentioned, it is often common to use a jet of air flowing over the mouth of the resonator as a source of excitation. However, as research done by as Khosropour and Millet has shown, this source of excitation produces edge tone vibrations that affect the spring-mass resonance of the system [69]. As an alternative, acoustical excitation can be produced using audio speakers. Speakers are useful because they can be controlled so that they emit only one frequency. However, as was already discussed, their presence in the neck affects the total effective mass and total effective stiffness of the resonator. In the extreme case, a speaker with very high acoustical impedance may dominate the acoustical vibrations of the resonator, masking the spring-mass resonant mode. In addition, speakers have their own resonant mode which usually falls within the typical

Helmholtz regime. This resonance may also have an effect on the behavior of the spring-mass resonant mode.

In order to keep the different modes of vibration separate from one another, it is important to keep in mind that there are only a few design parameters available for this purpose. These include the dimensions of the neck, the dimensions and the shape of the tank, and the type of excitation source. Therefore, the ability to use the Helmholtz principle to measure volume relies heavily on the optimization of these parameters so that a useful frequency range becomes available.

5.7. Temperature and Humidity

As equation (5.3-8) shows, the resonant frequency of a Helmholtz resonator depends directly on the speed of sound. As a result, a further cause for concern are any changes to the properties of the medium that will have an effect on the speed of sound. Two particular properties of concern are the temperature and composition of the gas inside the resonator [44].

In the case of propane powered vehicles, changes in temperature is a very critical issue since these vehicles are expected to operate within a wide range of environments. In addition, variability in the quality, purity, and pressure of the fuel within different locations will add extra uncertainty to the system.

Compensation for this type of variability can generally be done in two different ways. The first is to measure the physical quantities that are affecting the accuracy of the readings, such

as the temperature, pressure, and humidity of the vapor inside the tank. These data can be used to automatically compensate the readings from the Helmholtz sensor by using known equations. Although this method may seem the most logical solution at first, it has two serious drawbacks. First, it requires multiple sensors which makes it complex and costly. And second, it usually does not account for all the factors affecting the final result making its accuracy limited.

The second method consists of directly measuring the affected factor, which in this case is the speed of sound. This method takes into account all the factors that affect the speed of sound without having to measure any of them individually. Nevertheless, measuring the speed of sound is a challenging issue in itself which requires special instrumentation [44].

CHAPTER 6 EXPERIMENTAL PROCEDURE

A series of experiments were performed in order to demonstrate the feasibility of using the Helmholtz principle as a fuel level sensing technology for automotive applications. The purpose of these experiments was to develop a proof of concept model for the chosen method. They also provided an opportunity to confirm the accuracy of the results obtained through the theory and to learn about the severity of some of the problems described in chapter 5.

The approach used to evaluate the acoustical response of the experimental resonators is discussed in this chapter. The equipment used for this purpose is also described. The results obtained during the experimental phase are presented and analyzed in later chapters.

6.1. Signal Generation and Acquisition

Several experimental resonators were used in order to compare the response obtained through the theoretical models against the actual response. The excitation and measurement of the response were done using two different approaches. The first was to excite the cavity using random and uniform white noise while measuring the total response over a given frequency spectrum [69]. The second was to excite the cavity at discrete frequencies and to measure the response at those frequencies only [56, 57, 58, 59, 60, 61, 62].

6.1.1. White Noise Generation Method

Using white noise to excite the resonator is very useful as an exploratory technique because it makes it possible to measure the response of the resonator over a wide range of frequencies at

once. This approach gives a quick snapshot of the response of the system. Computationally, it is very simple and fast, which is an attraction for any type of software that may be used in an automotive computer.

In terms of equipment, all that is necessary is a generator of uniform white noise to excite the resonator over a wide range of frequencies. The response can be measured with a computer which monitors the pressure fluctuations in the cavity through a microphone. This time domain signal is converted by the computer into the frequency domain by using a Fast Fourier Transform (FFT). Any resonant frequencies can be identified as spikes in the FFT plot. The computer also allows the data to be stored for later analysis.

One of the shortcomings of this method is that, by its own nature, a lot of noise is added to the signal This often makes it difficult to distinguish the resonant peaks. The accuracy of the results are also dependent upon which frequencies are actually excited. This will vary since the random nature of the excitation does not guarantee that any particular frequencies will be generated.

Figure 6.1 shows an example of an FFT obtained from a Helmholtz resonator excited using random white noise. It is clear that there is one frequency (430Hz) which is more prominent and which corresponds to the spring-mass resonant mode of the system. However, it is also clear that other peaks also appear corresponding to other resonant modes. In practice, the response obtained through this method is not always as clear as is shown in *Figure 6.1*, making it difficult sometimes to determine the resonant frequency of the system.

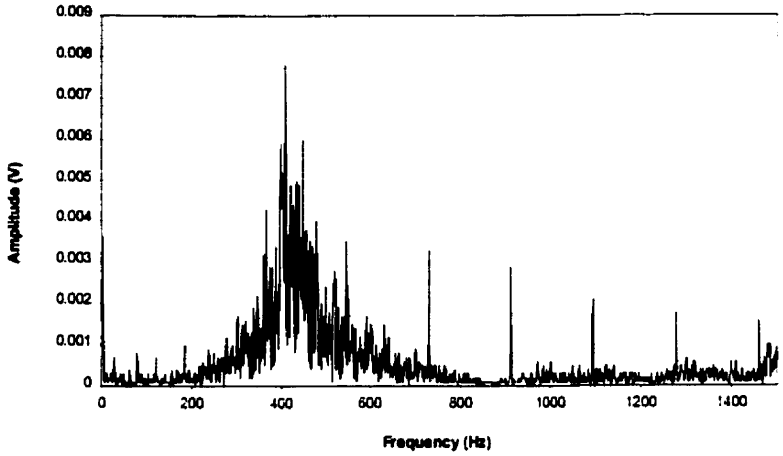

Figure 6.1: Response of a Helmholtz resonator to uniform white noise.

6.1.2. Frequency Sweep Method

Another approach is to excite the resonator at discrete frequencies over a desired band and to measure the response at each of these frequencies. The equipment that is needed for this is a controllable excitation source, a microphone, and a control unit for system synchronization, signal acquisition, and data processing.

A frequency sweep begins by exciting the system at the initial frequency of the chosen scan band. After a short delay which allows the system to settle (typically in the order of milliseconds), the signal acquisition begins. A sample of data is then collected at the excitation frequency and transformed from the time domain into the frequency domain by using an FFT. After the data have been collected, the system moves to the next frequency in the spectrum and repeats the same signal generation and acquisition. This process is repeated until the desired frequency band is exhausted. From each frequency that is tested, it is then possible to extract the amplitude of response of the system at that given frequency. By plotting all the individual resonating amplitudes against their corresponding frequencies, it is possible to see the response of the system over a desired frequency range.

The need to excite and sample at each individual frequency makes this method inherently slow and computationally demanding. However, this approach provides a much more accurate picture of the acoustical response of the system than can be obtained using a white noise generator. One reason is that each frequency is excited individually, thus making sure that the entire spectrum is covered. In addition, the discrete nature of this method allows three quantities to be measured:

6.1.2.1. Amplitude Response

The amplitude of the pressure fluctuations in the cavity can be measured by using a microphone. It is known from theory that the amplitude of the acoustic pressure in the resonator will reach a maximum at resonance [65]. Therefore, the resonant frequency can be found by keeping track of the amplitude of the response at each excitation frequency during the frequency sweep. The resonant frequency will be that where the amplitude reaches a maximum. *Figure 6.2* illustrates the response of a resonator with a resonant frequency of 185Hz.

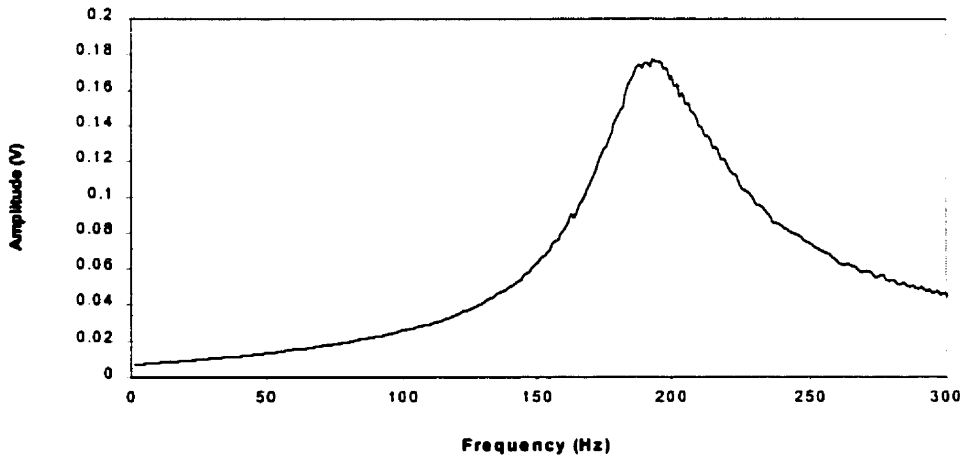

Figure 6.2: Amplitude response obtained using the frequency sweep method.

6.1.2.2. Phase Response

Another measure that can be used to infer the resonant point is a shift in phase between the driving signal and the response of the resonator [58, 59, 61, 62]. The phase difference between these two signals will be 90 degrees at the resonant point. A practical method to determine if the phase difference reaches 90 degrees is to consider the signal sent to the speaker and the signal received from the microphone as phasors. Since it is known that the dot product between two vectors is zero when they differ by ninety degrees, the dot product of these two phasors should also be zero when they differ by ninety degrees. Therefore if the dot product between the signal sent to the speaker and the signal received by the microphone is plotted at each frequency during the sweep, the resonant point will be identifiable where the plot crosses the zero line. During routine observations, it becomes clear that the plot of the phase differential may cross this line many times; however, the only crossing that is of interest is that which corresponds to the maximum amplitude measured in the microphone.

The purpose of measuring both the amplitude and the phase differential is to provide a means to distinguish different peaks in the amplitude plot that may otherwise appear to be resonant points. *Figure 6.3* shows a plot of the phase shift for a resonator passing through its resonant point. Note that this resonant point corresponds to the maximum amplitude recorded in *Figure 6.2* at 185Hz for the same resonator.

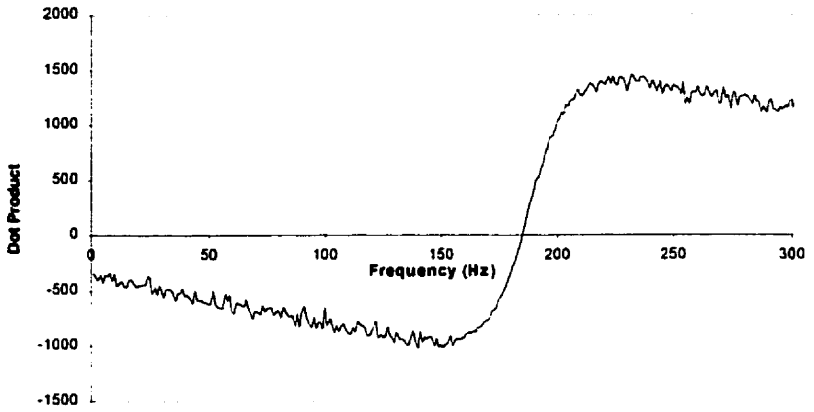

Figure 6.3: Phase shift between speaker and microphone.

6.1.2.3. Impedance Response

An alternative technique that was successfully tested during the experiments is to measure the impedance of the speaker, which reaches a minimum at resonance [56]. The impedance response can be inferred from changes in the current drawn by the speaker, which will reach a maximum when its electrical impedance reaches a minimum. This current may in turn be measured by placing a low resistance shunt in series with the speaker, and by measuring the voltage across the shunt. This voltage will drop to a minimum when the system reaches resonance.

A frequency sweep can be performed while measuring the voltage across the shunt at each individual frequency. This voltage will drop to a minimum when the system reaches its resonant point. This point will in turn correspond to the maximum amplitude measured in the microphone response, and to the phase transition point between the microphone and the speaker. *Figure 6.4* shows the plot of the shunt voltage corresponding to the resonator discussed in sections 6.1.2.1 and 6.1.2.2 which has a resonant frequency of 185Hz.

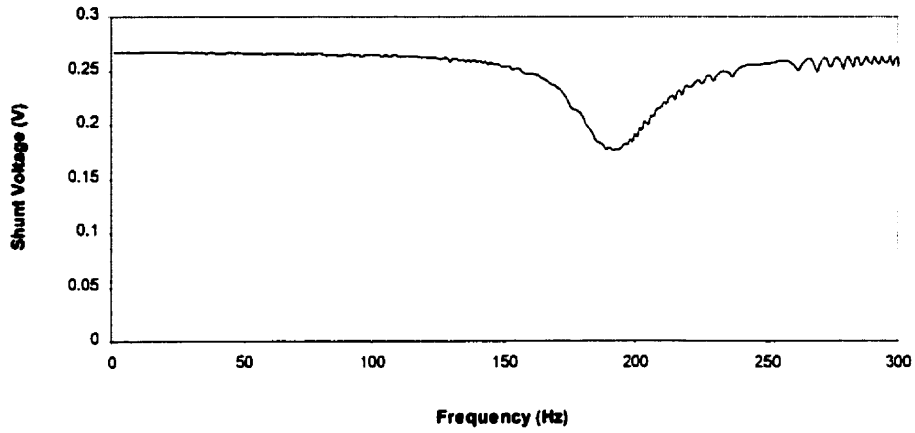

Figure 6.4: Impedance response obtained using the frequency sweep method.

6.2. INSTRUMENTATION

The instrumentation used for the experimental section of this project was built around a computer based data acquisition and control board. A very important part in the selection of the instrumentation was a recognition of the types of signals that needed to be generated and collected. Due to the nature of the project, it was known in advance that the system needed to be able to process data in the frequency domain. Using the theory and existing literature, it was also known that the frequencies of interest would likely lie in the range between 0 and 2000Hz. In order to meet these requirements, the equipment components that were used during the experimental phase of this project included a microphone, several speakers, and a computer. They are described below.

6.2.1. MICROPHONE

In order to measure pressure fluctuations inside the resonator, a Bruel & Kjaer condenser microphone Model 4176 was used. This microphone has a resonant frequency of 12.5kHz,

and a good free field response below 1000Hz [71]. In addition, the microphone cartridge is made of corrosion resistant materials that make it ideal for this application.

The microphone was driven by a Bruel & Kjaer power supply Model 2804. This battery driven power supply provides the proper excitation voltage for the microphone, as well as some amplification.

6.2.2. SPEAKER

As was mentioned before, audio speakers were used during the experimental phase of this project in order to provide a source of acoustical excitation. Speakers were preferred over air jets because of their ease of implementation, their controllability, and their relatively low cost. Furthermore, the experimental work performed for this thesis did not require the use of fuel in order to verify the relationship between frequency and volume. Instead, water was used which, in addition to the fact that durability was not a concern, made it possible to use ordinary speakers designed for home use.

The main concern in the selection of suitable speakers for the experiments was their frequency response. An ideal speaker was considered to have a constant amplitude at all frequencies. In practice however, this is not possible due to the characteristics of the speakers themselves. All speakers have a resonant frequency where the amplitude of their output reaches a maximum. This frequency normally falls somewhere within the typical Helmholtz range (below 1000Hz). Therefore, prior to using any speaker, it was necessary to record its resonant frequency so that its effect could be taken into account on the overall

performance of the resonator. The actual responses recorded for the different speakers used during the experiments are shown in chapter 7.

In addition to the resonant frequency of the speaker, some devices added to the driving circuit were also found to have an effect on the amplitude of the output. For instance, if an amplifier is used to drive the speaker, the amplifier electronics may filter out a part of the spectrum, thus affecting the output in this range. Therefore, all the electronics added to the circuit must be checked in order to ensure that they do not interfere with the proper excitation of the speaker at the desired frequency ranges.

Figure 6.5 shows the combined effect of the resonance of the speaker and an amplifier that filters the signal in the lower spectrum. These readings were taken by exciting the speaker in free air, while mounted on a soft surface. The shunt voltage readings show the electrical impedance response of the speaker, whereas the microphone readings show the amplitude of the output acoustical signal. The impedance response shows that the amplitude of the driving voltage increases only gradually in the lower frequency range as a result of the electronics in the amplifier. In addition, the resonant point corresponding to the speaker is recorded at 110Hz. It is clear from this figure that the characteristics of the excitation source must be controlled carefully in order to prevent unwanted effects from affecting the Helmholtz response of the system.

6.2.3. COMPUTER

A PC computer was used in order to integrate the data measurement and data analysis. This computer consisted of a Pentium 200, with 16Mb of RAM, and 2Gb of hard drive space. The

operating system used was Windows 95. The computer was outfitted with a data acquisition board and the required software in order to perform signal control and analysis.

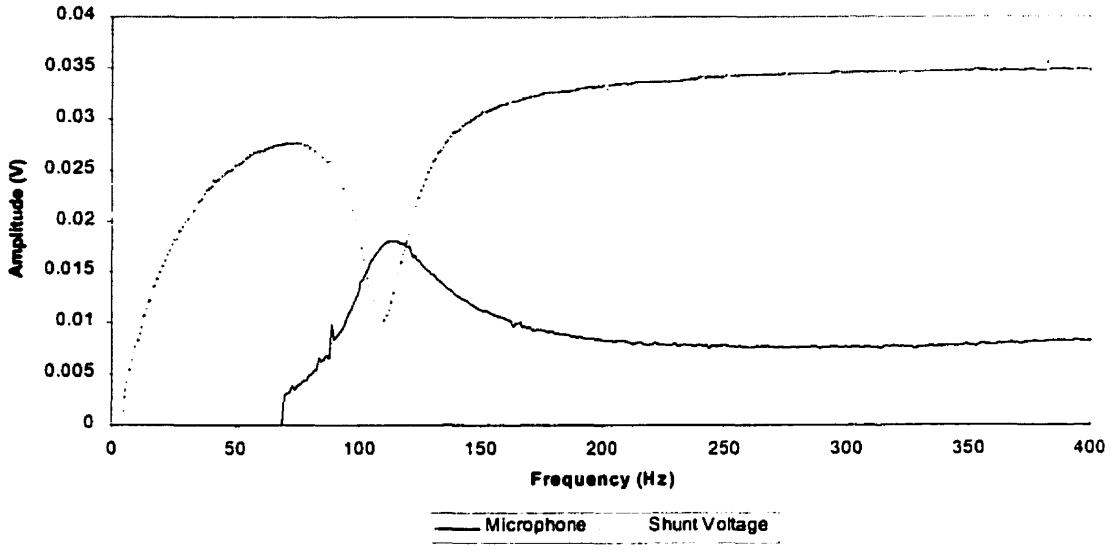

Figure 6.5: Combined frequency response of amplifier and speaker.

6.2.3.1. Data Acquisition Board

The signal generation and acquisition was achieved using a National Instruments data acquisition board, Model AT MIO 16 E10. A National Instruments SCB-68 connector block and cable were used to interface with the instrumentation. This connector block has a built in cold junction compensation sensor that allows the board to use thermocouples for temperature sensing. The board has 16 channels of analog input with internal multiplexing and buffering. The maximum acquisition rate is 100kHz distributed over all the active channels. Two analog output channels are also available with an output voltage range of +/- 10V. The maximum output sampling rate is also 100kHz distributed over the two output channels.

6.2.3.2. Software

Two programs were written using the LabVIEW programming language, version 5.0. The control panel of the first program is shown in *Appendix I.* This program is capable of controlling a speaker and outputting a signal consisting of random white noise. As the signal is sent to the speaker, the program monitors the response of the resonator through the microphone. The computer takes a sample of the response, processes the signal, and finally displays it on the screen. The signal processing includes a Hanning window to reduce spectral leakage, and an FFT which converts the signal from the time domain to the frequency domain.

As can be seen in *Figure 6.1*, the white noise generation method provides a very simplistic look at the collected data. The displayed data can also be difficult to interpret due to excessive noise, or because the frequencies of interest may have not been excited. As a solution to these problems, a second program was created that takes advantage of the frequency sweep method previously described. The control panel of this program is shown in *Appendix II.* This program also provides simultaneous excitation and data acquisition, but it scans one frequency at a time. The screen displays a time record of the amplitude, the impedance, and the phase responses.

6.2.4. Experimental Setup

A detailed wiring diagram of the equipment just described is given in *Figure 6.6.* Note that in this diagram, the speaker used can be easily interchanged according to the needs of each experiment. An amplifier may also be needed to drive larger speakers. If an amplifier is

used, it should be placed between the board and the shunt resistor so that the shunt records the actual current passing through the speaker.

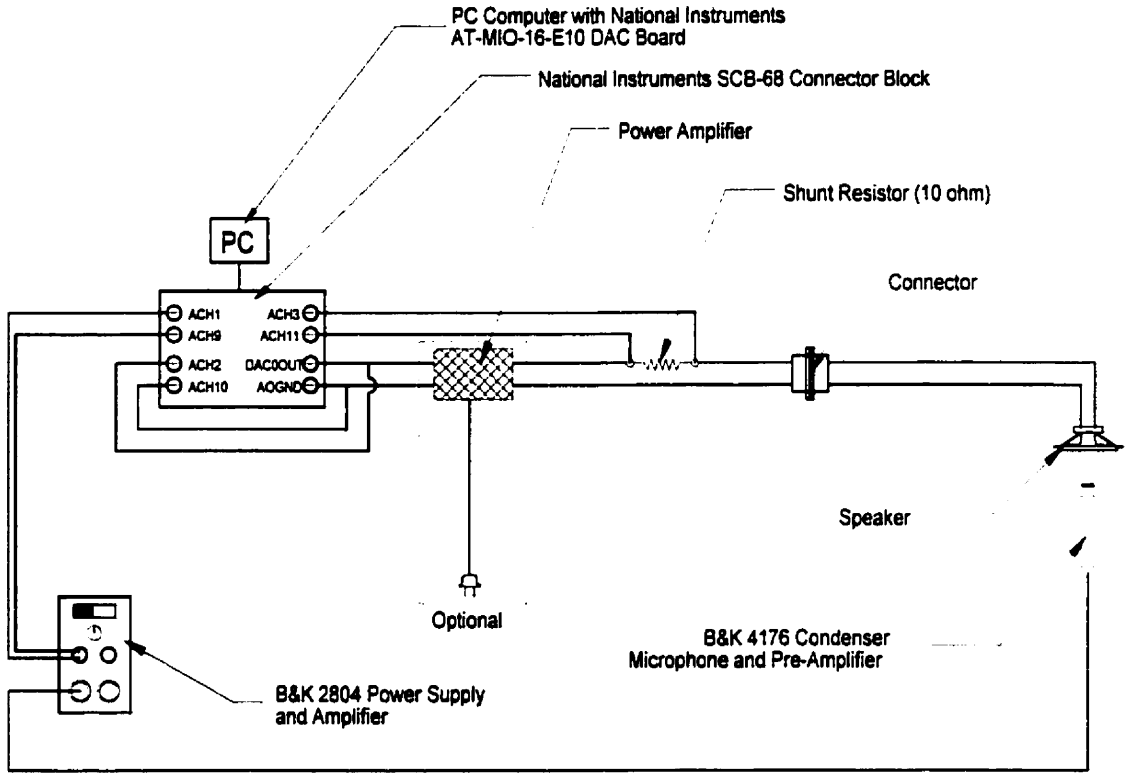

Figure 6.6: Wiring diagram of experimental setup.

A very important issue in the experimental setup is the location of the microphone with respect to the resonator. This location will in turn depend on how the speaker is mounted with respect to the neck. In general, the speaker may either be mounted hermetically onto the neck of the resonator (coupled), or it may be located at a distance away from the mouth (uncoupled).

If the speaker is coupled, not only will the resonator react to the speaker, but the speaker will also react to the resonator. The speaker will control the frequency of the system, but its amplitude of vibration will depend on the amplitude of the response of the resonator. As a

result, the combined system will have only one resonant frequency which will depend on both the Helmholtz frequency and the resonant frequency of the speaker.

For the coupled case, the microphone can be located either near the diaphragm of the speaker or inside the resonator itself. Furthermore, if the housing of the speaker allows access to the diaphragm from the outside, the microphone can be located entirely in the outside of the resonator since the diaphragm will reflect the acoustic response of the entire resonator (see *Figure 6.7*).

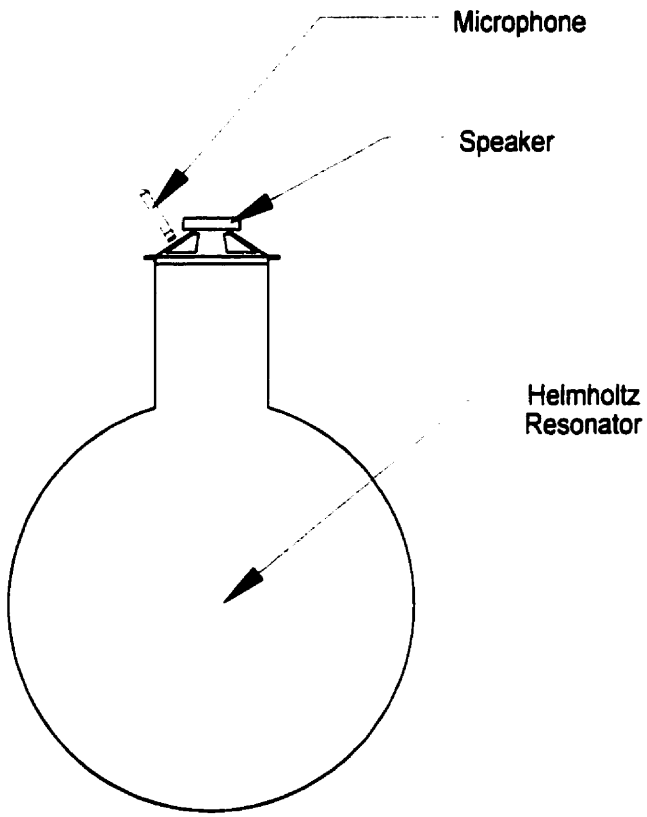

Figure 6.7: Microphone location in coupled resonator.

If the speaker is uncoupled from the resonator, the response of the resonator will have no effect on the response of the speaker. Therefore, the microphone must be mounted inside the

cavity or the neck of the resonator in order to detect its resonance. *Figure 6.8* illustrates this mounting approach.

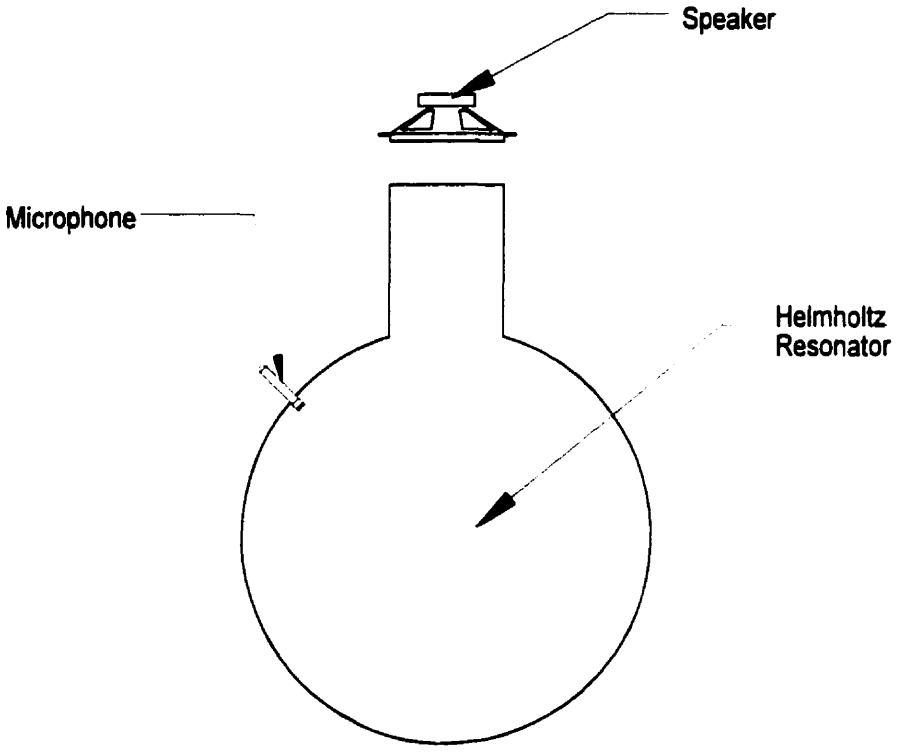

Figure 6.8: Microphone location in uncoupled resonator.

It is important to note that for the first mounting method, the acoustical impedance of the speaker must be low enough so that the Helmholtz resonant mode is detectable at the diaphragm of the speaker. In addition, since the movement of the speaker diaphragm is directly affected by the resonator, impedance changes in the speaker can also be used to detect resonance with the use of a shunt resistor, as was described in section (6.1.2.3). It is very important to point out that this is not the case when the speaker is uncoupled from the resonator. This means that measuring the impedance response of the system is only useful when the speaker and the resonator are coupled.

CHAPTER 7 RESULTS

Background research into the Helmholtz method indicated that the three most important aspects of a resonator are the dimensions of the cavity and neck, the shape of the cavity, and the excitation source [56, 57, 58, 59, 60, 61, 62, 65, 66, 67, 68, 69, 70, 72, 73]. In order to investigate these three elements, five experiments were conducted that explored the behavior of resonators having different dimensions, shapes, and speaker locations. This chapter discusses the results obtained.

7.1. 0.75L GLASS JAR:

The first experiment was set up in order to test the basic relationship between volume and frequency as is given in equation (5.3-8). For this experiment, it was decided to use a small glass jar with a volume capacity of 0.75L. This jar was chosen because of the rigidity of its walls, and because its relatively small dimensions made it less prone to standing wave formation. *Figure 7.1* shows the jar dimensions.

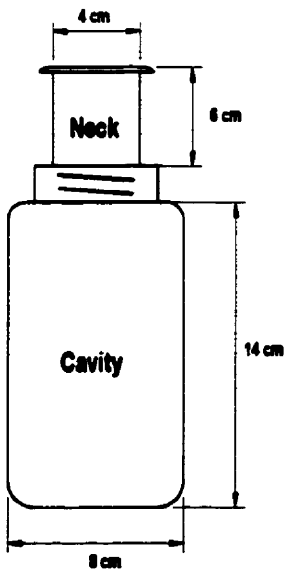

Figure 7.1: Glass jar dimensions.

7.1.1. Performance Prediction

The first step in the process was to calculate the predicted resonant frequency of the jar according to the theory. The resonant frequency of the jar was calculated using two different methods. The first was the commonly accepted equation developed by Helmholtz (Equation (5.3-9)). The second was equation (5.4-1) developed by Troke to include boundary layer effects in the neck.

Prior to applying these equations, it was necessary to adjust the effective length L' to reflect the presence of the speaker at the end of the neck. It was already mentioned in Section 5.3 that the correction commonly used for the Helmholtz model is $1.22R$. For the purpose of the calculations, it was assumed that the speaker diaphragm was essentially flat. As a result, the compensation added to L' was cut in half to $0.61R$ in order to reflect the fact that the neck had no direct interaction with the outside. The same correction was applied to the Troke equation. The results of these calculations are summarized in *Table 7.1*:

Table 7.1: Predicted Helmholtz resonance for glass jar.

Model	Helmholtz	Troke
Equation	$\omega_o = c\sqrt{\frac{S}{L'V}}$	$\omega_o = c\frac{D}{\sqrt{L'V}}$
L'	$L + 0.61R$	$L + R$
c	344 m/s	344 m/s
Predicted Resonance	**285 Hz**	**313 Hz**

As is apparent from these calculations, the results predicted by both methods differ considerably. Nevertheless, it is clear that the resonant frequency of the jar should be expected to lie at a relatively low frequency near 300Hz. Keeping this in mind, it is still important to check that no unwanted resonant modes may occur inside the cavity around this

frequency range. As was previously discussed, unwanted resonant modes can occur in three different places: the cavity, the neck, and the speaker.

The response of the cavity can be verified by calculating the wavelength at the highest predicted frequency by using the following equation [74]:

$$\lambda = \frac{c}{f} \tag{7.1.1-1}$$

Using a frequency of 313Hz and a speed of sound of 344m/s, this equation predicts the wavelength to be 1.09m. Since this is more than six times the largest dimension of the jar, there is little reason to believe that standing waves will form inside the cavity.

The next thing that must be checked is the quarter wave resonant frequency of the neck. This frequency should be high enough so that it does not interfere with the spring mass resonant mode of the resonator. Using equation (5.6-1) with n = 1, this frequency is predicted to be 1433.33Hz, clearly out of the range of concern.

Finally, the speaker response must be obtained experimentally. *Figure 7.2* shows the response of the speaker in free air. This response was achieved by resting the speaker on a soft mount, and by placing the microphone near the diaphragm. This figure shows that the speaker has a resonant point at 415 Hz.

In order to measure the interaction between the neck and the speaker, their combined response was measured in the absence of the cavity of the resonator. *Figure 7.3* shows that the resonant point of the speaker at 415Hz is not affected considerably by the presence of the

neck. Also, no other resonant peaks due to the neck are seen in this frequency range, thus confirming the previous prediction.

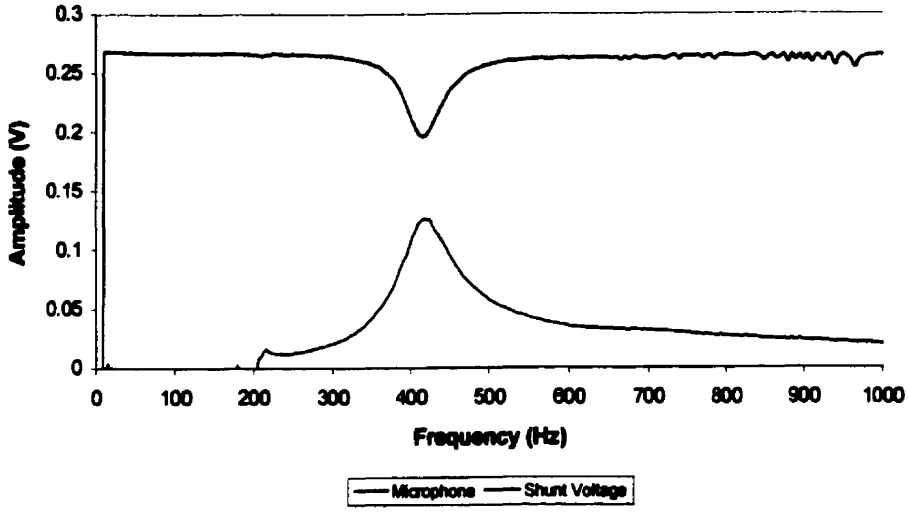

Figure 7.2: Response of speaker without resonator neck.

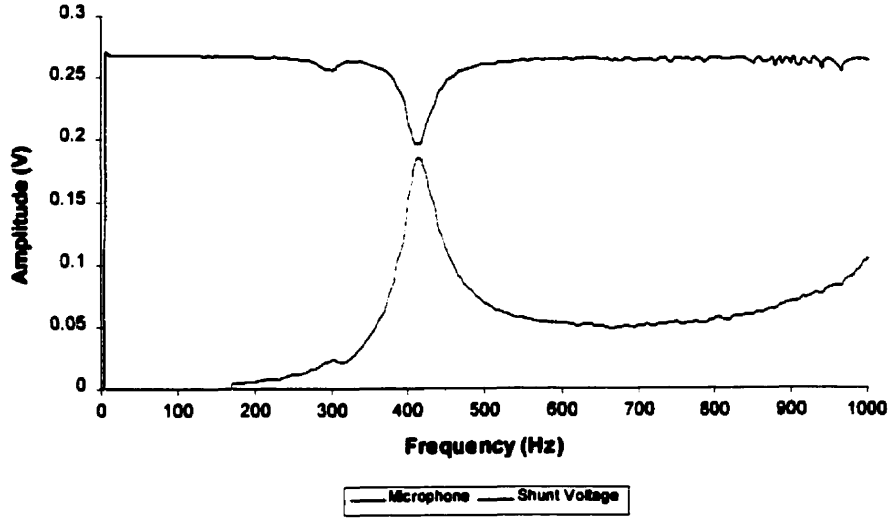

Figure 7.3: Response of speaker with resonator neck.

7.1.2. Experimental Setup

In order to measure the actual response of the resonator, the jar was instrumented with a speaker and a microphone. The experimental setup for this jar is shown in *Figure 7.4*.

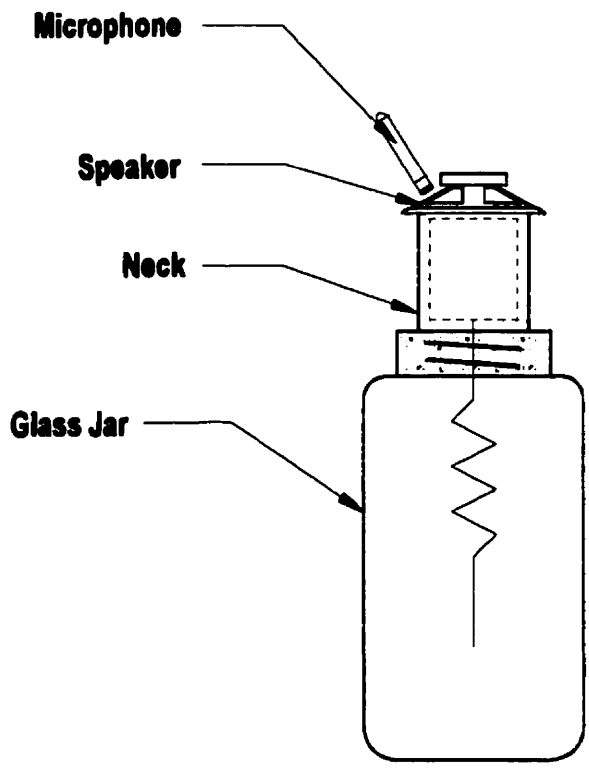

Figure 7.4: Mounting of instrumentation on glass jar.

The speaker was selected from among several choices available because of its low impedance. The diameter of the speaker was 4.5cm, and its rating was given as 0.2Watt and 8Ω. The microphone was mounted externally so that no wiring had to be run into the cavity. This was important because of the difficulty in cutting a hole through the glass. The actual microphone location during the experiments was about 4.0mm away from the speaker cone.

7.1.3. RESULTS

Using the set up shown in *Figure 7.4*, the resonant frequency of the resonator was determined using the frequency sweep method, and by simultaneously monitoring the microphone, the speaker impedance, and the phase differential.

Figure 7.5 shows that the resonant frequency of the speaker and resonator system when empty (0.75L air volume) is 391 Hz. This value is higher than that predicted in *Table 7.1* for the resonator alone, but lower than the resonance measured for the speaker alone. This confirms that there is an interaction between the speaker and the resonator. To investigate this interaction further, the same test was repeated while changing the internal volume of the resonator by adding water to it in 0.118L increments.

Figure 7.5 shows the change in resonant frequency with volume as detected by the microphone. *Figures 7.6* and *7.7* also correlate this effect in terms of impedance response and phase shift. It is clear that the resonant frequency increases with increasing water volume (dropping air volume), as predicted by equation (5.3-8). This can also be explained intuitively, since a drop in air volume means an increase in stiffness, and therefore an increase in resonant frequency.

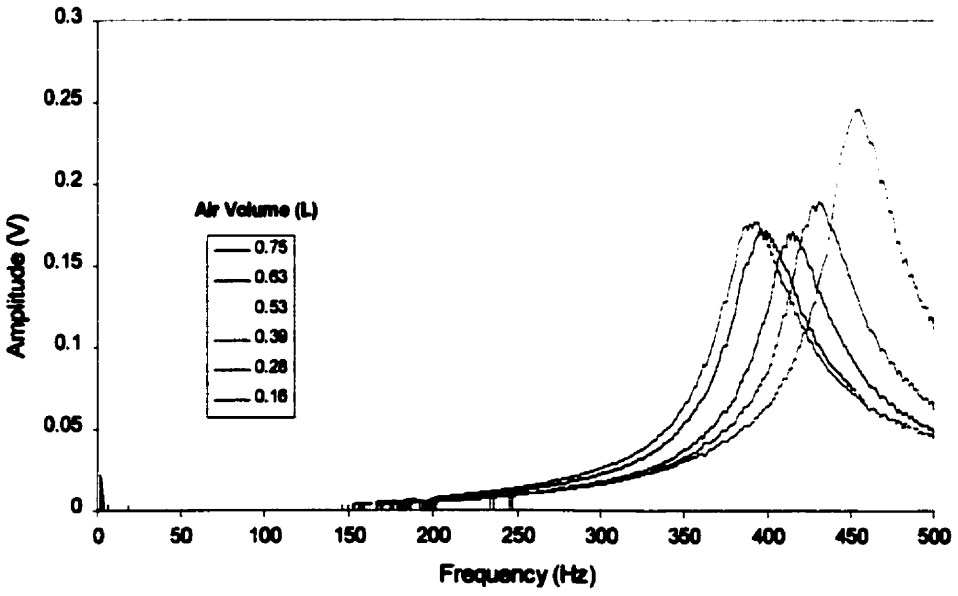

Figure 7.5: Amplitude response of glass jar.

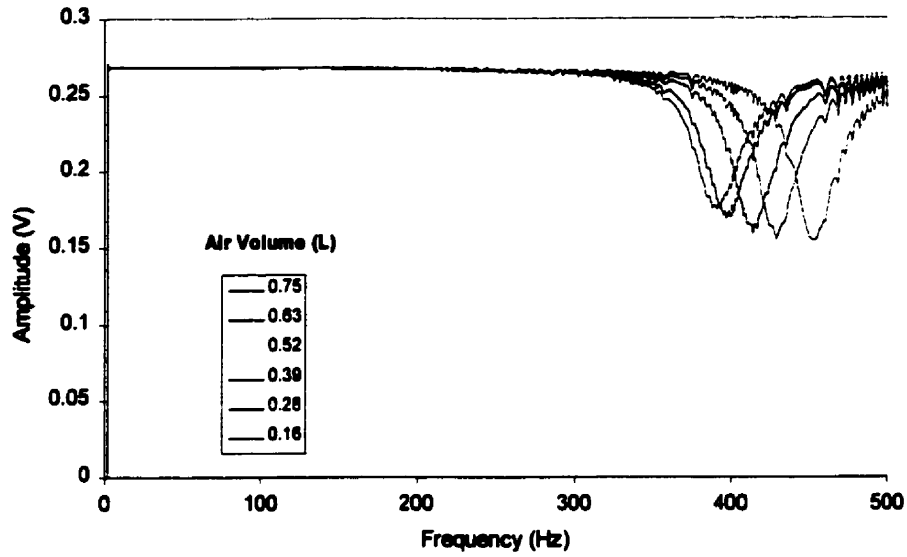

Figure 7.6: Impedance response of glass jar.

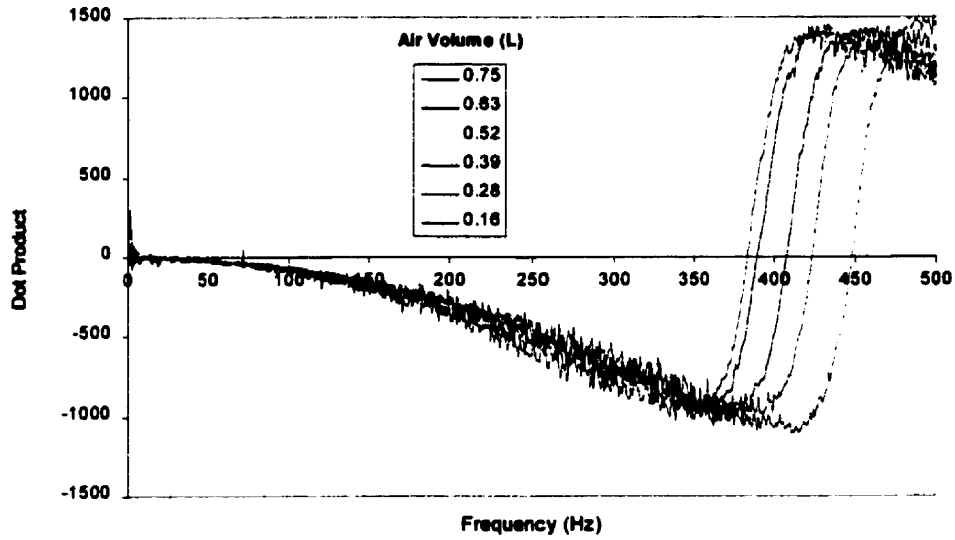

Figure 7.7: Phase shift response of glass jar.

Figure 7.8 shows a plot of resonant frequency as a function of air volume. The three curves shown in this graph correspond to the predicted behavior using Helmholtz's equation and Troke's equation, and the experimental results. Note that the volume used in the calculations was the volume of air in the jar, which decreased as water was added.

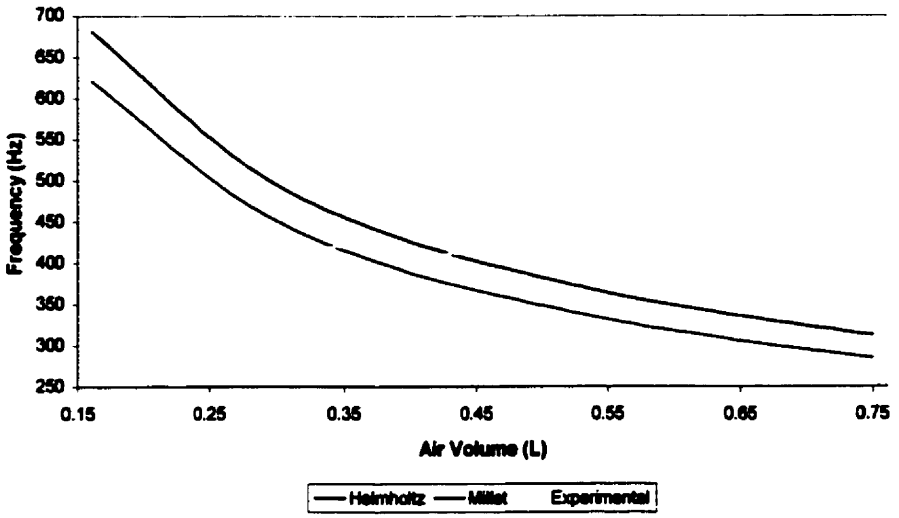

Figure 7.8: Resonant frequency as a function of air volume.

Figure 7.8 shows that the predicted Helmholtz response is consistently lower than the response predicted by Troke. The experimental data show that even though some correlation between volume change and frequency response was measured, the resonant mode of the system always remained very close to the resonant mode of the speaker (415Hz). In fact, at lower air volumes, the experimental resonant frequency appears to be dampened by the speaker, whereas at higher air volumes the experimental resonant frequency appears to be enhanced by the resonance of the speaker. An interesting feature of this plot is the point where the experimental curve crosses the predicted curves. This point corresponds to the natural frequency of the speaker.

Figure 7.9 shows a logarithmic plot of the theoretical and the experimental results. In this case, the volume used is in cubic meters and the frequency is in Hertz. The slope calculated in both theoretical lines is –0.5, as was predicted in the regression analysis of the model in section (5.5). The regression equation of the line obtained experimentally has a slope –0.1, and a linear correlation coefficient r of 0.998. This suggests a strong logarithmic

relationship between volume and resonant frequency, although this relationship differs somewhat from the predicted behavior.

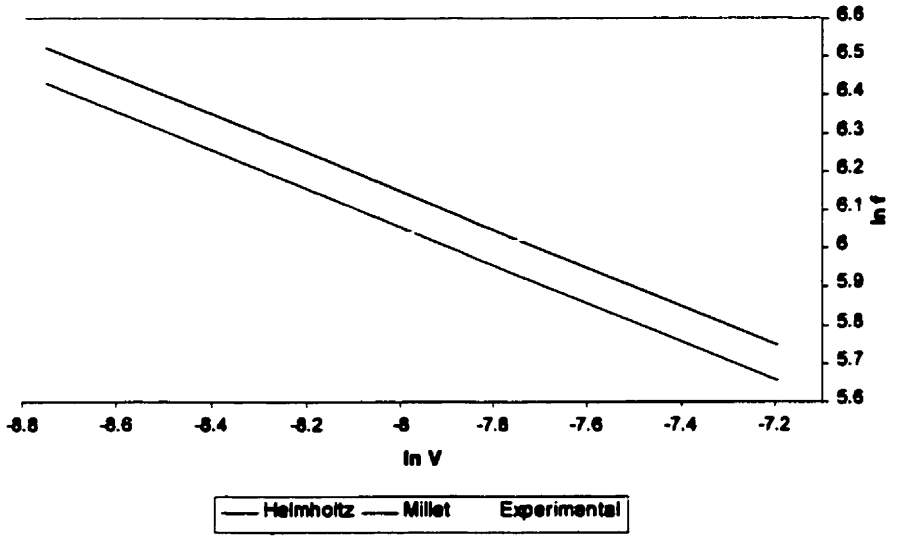

Figure 7.9: Logarithmic plot of resonant frequency as a function of air volume.

7.2. 3.8L RUBBERMAID CONTAINER – COUPLED DESIGN

The discrepancies between the predicted and the experimental values obtained in the first set of experiments prompted an investigation of the relationship between the resonant mode of the speaker and that of the resonator. For this purpose, a second experiment was set up using a slightly larger container.

For this experiment, it was decided to use a plastic container with a volume capacity of 3.8L. This container was chosen because of the desire to insert the microphone into the resonator. The plastic walls made it very easy to cut the necessary access hole which would have been extremely difficult in the glass jar. The downside to this choice was the possibility of introducing new errors due to the greater compliance of the container walls. In general, the resonance frequency of a Helmholtz resonator drops with lower wall stiffness [72]. The size

of the container was again chosen to minimize the probability of standing wave formation. *Figure 7.10* shows the container dimensions.

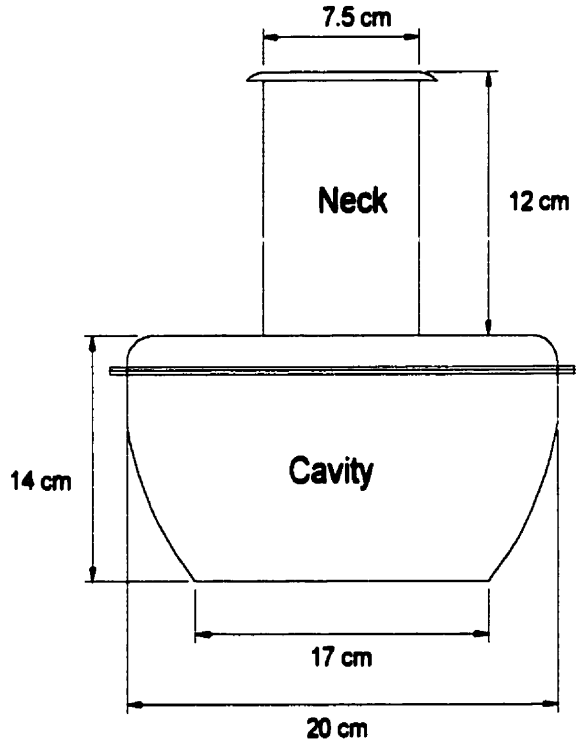

Figure 7.10: Dimensions of 3.8L experimental resonator.

7.2.1. Performance Prediction

The same analysis that was done for the first resonator was repeated with the second one. Note that since the speaker was again mounted hermetically on the neck, it was necessary to adjust L' the same way as it was done for the glass jar. *Table 7.2* shows the predicted behavior for the 3.8L resonator.

Table 7.2: Predicted Helmholtz resonance for 3.8L coupled resonator.

Model	Helmholtz	Troke
Equation	$\omega_o = c\sqrt{\frac{S}{L'V}}$	$\omega_o = c\frac{D}{\sqrt{L'V}}$
L'	$L + 0.61R$	$L + R$
C	344 m/s	344 m/s
Predicted Resonance	**154 Hz**	**166 Hz**

The wavelength for 166Hz was calculated as 2.07m using equation (7.1.1-1). Since this wavelength is over ten times the largest dimension of the resonator, no standing waves were expected inside the cavity. Using equation (5.6-1), the quarter wave resonance of the neck was predicted to be 700Hz.

The response of the speaker used in this experiment was also measured while on its own, and when mounted onto the neck. *Figures 7.11* and *7.12* show that resonant frequency of this speaker dropped from about 210Hz without a neck, to about 175Hz with the neck. The explanation for this drop lies on the interaction of the speaker with the neck. The presence of the neck affects the boundary conditions of the speaker. These two components then act as a system as described by Kleppe, and therefore have a combined resonant frequency[73]. It is important not to confuse this mechanical resonant mode with the acoustical quarter wave resonant mode of the neck which occurs independently. *Figure 7.12* shows this quarter wave resonance as a peak near the predicted value of 700Hz.

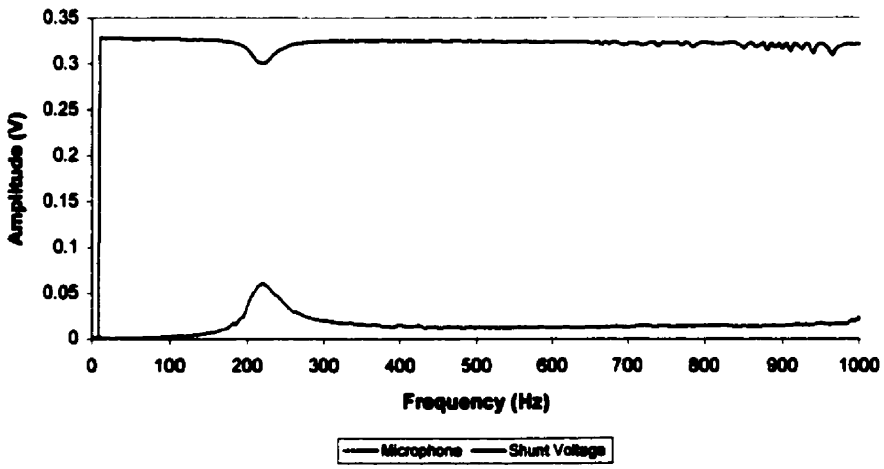

Figure 7.11: Response of speaker without resonator neck.

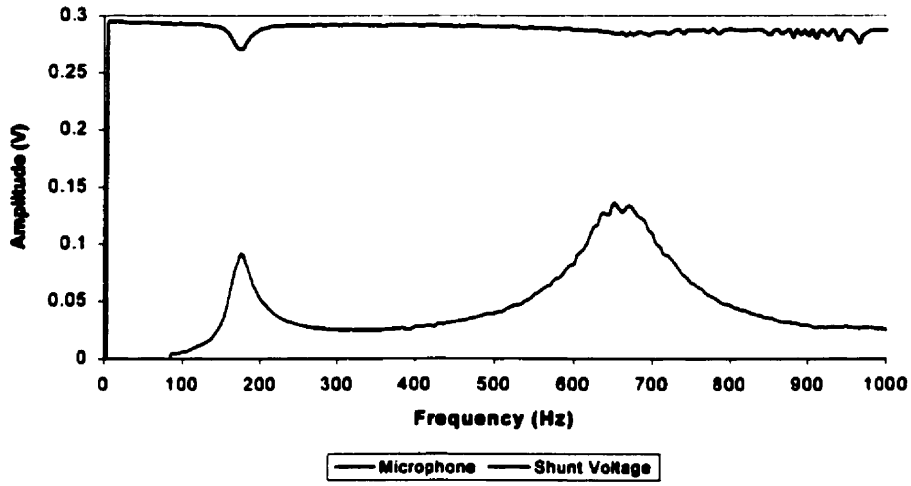

Figure 7.12: Response of speaker with resonator neck.

7.2.2. EXPERIMENTAL SETUP

The plastic container was instrumented with the speaker and the microphone. The experimental setup for this case is shown in *Figure 7.13*.

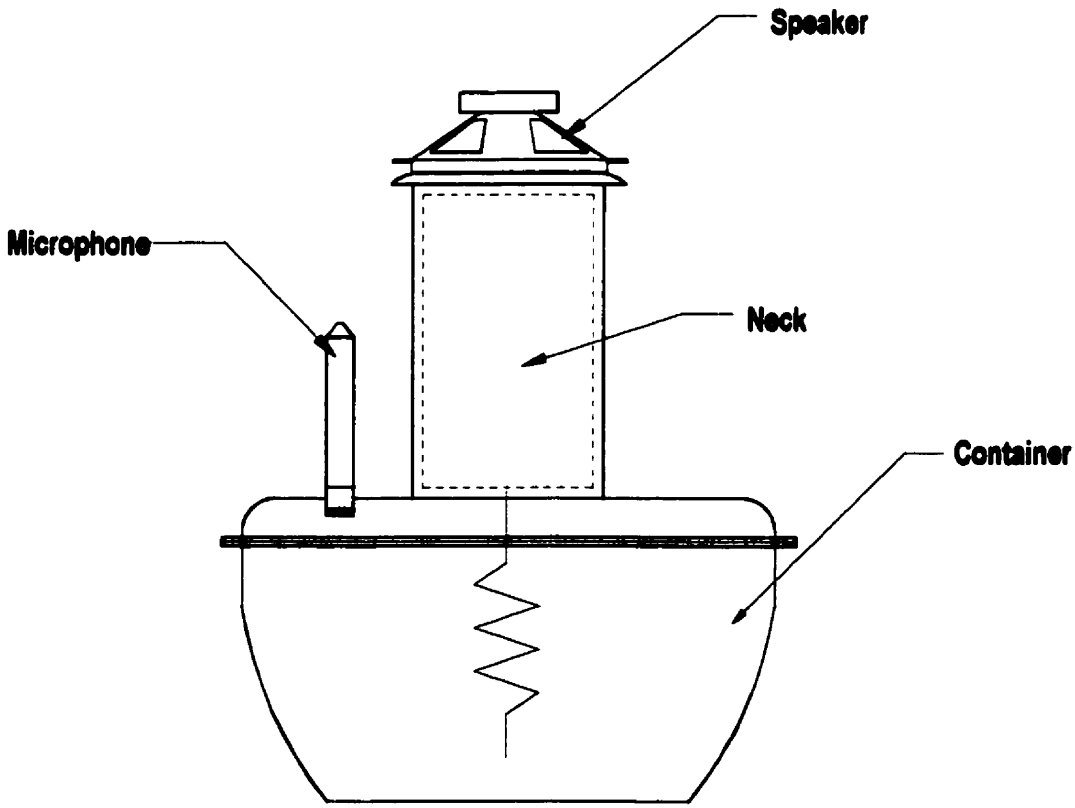

Figure 7.13: Location of instrumentation on 3.8L container.

The diameter of the speaker was 7.5cm, and its rating was given as 1.5Watt and 6Ω. This time the microphone was mounted internally, but very close to the top so that it would not become immersed as water was added.

7.2.3. Results

The microphone response, impedance response, and phase shift were measured while adding water to the container in 0.6L increments. The resulting data are plotted in *Figures 7.14, 7.15,* and *7.16.* It is clear that the response of this container is very similar to that observed in the glass jar, with the resonant frequency increasing as the air volume of the chamber decreases.

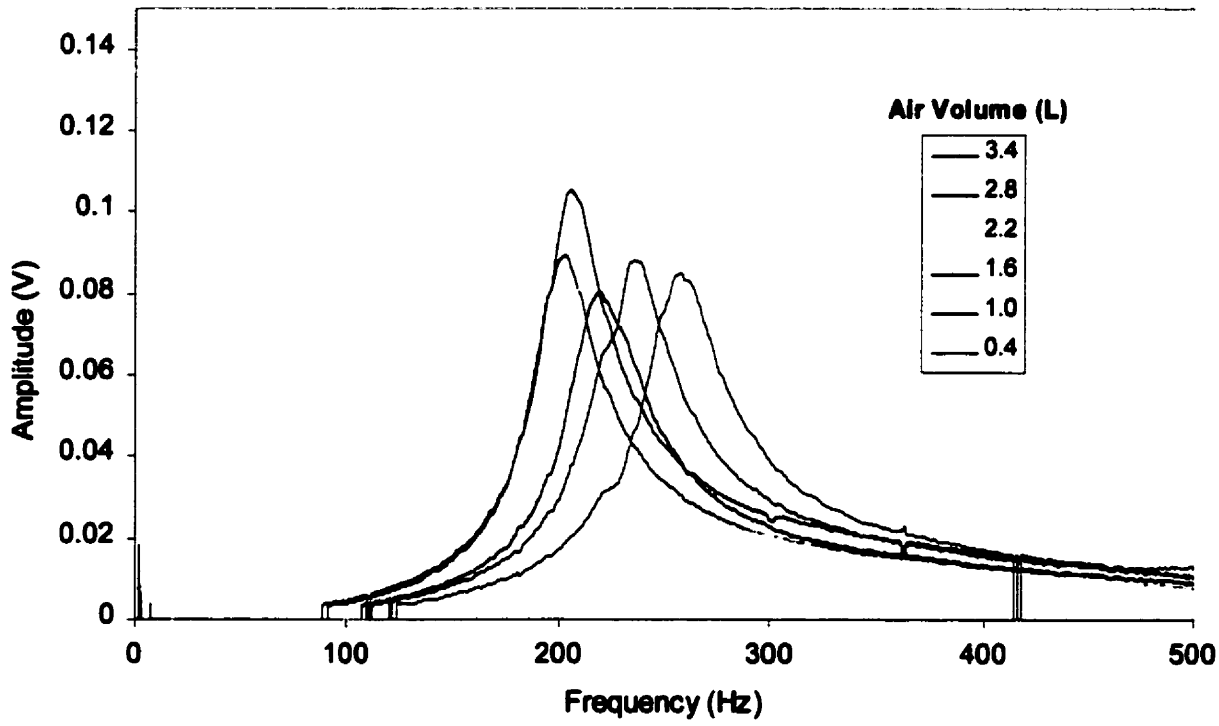

Figure 7.14: Amplitude response of 3.8L coupled resonator.

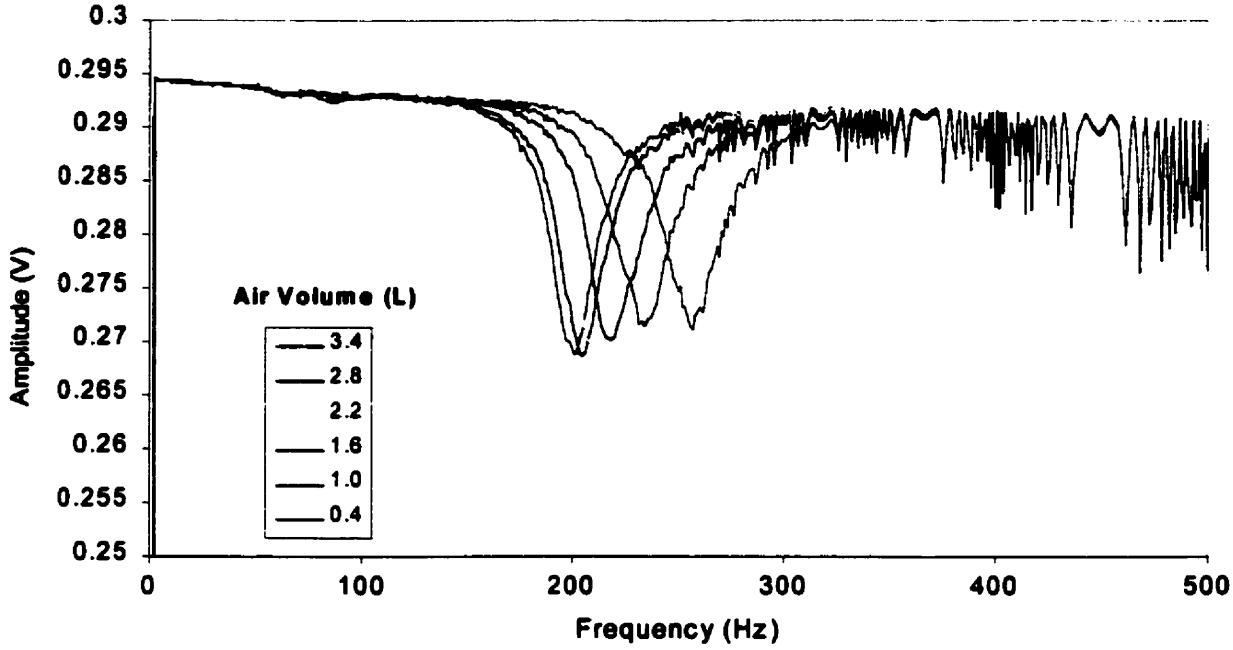

Figure 7.15: Impedance response of 3.8L coupled resonator.

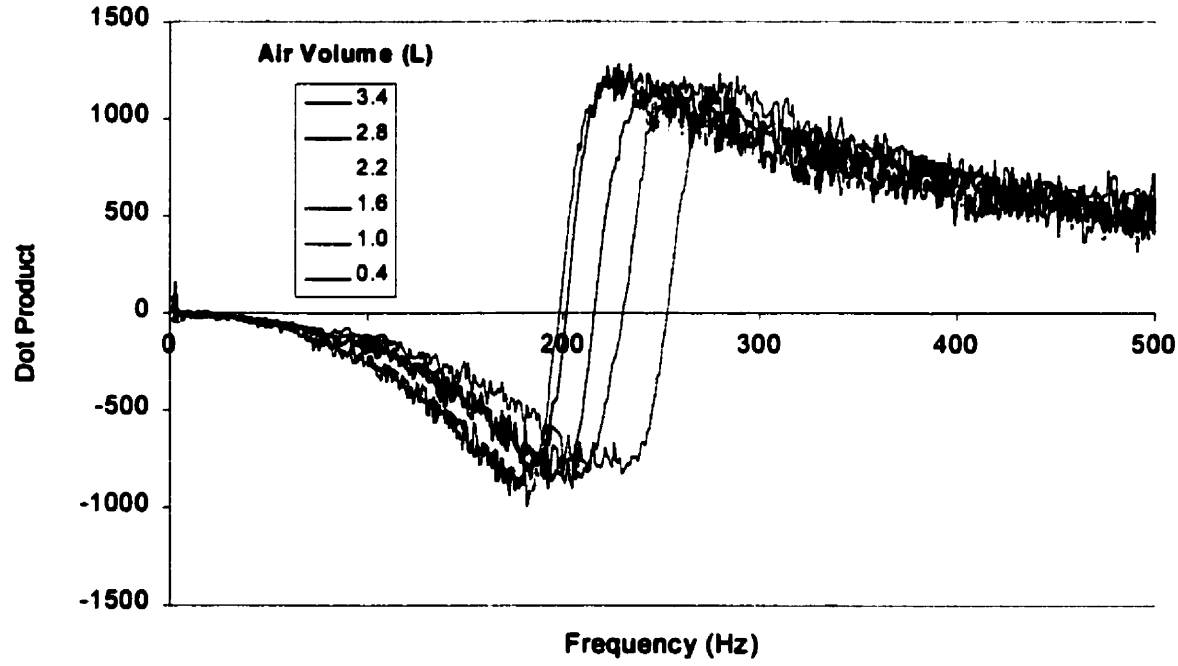

Figure 7.16: Phase shift response of 3.8L coupled resonator.

Figure 7.17 shows a plot of the resonant frequency as a function of volume of air. Note the similarity between this plot and that obtained for the glass jar (*Figure 7.8*). Again, the curve

obtained experimentally crosses the predicted curves near the resonant frequency of the speaker (210Hz). Also, the spring-mass resonance of the system seems to be dampened at lower air volumes, and enhanced at higher air volumes.

Figure 7.18 shows a logarithmic plot of the theoretical and the experimental results. The slope measured in both theoretical lines is again –0.5, as was predicted in the regression analysis of the model. In this case, the slope of the line obtained experimentally is approximately –0.15, very close to that recorded for the glass jar. The linear correlation coefficient r in this case is 0.994, again showing a strong logarithmic relationship between volume and frequency.

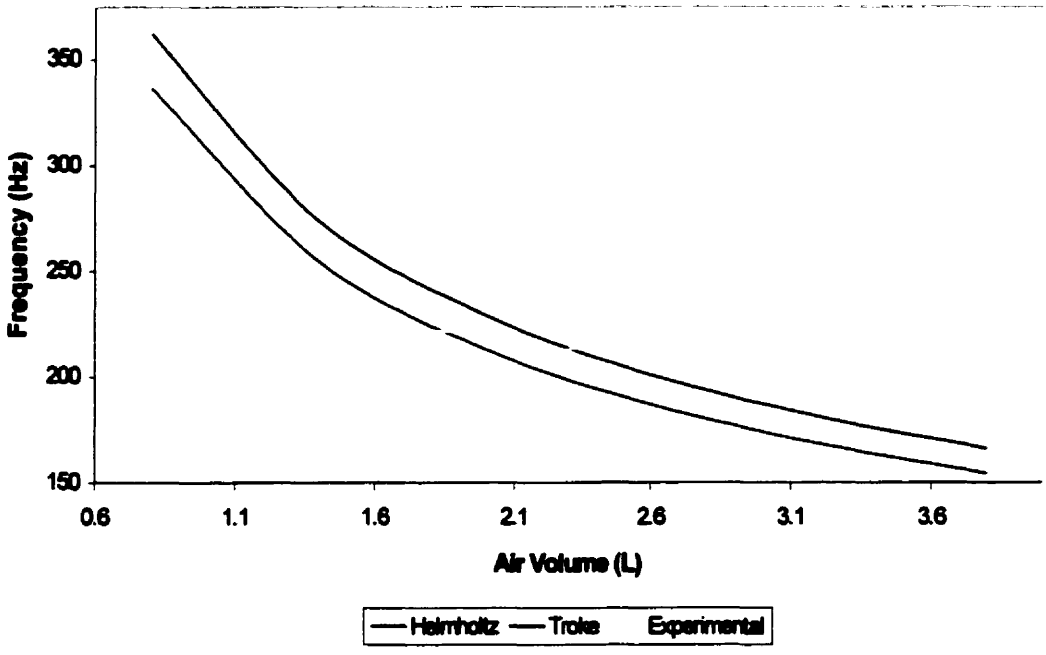

Figure 7.17: Resonant frequency as a function of air volume.

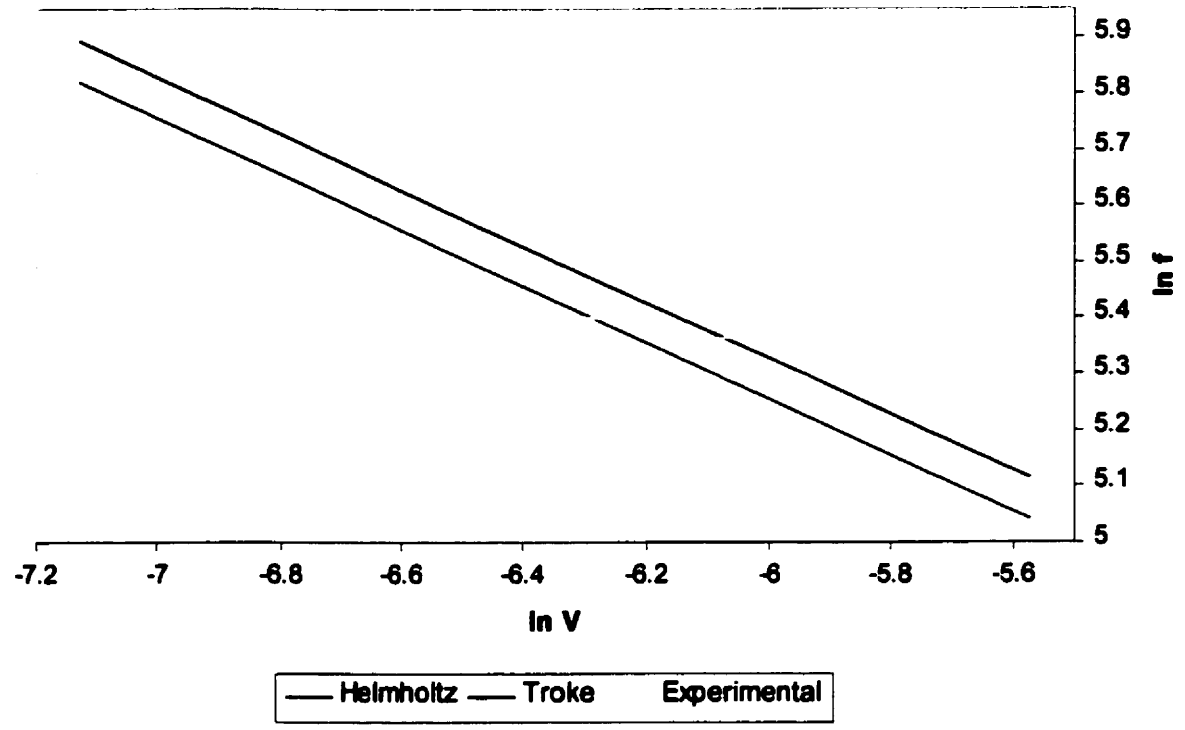

Figure 7.18: Logarithmic plot of resonant frequency as a function of air volume.

7.3. 3.8L RUBBERMAID CONTAINER – UNCOUPLED DESIGN

Even though the first two sets of experiments have shown a clear logarithmic correlation between volume and resonant frequency, the results also show that there is an interaction between the speaker, the neck and the resonator. To further investigate this phenomenon, a third experiment was set up that uncoupled the speaker from the resonator. Using this approach, the resonator is only excited by an incoming acoustic wave travelling through space. This allows the speaker and the container to resonate individually. For this experiment, it was decided to use the plastic container with 3.8L volume capacity and the same neck as before.

7.3.1. Performance Prediction

The analysis that was performed on the second resonator was repeated, but this time the full value of L' was used to account for the fact that the speaker was no longer coupled to the neck. The results are summarized in *Table 7.3*.

Table 7.3: Predicted Helmholtz resonance for 3.8L uncoupled resonator.

Model	Helmholtz	Troke
Equation	$\omega_o = c\sqrt{\frac{S}{L'V}}$	$\omega_o = c\frac{D}{\sqrt{L'V}}$
L'	$L + 1.22R$	$L + D$
c	344 m/s	344 m/s
Predicted Resonance	**143 Hz**	**149 Hz**

The wavelength for 149Hz was calculated as 2.29m using equation (7.1.1-1). This wavelength is over eleven times the largest dimension of the resonator, leaving little reason to believe that standing waves would form inside the cavity.

7.3.2. Experimental Setup

The plastic container was instrumented with the speaker and the microphone. The experimental setup for this case is shown in *Figure 7.19*.

A more powerful speaker was used for these experiments in order to ensure that sufficient acoustical energy would reach the mouth of the resonator. The resonant frequency of this speaker was measured as 120Hz. The microphone was mounted the same way as it was in the previous experiment.

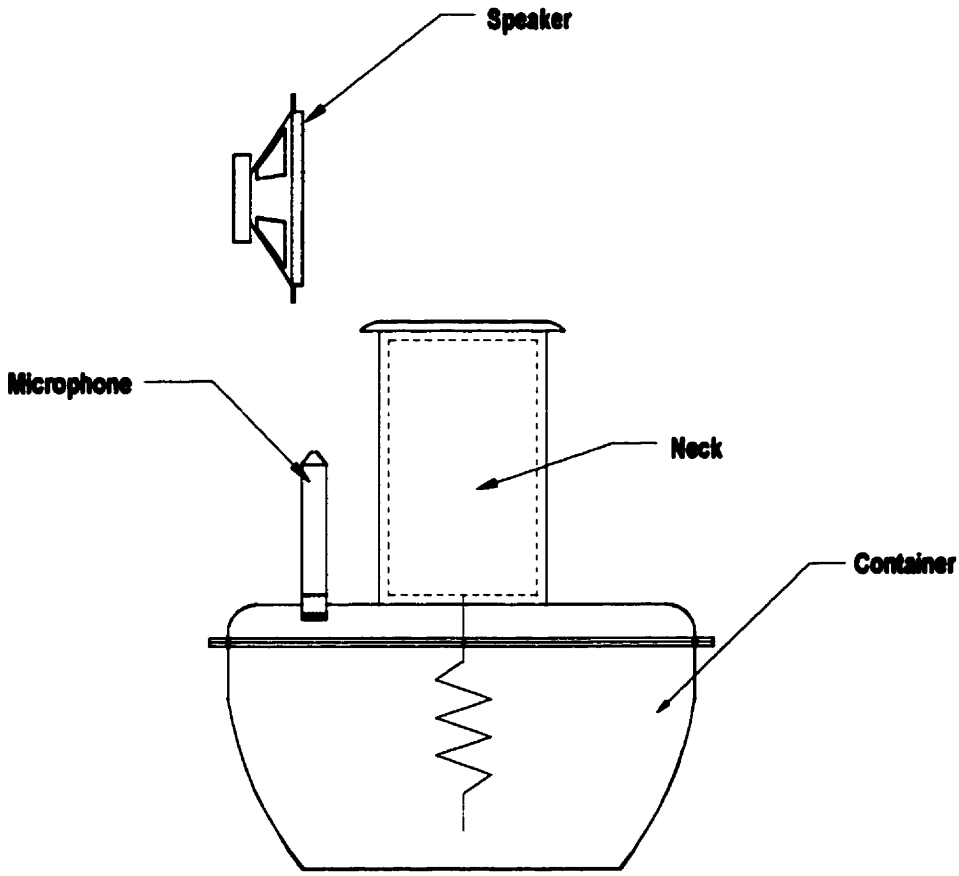

Figure 7.19: Experimental setup for uncoupled resonator.

7.3.3. RESULTS

The microphone response, impedance response, and phase shift were measured while adding water to the container in 0.6L increments. The resulting data are plotted in *Figures 7.20, 7.21*, and *7.22*.

It is clear from these results that the behavior of this resonator varies significantly from the coupled case studied in section (7.2), despite the fact that the two do not differ geometrically. The separation of the speaker resonant mode and the spring-mass resonant mode can be seen in *Figure 7.20*. Two peaks are prominent in this plot. The first, at around 120Hz, corresponds to the resonant frequency of the speaker. As the speaker resonates, the greater

intensity of the acoustical excitation is picked up by the microphone inside the container. The second peak corresponds to the spring-mass resonant mode of the cavity and neck. This peak shifts to the right between 150 Hz and 260 Hz as water is added to the container. An additional feature in this plot is the increase in total amplitude as the two resonant peaks merge together.

A further example of the uncoupling between the speaker and the resonator is seen in *Figure 7.21*, which shows the impedance change in the speaker. This plot shows that the speaker behaves the same throughout the experiment because it is not affected by the resonator. The disadvantage of this of course is that uncoupling the speaker makes it impossible to measure the resonant frequency using the impedance response of the speaker.

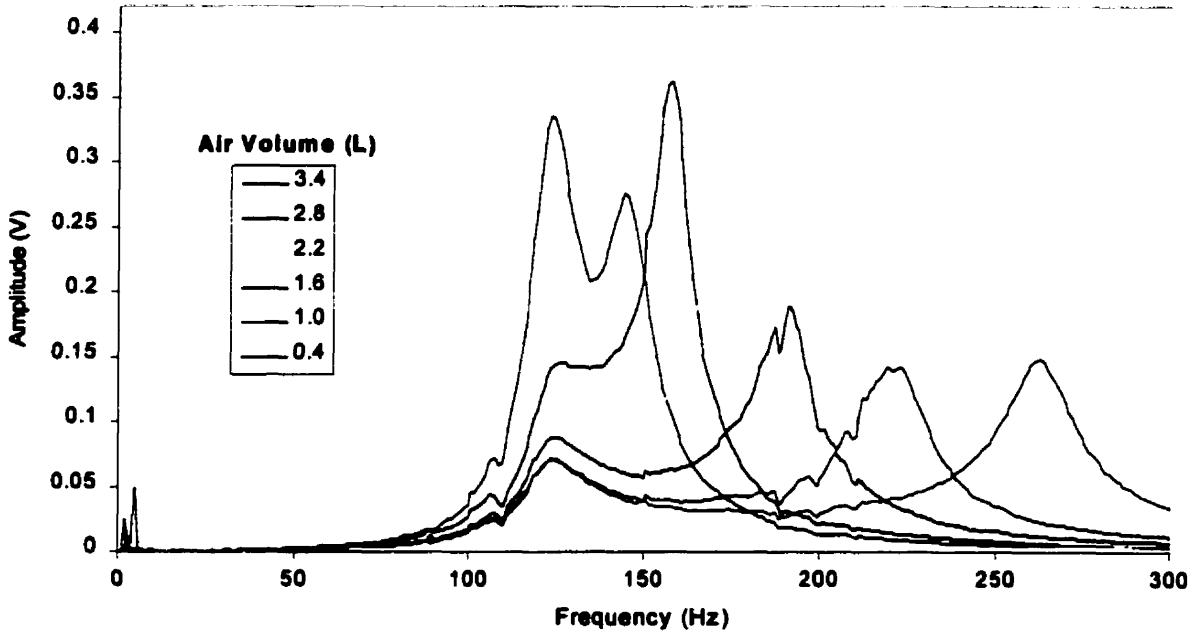

Figure 7.20: Amplitude response of 3.8L uncoupled resonator.

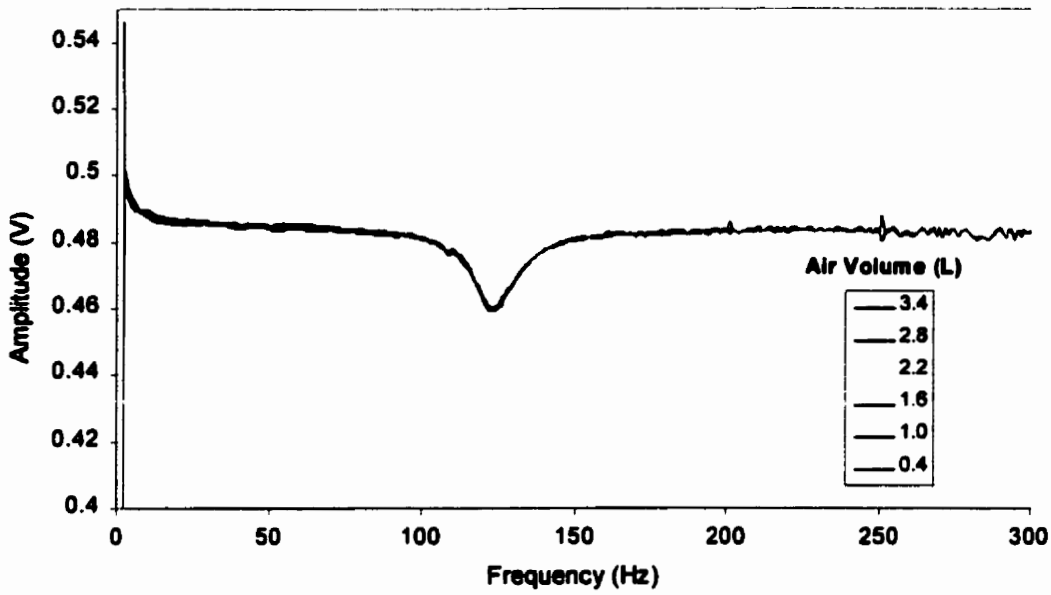

Figure 7.21: Impedance response of 3.8L uncoupled resonator.

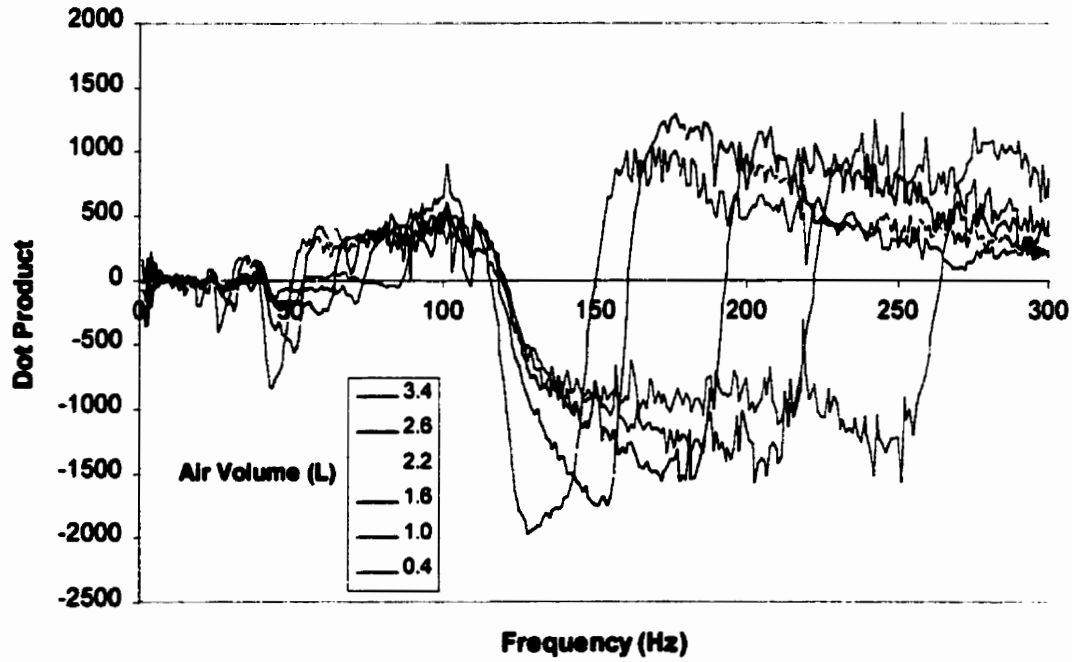

Figure 7.22: Phase shift response of 3.8L uncoupled resonator.

Figure 7.23 shows a plot of the spring-mass resonant frequencies (corresponding to the second peak measured by the microphone) as a function of air volume. This plot shows that

the experimental curve again departs from the predicted values as the excitation frequency moves away from the resonant frequency of the speaker. However, the severity of this departure is not as great as when the speaker was coupled.

Figure 7.24 shows a logarithmic plot of the theoretical and the experimental results. The slope calculated in both theoretical lines is again –0.5, as was predicted in the regression analysis of the model. However, the slope of the line obtained experimentally is –0.4, much closer to the predicted value than in the coupled example. Furthermore, the correlation coefficient r for this case is 0.999, thus showing a strong logarithmic relation between volume and resonant frequency.

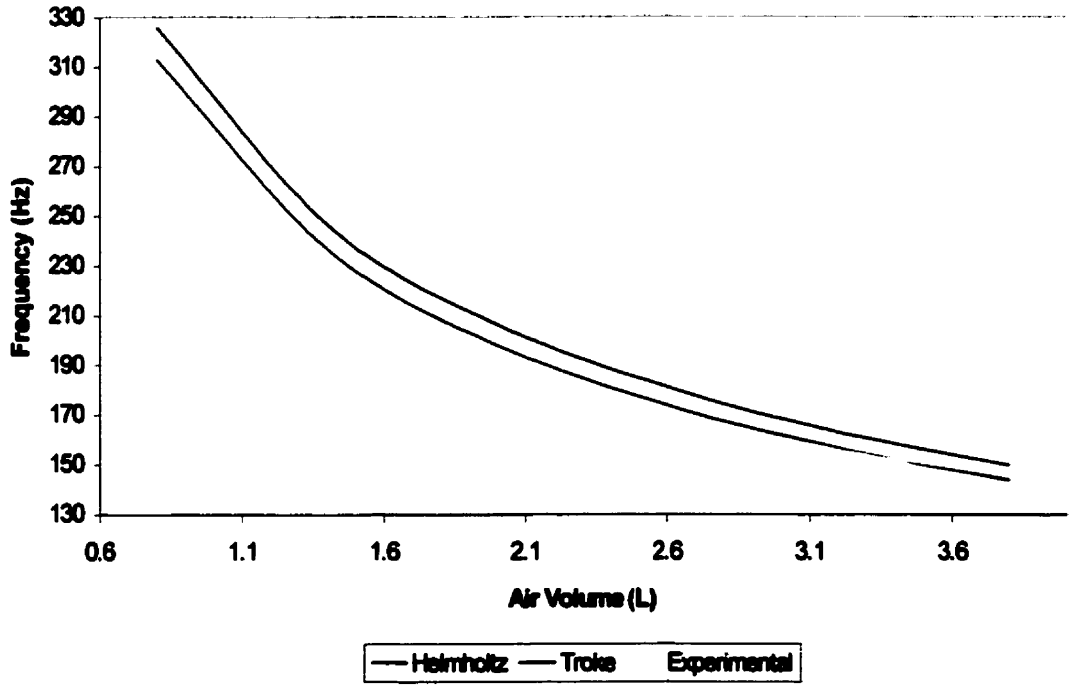

Figure 7.23: Frequency response as a function of air volume.

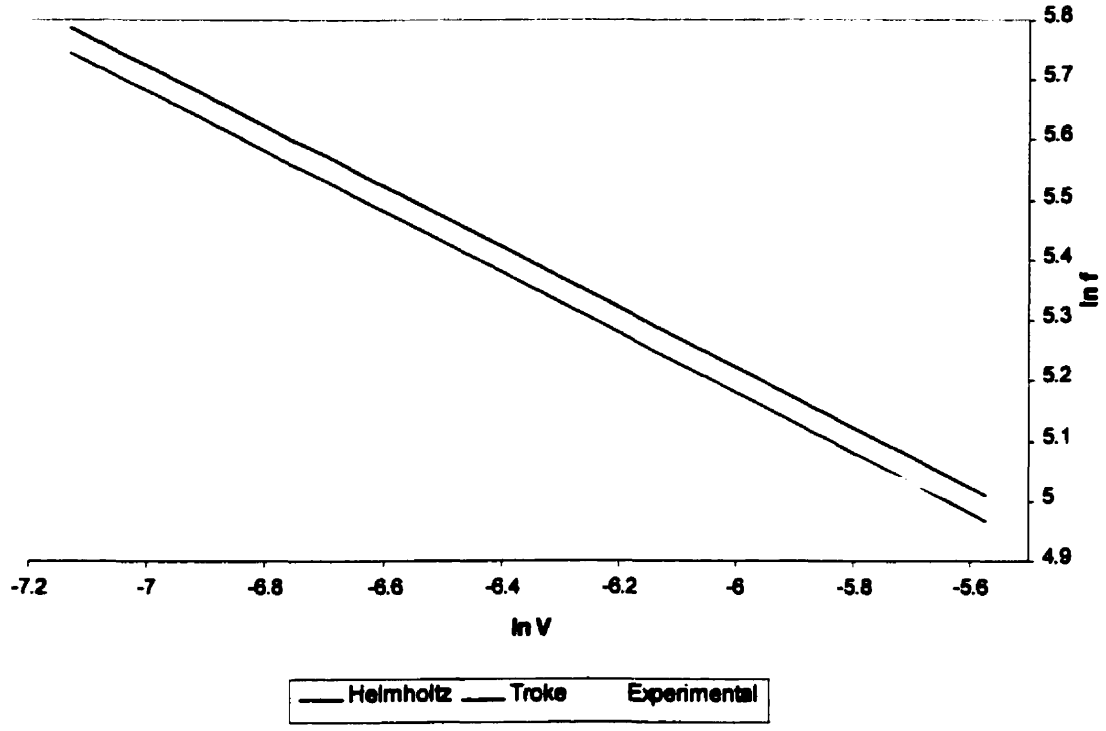

Figure 7.24: Logarithmic plot of resonant frequency as a function of air volume.

7.4. LARGE TANKS – SIMPLE GEOMETRY

The experiments described in sections 7.1, 7.2, and 7.3 demonstrate the feasibility of using the Helmholtz method to measure volume in a small container. However, as was previously mentioned, larger tanks present a potential problem if the wavelength of the excitation source reaches a dimension close to those of the tank. To further investigate this problem, the Helmholtz method was applied to a large tank having a simple geometry. The tank used was a custom made propane tank having a simple cylindrical geometry with rounded ends. *Figure 7.25* shows the dimensions of the tank.

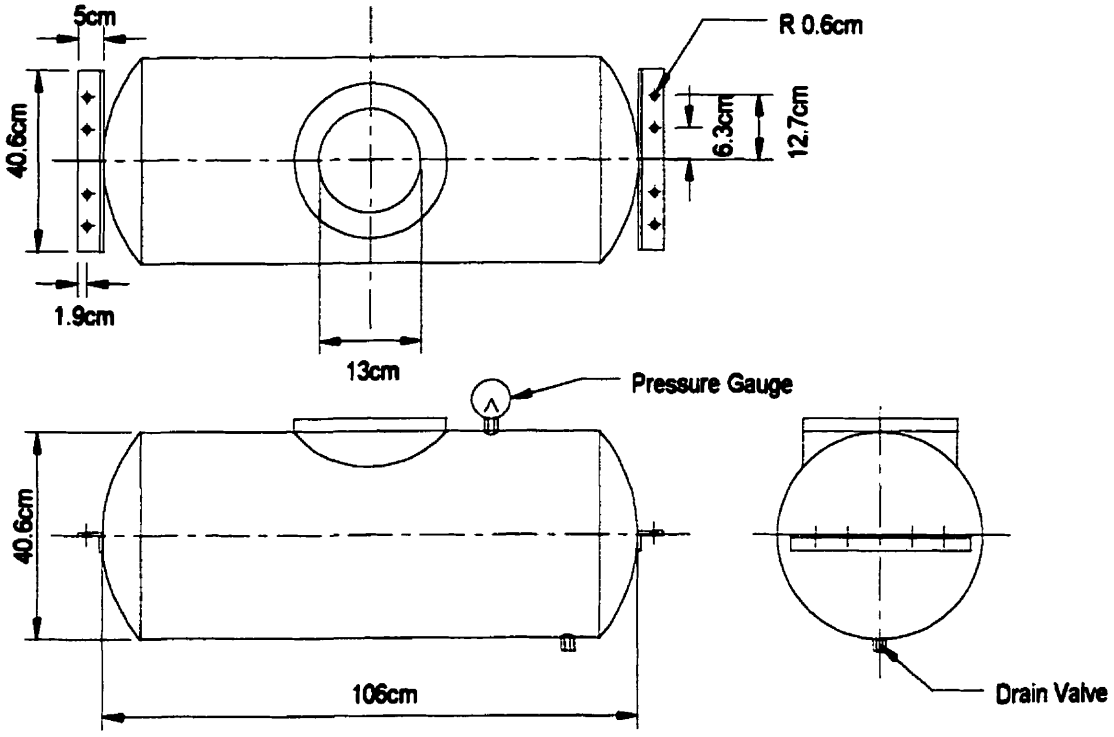

Figure 7.25: Dimensions of propane tank.

Being a steel tank designed to store fuel at high pressures, the walls could be assumed to be very stiff. The neck was built into the top of the tank and had a diameter of 13.5cm and a length of 4.5cm.

7.4.1. Performance Prediction

From the experience gained in the previous experiments, it was decided to perform this experiment using a speaker uncoupled from the neck of the tank. The reason for this was that previous experiments revealed a clear interaction between the speaker resonance and the spring-mass resonant mode of the tank when the speaker was coupled. In contrast, performing an uncoupled experiment yields the pure acoustical response of the Helmholtz resonator independent of the excitation source used. Having the pure acoustical response of

the system is more useful in examining the true behaviour of the tank since the errors introduced by the speaker are removed.

The preliminary analysis that was performed on the propane tank was the same as was done for previous resonators. The total volume of the tank when empty was 131.8L. The results are summarized in *Table 7.4.*

Table 7.4: Predicted Helmholtz resonance for propane tank.

Model	Helmholtz	Troke
Equation	$\omega_o = c\sqrt{\frac{S}{L'V}}$	$\omega_o = c\frac{D}{\sqrt{L'V}}$
L'	$L + 1.22R$	$L + D$
c	344 m/s	344 m/s
Predicted Resonance	**50.5 Hz**	**47.9 Hz**

The wavelength for 50.5Hz was calculated as 6.81m using equation (7.1.1-1). Since this wavelength is over six times the largest dimension of the resonator, no standing waves were expected inside the tank. Using equation (5.6-1), the quarter wave resonance of the neck was predicted to be 1911Hz.

7.4.2. Experimental Setup

The speaker was mounted on a support stand at a distance of 60cm away from the top of the neck. Having such a large gap between the speaker and the neck allowed for a minimized coupling between the resonator and the speaker. However, at such a large distance a much more powerful speaker was needed in order to produce sufficient acoustical energy to excite the resonator. In addition, since the operating frequency range was so low (around 50Hz), it was also necessary to use a speaker with a good frequency response in the lower range. These two requirements were met by using a Bass speaker, or sub-woofer. The speaker used

for this experiment had a 20cm diameter cone and a 50oz magnet. Its power rating was 600Watt and its electrical impedance 8Ω.

Since the speaker was uncoupled, it was necessary to use a microphone to record the acoustical response of the tank. The microphone was inserted though an access hole at the top of the tank (labeled pressure gauge in *Figure 7.25*), and located just inside the wall. The impedance response of the speaker was not recorded during the experiments since the lack of coupling meant that this signal carried no useful information.

7.4.3. RESULTS

The microphone response and phase shift response were measured while adding water to the tank in 3.8L increments. The water was mixed with a rust inhibitor agent to prevent the degradation of the steel tank. The tank was only filled to 80% of full capacity since this is the maximum allowable volume when filling a propane tank. The resulting data are plotted in *Figures 7.26* and *7.27*.

Figure 7.26 shows that there is only one prominent peak for each volume in the range between 0 and 200Hz. This peak moves to the right as the volume of liquid inside the tank is increased. The same shift is observed in *Figure 7.27* with the phase response.

Figure 7.28 shows a plot of the spring-mass resonant frequency as a function of air volume. This plot shows that the experimental curve is very close to values predicted by both models. Note that in this case, the results predicted by the Troke model are higher than the results predicted by the Helmholtz model.

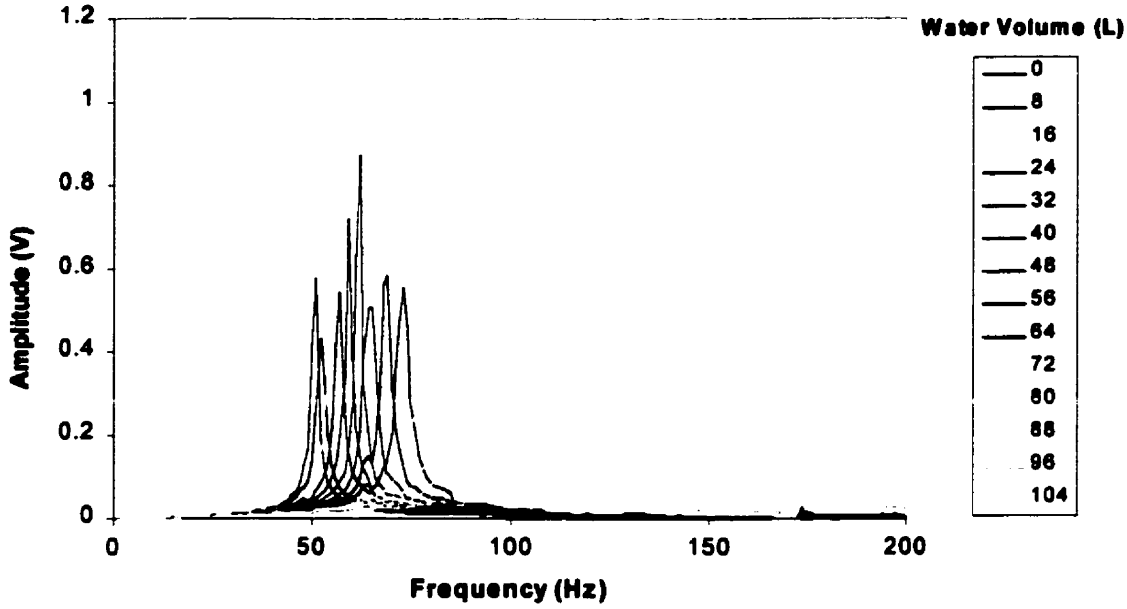

Figure 7.26: Amplitude response of propane tank.

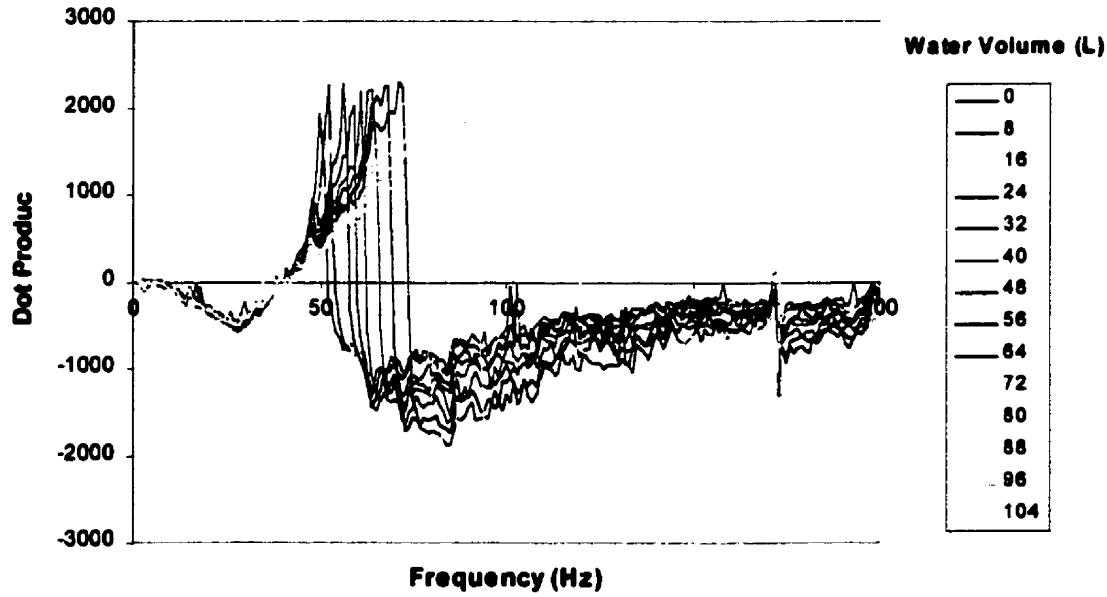

Figure 7.27: Phase shift response of propane tank.

Figure 7.29 shows a logarithmic plot of the theoretical and the experimental results. The slope calculated in both theoretical lines is again –0.5, as was predicted in the regression analysis of the model. However, the slope of the line obtained experimentally is –0.54, much closer to the predicted value than in previous experiments. Furthermore, the correlation coefficient *r* for this case is 0.999, again showing a strong logarithmic relation between volume and resonant frequency.

Figure 7.29 shows that it is possible to use the Helmholtz principle to measure volume in a large tank. A key issue is to maintain the wavelength of the excitation source as large as possible by working with very low frequencies. The simplicity of the geometry of the tank also makes the formation of unwanted standing waves less probable.

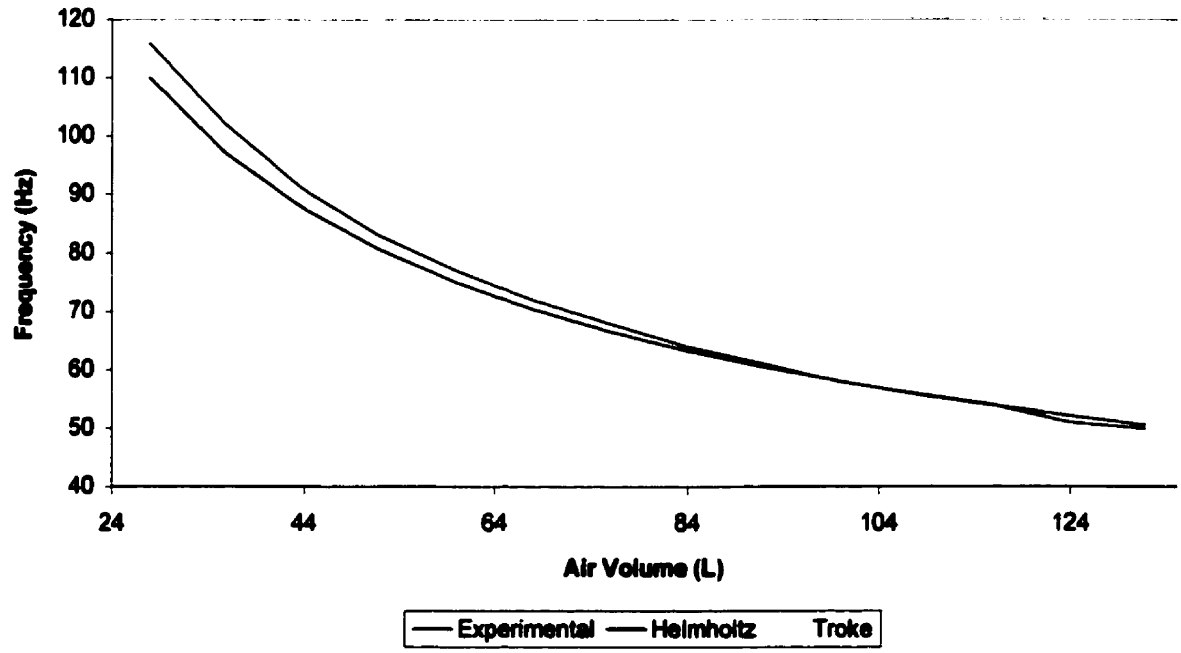

Figure 7.28: Frequency response as a function of air volume.

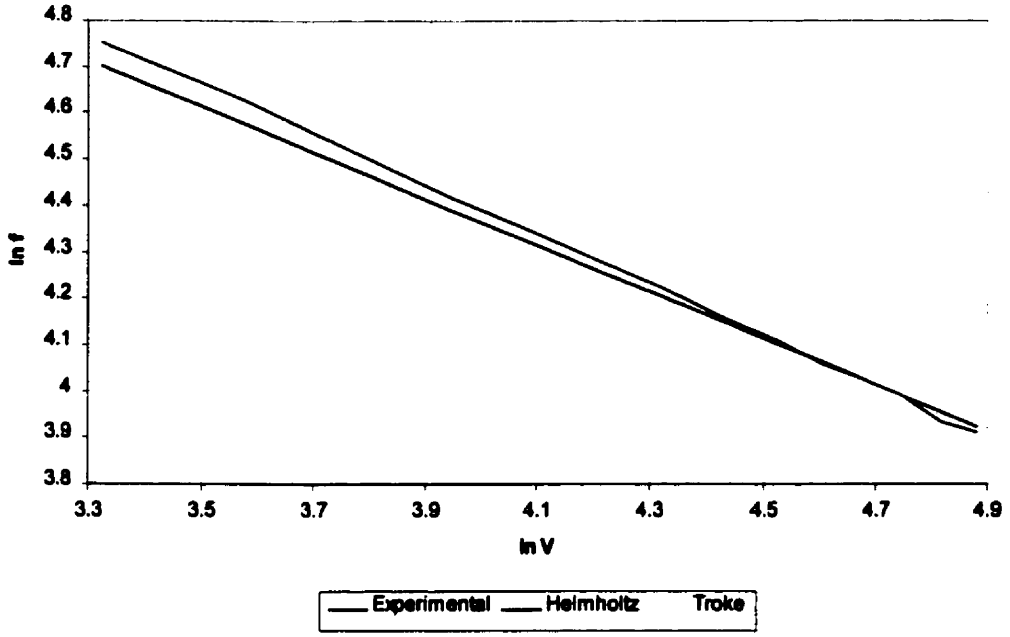

Figure 7.29: Logarithmic plot of resonant frequency as a function of air volume.

7.5. LARGE TANKS – COMPLEX GEOMETRY

To further investigate the effect of size and geometry on a Helmholtz resonator, another experiment was performed using a steel tank from a gasoline powered Chevrolet Lumina. This tank is characterized by having a wedge shape designed to fit under the back seat of the car, and in front of the rear suspension. This makes its shape very complex since the tank has many geometrical contours and varying dimensions throughout. In addition, the tank also has internal baffles designed to reduce the sloshing effects of the fuel during driving. The presence of these baffles adds to the complexity of the geometry of the tank, while at the same time dividing the tank into separate compartments. A tank with such a complex geometry is much more prone to the formation of standing waves at different wavelengths because of the wide range of dimensional features. This made this tank an interesting

specimen to investigate. *Figure 7.30* shows and exploded view of the tank depicting the top and bottom halves, as well as the internal baffles.

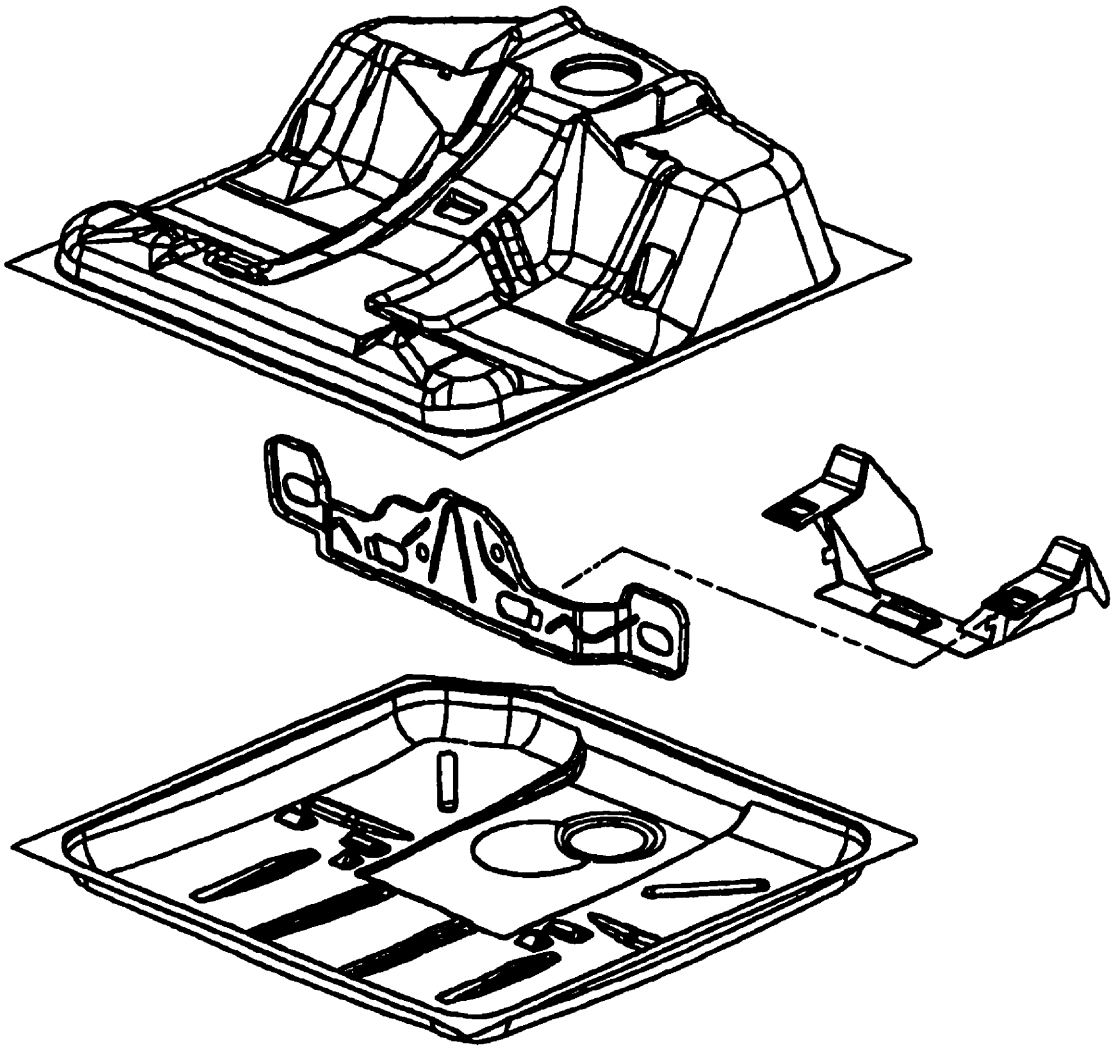

Figure 7.30: Exploded view of Lumina tank showing internal baffles.

The tank itself was made of steel, although one of the baffles was made out of molded plastic. A plastic neck measuring 4cm in length and 7.5cm in diameter was added to the top access hole to complete the resonator.

7.5.1. Performance Prediction

This experiment was also performed with the speaker uncoupled from the neck. The total volume of the tank when empty was 56.8L. The predicted behavior of this tank when empty is summarized in *Table 7.5*.

Table 7.5: Predicted Helmholtz resonance for propane tank.

Model	Helmholtz	Troke
Equation	$\omega_o = c\sqrt{\frac{S}{L'V}}$	$\omega_o = c\frac{D}{\sqrt{L'V}}$
L'	$L + 1.22R$	$L + D$
c	344 m/s	344 m/s
Predicted Resonance	**49.6 Hz**	**50.8 Hz**

The wavelength for 50.8Hz was calculated as 6.77m (using equation (7.1.1-1)), which is over six times the largest dimension of the tank (0.75m.). Using equation (5.6-1), the quarter wave resonance of the neck was predicted to be 2150Hz.

7.5.2. Experimental Setup

In order to make the results from this experiment comparable with those obtained with the propane tank, the same basic setup and equipment was used for this experiment. This time, the speaker was mounted at a distance of 80cm away from the top of the neck.

The microphone was inserted though an opening on the side of the tank used for venting during filling. Once inside, the microphone was mounted five centimeters below the top of the tank.

7.5.3. RESULTS

The microphone response and phase shift response were measured while adding water to the tank in 3.8L increments. The tank was only filled up to 49.2L in order to prevent the microphone from becoming immersed in the water. The resulting data are plotted in *Figures 7.31* and *7.32*.

Figure 7.31 is much more difficult to interpret than similar results obtained for previous resonators. One peak is prominent between 38Hz and 44Hz corresponding to the first 26.5L of water added. This peak moves to the right with increasing volume, but not as predicted (its shift is linear when it should be logarithmic). After 26.5, this peak disappears and other peaks become prevalent at around 80Hz. These new peaks are unrelated to the Helmholtz resonance, and behave erratically as the volume of water is further increased. After passing 41.6L, another peak appears which moves to the right at 45.4L and 49.2L. It is uncertain whether these peaks correspond to the Helmholtz resonance.

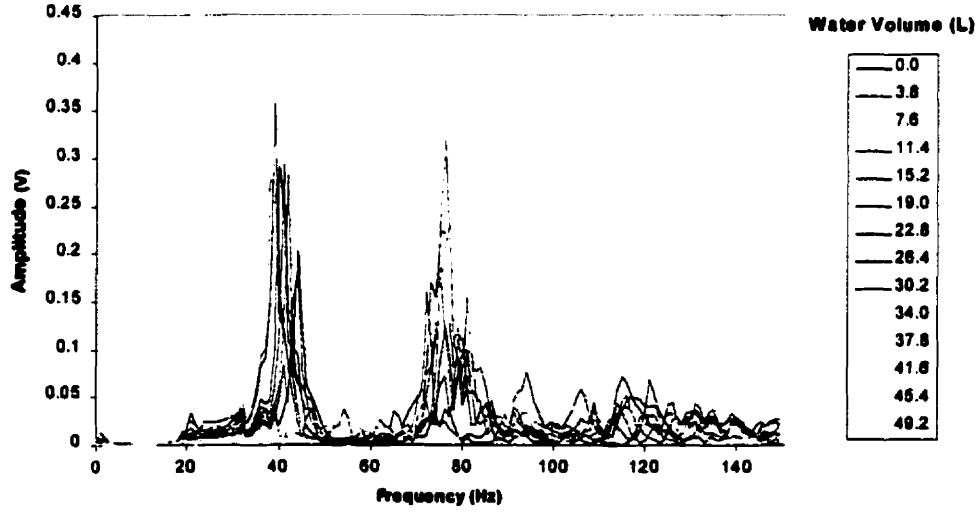

Figure 7.31: Amplitude response of Lumina tank.

The phase response illustrated in *Figure 7.32* shows the same erratic behavior that *Figure 7.31* has.

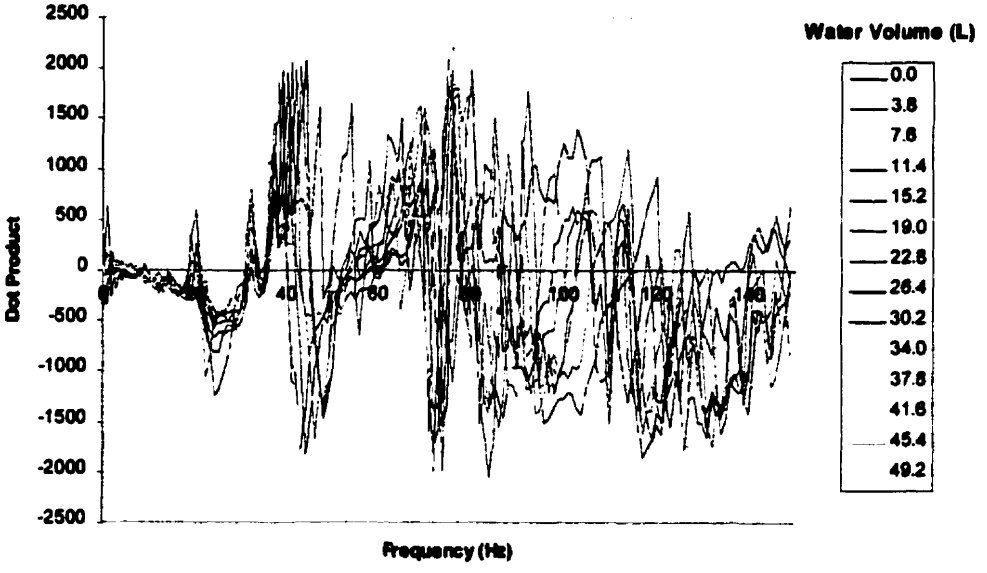

Figure 7.32: Phase shift response of Lumina tank.

It is clear from these two figures that the Helmholtz resonance of the Lumina tank does not behave as predicted by the theory. The complexity of the tank causes other acoustical resonant modes to interfere with the Helmholtz mode. Such unpredictable behavior demonstrates that the geometry of the tank is critical in order to implement the Helmholtz method.

7.6. Effect of Tilting

Another important factor that required further investigation was the susceptibility of the Helmholtz resonant mode to changes in the shape of the cavity. These changes take place due to movement of liquid inside the tank if the vehicle tilts. This effect was investigated using the 3.8L plastic container with the 0.5Watt speaker hermetically coupled to its neck.

Two experiments were conducted. In the first, 1.2L of water were added to the container. Subsequently, the Helmholtz resonance was measured while tilting the resonator 0, 10, 20, and 30 degrees. The same experiment was repeated with 2.2L of water. The results are plotted in *Figures 7.33* to *7.38*.

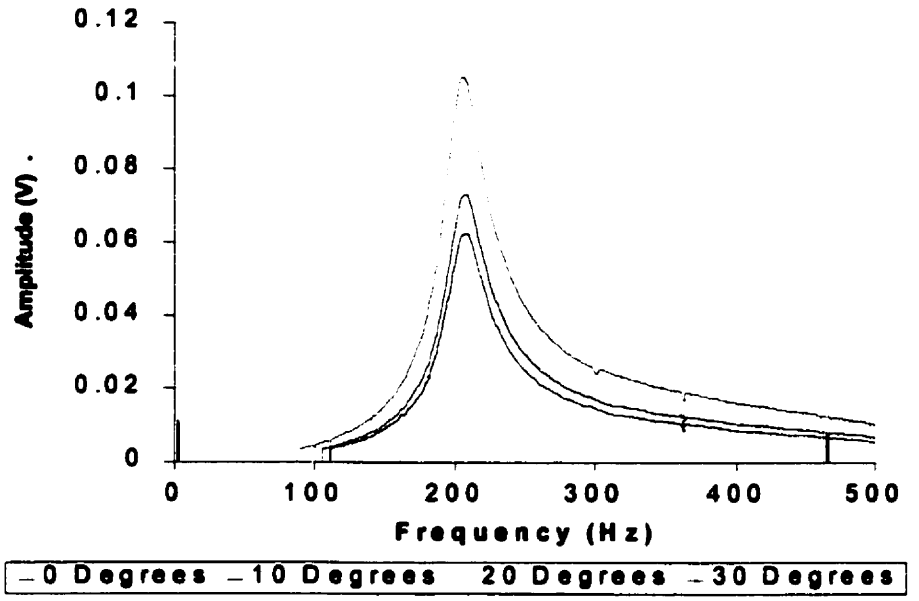

Figure 7.33: Amplitude response with change in tilting angle for container with 1.2L of water.

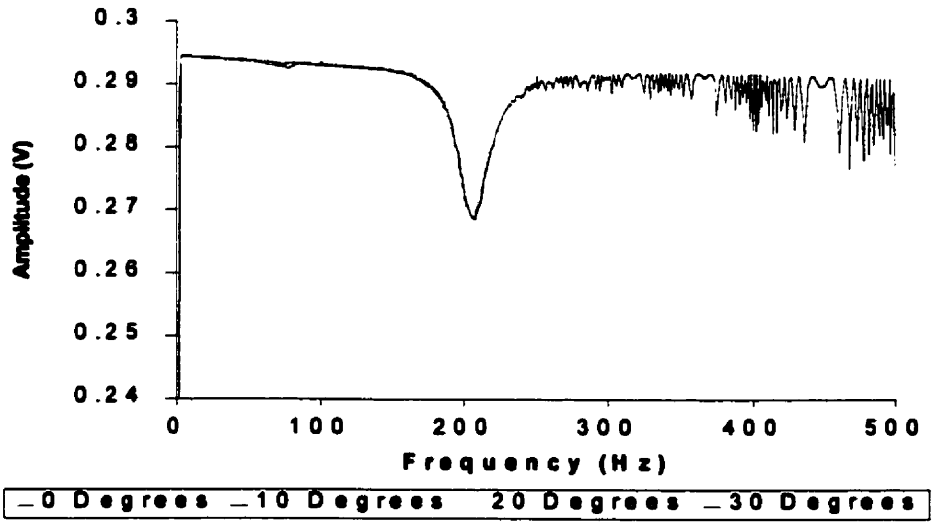

Figure 7.34: Impedance response with change in tilting angle for container with 1.2L of water.

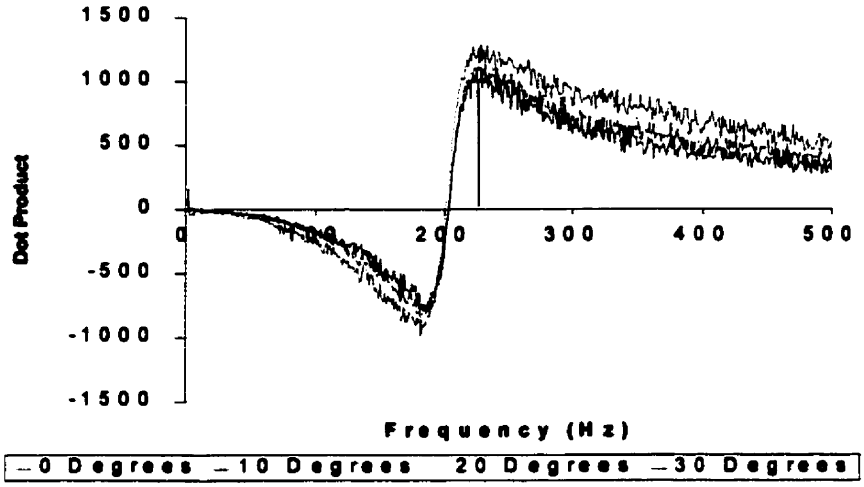

Figure 7.35: Phase response with change in tilting angle for container with 1.2L of water.

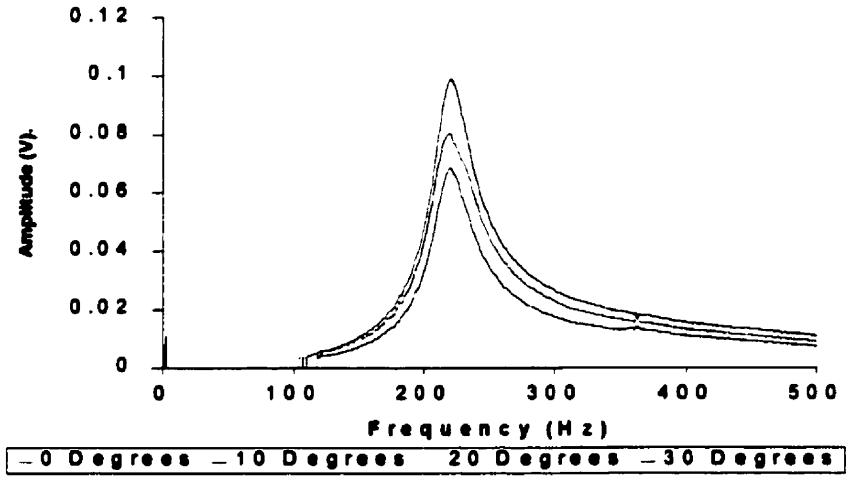

Figure 7.36: Amplitude response with change in tilting angle for container with 2.2L of water.

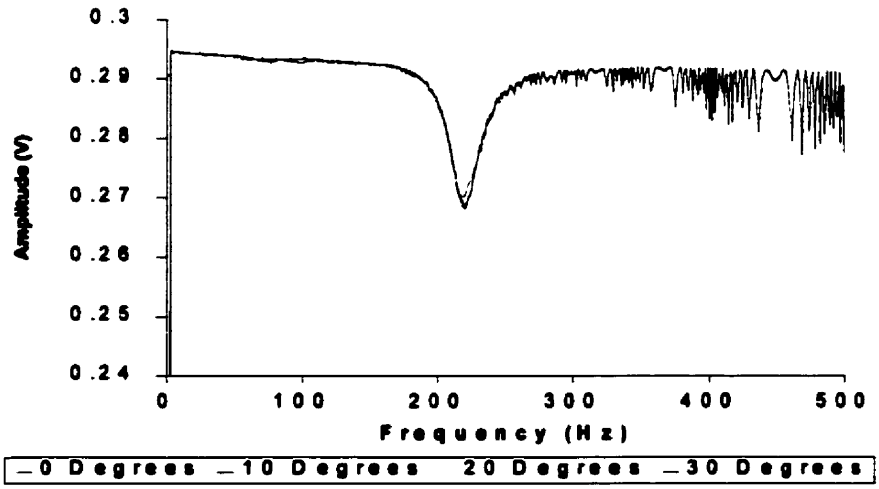

Figure 7.37: Impedance response with change in tilting angle for container with 2.2L of water.

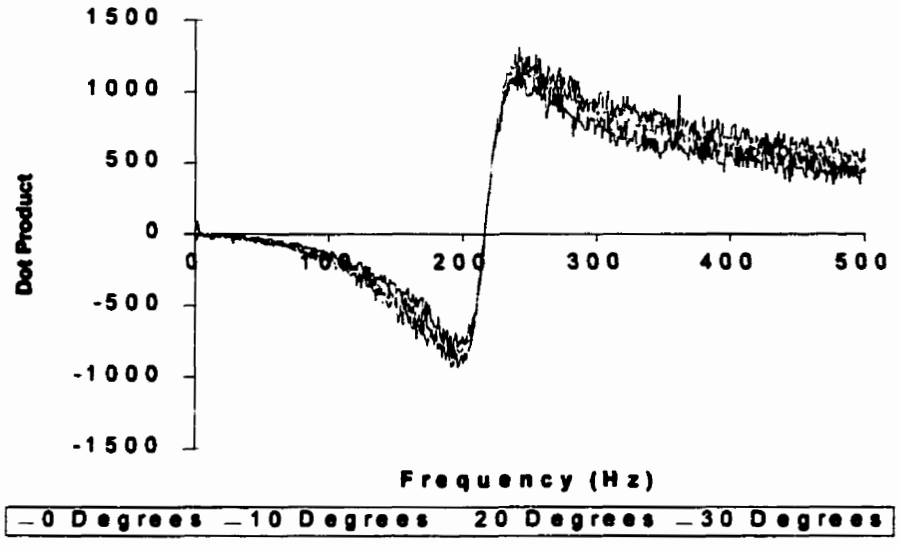

Figure 7.38: Phase response with change in tilting angle for container with 2.2L of water.

These plots show that although there is a definite change in the resonant frequency of the system when the volume of water is increased from 1.2L (205Hz) to 2.2L (220Hz), tilting the container has little effect on this response. This is consistent with both theoretical models presented in this study which correlate resonant frequency to the volume of the resonator, but not to its shape.

CHAPTER 8 DISCUSSION

It is clear from the results presented in chapter 7 that it is possible to use the Helmholtz resonator principle in order to measure the amount of liquid stored in a tank. The results show a clear correlation between volume and resonant frequency that, with proper design, is easy to measure. However, these results also demonstrate that there are several points of concern with this method that must be addressed before it can be applied in a practical situation.

For instance, the size and shape of the tank raise a very difficult problem. As was shown in section 7.5, some tanks have such a complex acoustic behavior as a result of their geometrical attributes that they cannot be used with the Helmholtz method. The presence of other acoustic resonating modes in the cavity makes the behavior of the spring-mass mode very erratic. Such behavior limits the usefulness of this technology in certain applications that use tanks with complex shapes, such as gasoline tanks.

In addition, even if the size and shape of a tank are suitable for the Helmholtz method, the design of the software and hardware will also play a critical role on its acoustical behavior. For instance, the operating frequency range is affected not only by the speaker design, but also by its location. The design of the neck also affects the acoustic behavior of the tank. In fact, this is the primary design parameter that can be used to tailor the frequency range of the tank. Finally, the type of instrumentation required is affected by both the location of the speaker and the scanning strategy used to find the resonant frequency. The following sections contain a detailed discussion on these topics.

8.1. TANK SIZE AND SHAPE

The first factor that must be examined during the implementation of the Helmholtz method is the geometry of the tank itself. Most literature relating to experimental work with Helmholtz resonators quote the use of resonators with dimensions that are much smaller than the wavelength of the resonant frequency [67, 68, 69, 70, 75, 76]. These dimensions are usually kept below about one sixth of the wavelength in order to avoid a quarter wave resonant mode. In fact, the equations developed in chapter 5 assume that the dimensions of the cavity are much smaller than the wavelength.

This requirement is not difficult to meet with small resonators since the wavelength remains acceptable even at high frequencies. However, larger cavities such as those found in automotive fuel tanks require very large wavelengths in order to prevent erratic behavior. This can only be done with very low frequencies, usually below 100Hz. Such low frequencies pose a problem from the point of view of instrumentation because equipment designed to work in those ranges tends to be less accurate and more expensive.

In some cases, size alone is not the problem. As was shown in section 7.5 with the Lumina tank, even if the wavelength greatly exceeds all the dimensions of the tank, unwanted resonant modes may appear due to the shape of the tank. These modes are probably two and three dimensional standing waves which are very difficult to predict.

8.2. OPERATING RANGE

As the experimental results have shown, the actual behavior of a Helmholtz resonator is affected by the type of hardware and software used. However, the idea of using the spring-mass resonant mode to measure volume will remain practical as long as this behavior is repeatable. In order to achieve this, it is necessary to find a range where the Helmholtz resonant frequency of the system can vary with changing volume without being disturbed by other acoustical resonant modes or by the electronic equipment. In finding such a range, it is necessary to take into account the following points:

a) Due to the logarithmic relation between frequency and volume, the resolution of the system will decrease as the operating range is moved into the lower frequency range. This means that at the lower end of the spectrum the amount of change of the resonant frequency per unit of change in volume will be smaller, and thus the resolution will be smaller. This makes working at higher frequencies advantageous.

b) At the same time, the wavelength of the resonant frequency will drop as the frequency increases. Since it is always desirable to work with the largest possible ratio between wavelength and tank dimensions, the higher end of the spectrum becomes unattractive because it makes the tank more susceptible to the formation of standing waves.

c) Furthermore, as the comparison between the coupled and uncoupled resonators confirmed, the resolution of the system is also affected be the presence of the speaker on the neck of the resonator. The extent of this effect will depend on the acoustical impedance of the speaker.

d) The electronic hardware used to drive the speaker may also have an effect on the overall behavior of the system. The example of an amplifier that filters the lower end of the spectrum was given in chapter 6. In designing the system, it is important to have a very good understanding of the effect of each electronic component on the actual output of the speaker. It is particularly important to make sure that this output is not affected in the Helmholtz regime of the tank.

e) Since this is an acoustically driven system, there is always the possibility that external acoustical noise may affect the desired response. The fact that this technology is being developed for an automotive application should take into account any acoustical resonant modes in the vehicle that may affect the operation of the system. *Appendix III* shows a guide to the commonly accepted frequency ranges for noise emanating from passenger vehicles. This type of chart should be kept in mind when selecting the operating frequency range.

f) As was shown in the experiments, other acoustical resonant modes different from the spring-mass mode may appear in the system. This is perhaps the most challenging issue in the application of this technology. The dimensions and the shape of the tank are critical in order to prevent standing waves from forming. Yet it is unlikely that these considerations could be used in the design of the tank since modern fuel tanks are designed to fill preciously scarce space under the frame of the vehicle. Therefore, other factors such as the dimensions of the neck must be used to shift the working range to an acceptable area.

g) Another issue of concern is the amount of noise emanating from the fuel level sensor. Automotive companies spend a great deal of effort trying to minimize acoustical noise inside and outside of vehicles. Since the measuring technique proposed here uses acoustics, passenger comfort should always be kept in mind. It is important to note that, during the experiments, it was possible to obtain a very good signal to noise ratio without having to use excessively loud excitation noise.

h) The last area of concern has to do with the cost of the equipment. Acoustical hardware capable of giving a good response in the lower end of the spectrum tends to be very costly. Therefore, the search for a working frequency range should also take into account the frequency ranges where the hardware is capable of providing acceptable performance at a reasonable cost.

It is clear from this summary that there are several conflicting factors affecting the design of an effective Helmholtz based fuel level sensor. Points a) and b) give a good example of the difficult choices that the designer faces, such as a balance between resolution and standing wave suppression. In order to deal with these issues, the designer has only a few design factors available. These include the dimensions of the neck, the size and shape of the tank, and the dimensions, characteristics, and location of the speaker.

8.3. Neck Design

The design of the neck of the resonator is the most important tool that can be used to manage the overall response of the system since its dimensions can be used to shift the resonant

frequency. In designing the neck, there are three design factors that are of importance: its length, its diameter, and the ratio between these two quantities.

The length and diameter of the neck can both be used to change the effective mass of the plug of air inside of it. This in turn has a direct effect on the resonant frequency of the system. Therefore, these dimensions can be used to shift the working range away from undesirable resonant modes.

The ratio between length and diameter can have an effect on the proportion of viscous losses in the neck. However, this will only be of significance in extreme cases when the neck is too narrow [65]. In general, the ratio of the dimensions of the neck do not affect the resonance of the system as long as the neck maintains the same total volume. This gives some leeway to the designer in order to fit a neck with the required volume into a limited space.

It is also necessary to reiterate here the relation of the neck dimensions with the formation of standing waves inside of it. The neck used in the 3.8L resonator illustrated how these resonant modes may appear near the operating spring-mass range if the neck has the appropriate dimensions.

A very important characteristic of equations (5.3-8) and (5.4-1) is that they limit the usable frequency range for a given tank volume. This means that for a given tank size, there will be an upper limit placed on the obtainable resonant frequency. The equations show that in order to obtain a higher frequency, a larger neck diameter is necessary. Eventually, if the desired resonant frequency is too high, the required diameter will become impractical, possibly even larger than the tank itself. This is illustrated in *Table 8.1*, which shows the relation between

the neck diameter and the resonant frequency for a typical 60L (assuming the neck length is zero). These results were obtained using the equation developed by Troke [68].

Table 8.1: Minimum neck diameter as a function of resonant frequency.

Desired Resonant Frequency (Hz)	Minimum Neck Diameter (m)
25	0.018
50	0.047
100	0.189
150	0.426
250	1.184
400	3.031
600	6.819

This table shows that, according to the theory, a neck with a minimum 6.819m diameter would be necessary to make a 60L tank resonate at 600Hz. It is clear that such a diameter would in all likelihood be larger than the tank itself.

8.4. Excitation Source

In transferring this technology to an automotive application, the use of speakers to provide the necessary acoustical excitation seems appropriate. Speakers provide a very simple and cost effective source of acoustic excitation which could be easily adapted to the harsh environment of a fuel tank. Furthermore, a properly selected and installed speaker can be used both as the source of excitation and as the sensor. From an automotive perspective, this provides a specially attractive device since it minimizes the hardware needed, especially inside the tank. This helps both the cost and the reliability of the system.

A further advantage of speakers is that even though they are electrically driven, they can be made to work at low voltage and current levels. This is a very important point for this

application since it involves their installation in a highly flammable environment. Float arm fuel level sensors also require a flow of current through an exposed variable resistor, but proper design using low level voltages and currents has shown that this is not a detriment to safety.

In terms of reliability, the construction of a speaker is comparable in many ways to that of existing rotary arm fuel level sensors. For instance, a speaker only requires the use of a magnet, a coil, a diaphragm, and a housing. In contrast, modern float level sensors require a coil (or resistor card) and a housing. Moreover, the complexity of the float and arm is comparable to that of the diaphragm and magnet in the speaker. It is obvious from this comparison that by selecting the proper materials, the construction of a speaker capable of working inside a fuel tank should be possible.

Choosing a proper speaker has its own challenges. The most important factor in selecting a speaker has to do with its acoustical impedance. A high impedance speaker will tend to dominate the spring-mass response of the system making it difficult to detect the Helmholtz resonant mode. Therefore, a low impedance speaker is desirable in order to minimize its influence on the resonance of the system. In addition, this makes it possible to detect changes in the response of the speaker as the tank reaches its resonant modes. As was just discussed, this is very desirable from the perspective that it reduces instrumentation.

Another characteristic of the speaker that is important is its resonant frequency. As the experiments demonstrated, the resonance of the speaker will have a definite effect on the overall response of the system. This is made particularly clear when the results obtained for

the coupled and the uncoupled resonators in sections 7.2 and 7.3 are compared. These experiments show that the speaker resonance and the Helmholtz resonance combine together to form a single resonant frequency. Nevertheless, this effect should not be a problem as long as the overall response is always predictable. As a benefit, this effect can be used as another tool that can be used to tailor the working frequency range of the system.

8.5. Scanning Strategy

This study has also illustrated two different strategies that can be used to obtain the resonant frequency of a Helmholtz resonator. The first uses white noise to excite the cavity and has the advantage of being computationally very fast. This allows a very fast update rate for the computer scanning the liquid level. However, this method has the inherent disadvantage that it requires a microphone. Its accuracy is also limited due to the random nature of the excitation.

The second strategy uses the frequency sweep method, which provides a very stable and clear response. This method has the advantage that it can be used without a microphone if the speaker is coupled to the neck. However, obtaining the resonant frequency of a Helmholtz resonator using a frequency sweep is also inherently slower due to the finite amount of time required to scan each frequency interval.

CHAPTER 9 CONCLUSIONS

The background research presented in this paper revealed that pneumatic techniques are superior to conventional level sensing for use in moving vehicles. Previously reported results demonstrated the possibility of using a pneumatic method to remove most errors due to tilting or sloshing in gasoline tanks. However, no attempt has been made to incorporate this technology into propane vehicles.

This current study demonstrated the use of the Helmholtz resonant method as a potentially viable pneumatic method for use in propane tanks. Five experiments were performed to uncover the characteristics and potential problems of this method in tanks of different sizes and shapes.

The results demonstrated that this method works better in tanks with simple shapes such as are found in propane vehicles. The appearance of intrusive acoustical modes was shown in a tank with a complex shape. Such behavior prevents the use of this technology even if the wavelength of the excitation source is much larger than the dimensions of the tank. Altogether, propane tanks seem to be the best suited for the Helmholtz method since they generally have a much simpler geometry than gasoline tanks and their walls are much stiffer. Conversely, conformal gasoline tanks appear to be the poorest due to their complicated shapes.

The experiments also demonstrated that it is possible to use the Helmholtz method without a microphone as long as the speaker is coupled to the neck. This makes this method attractive

for automotive use because it requires very little hardware. Nevertheless, using an uncoupled speaker with a microphone proved to be a valuable laboratory technique that can be used to characterize the pure acoustical behavior of a resonator. Uncoupled resonators were shown to behave closer to the response predicted by the theory than coupled resonators.

CHAPTER 10 FUTURE RECOMMENDATIONS

Although the principles of using the Helmholtz method to measure volume are covered in this paper, further research is needed in order to implement this system successfully into a propane vehicle. This chapter is an overview of the main topics that still require investigation. In addition, the end of this chapter includes a number of proposed steps that should be taken in order to complete this project.

10.1. Effect of Temperature and Humidity Changes

The dependence of the Helmholtz method on the conditions inside the tank remains an issue of concern. As was discussed before, the speed of sound depends on the properties of the medium, such as temperature and humidity. This problem has not yet been addressed, but it is clear that some form of calibration will have to be added to the system if it is ever to be used in a vehicle.

Two methods are proposed in here as possible solutions to this problem. The first is to use temperature measurements inside the tank to calibrate for changes in the speed of sound. This method does not take into account all the factors that affect the speed of sound, but it is easily implemented using thermocouples. A second method would consist of measuring the actual speed of sound in the tank. This is much more difficult to do, but would offer better accuracy.

10.2. Effect of Tilting and Sloshing

Tilting and sloshing of the fuel in the tank are the primary sources of error for float based level sensors. Future experiments should demonstrate the effects of these phenomena on the accuracy of the Helmholtz method. An experimental setup is currently under construction for this purpose. This machine is capable of sliding a propane tank on a track to simulate slosh. The frame also allows the tank to rotate in two different axis to simulate the effect of tilt. *Appendix IV* shows an assembly drawing of this fixture.

10.3. Other Required Areas of Study

Further research in this project should concentrate in propane tanks. The propane tank used in this current study was designed with these future experiments in mind. The following steps in the project should be:

1. To find a speaker with a low acoustical impedance which can be coupled to the neck of the propane tank. The behavior of the coupled system should be matched as closely as possible to the behavior recorded in this study in order to maintain the highest possible resolution.

2. This speaker should be used to conduct tests on the effects of tilt, slosh, and temperature fluctuations. These tests should be done at atmospheric pressure to simplify the study of these phenomena.

3. If the technology is shown to work under these conditions, the next step should be to develop a Helmholtz resonator that can work in a high pressure environment. A

preliminary design of such a sensor is shown in *Figure 10.1*. The danger of using propane should not be underestimated. These tests should be conducted using a different fluid (i.e. water mixed with rust inhibitor), and by pressurizing the tank using a gas with similar acoustical behavior to propane, such as Freon 12.

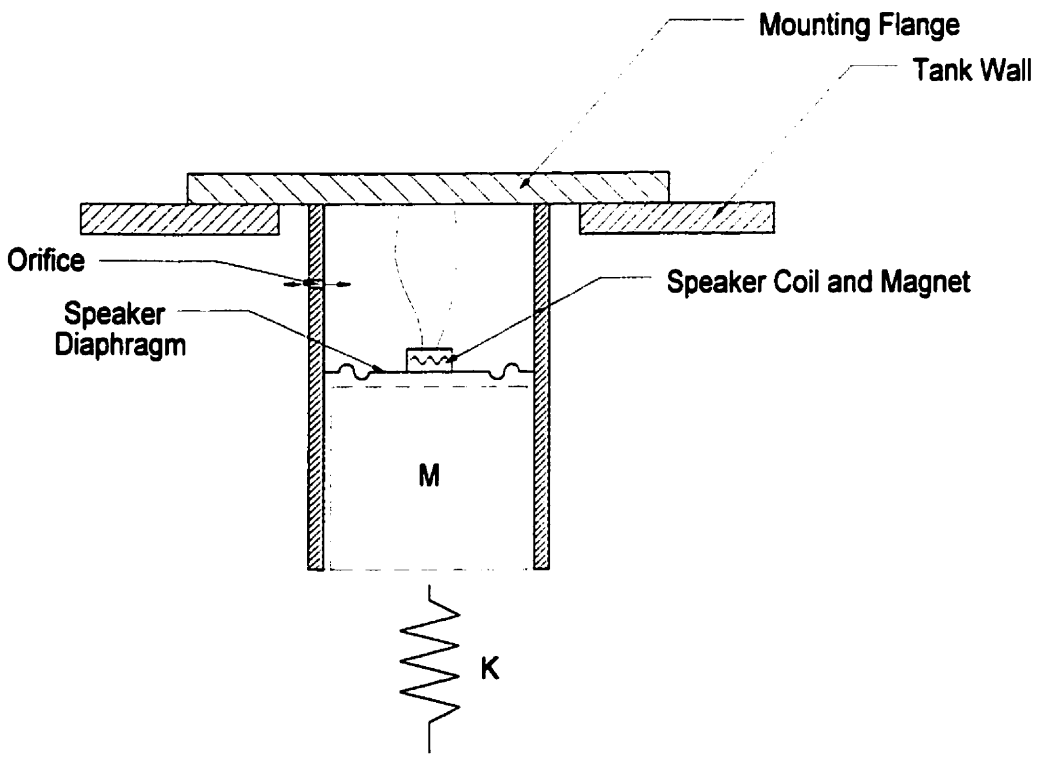

Figure 10.1: Proposed Helmholtz resonator design for use inside a propane tank.

10.4. PROPOSED SENSOR DESIGN FOR PROPANE ENVIRONMENT

Figure 10.1 illustrates the proposed design. It consists of a cylinder divided into two separate chambers by an electrically driven diaphragm (speaker). The lower part of the chamber forms the air plug that acts as the mass in the Helmholtz resonator. The air in the tank acts as the spring. Since the tank is pressurized, the back of the diaphragm cannot be directly exposed to the outside pressure. Therefore, the top chamber acts as a buffer which allows the pressure in the tank to increase with the movement of the speaker. A small orifice allows the

pressure of the top chamber to equalize with the rest of the tank, but limits the speed in which this happens in order to allow the mass spring system to work. If the air flow into this cavity was not restricted, the diaphragm would be unable to cause a significant pressure change in the tank, making the resonator unable to function.

The proposed design is a combination of the design proposed by Kobayashi et. al and the Helmholtz approach [53]. These two methods were thoroughly studied in the context of propane tanks. However, since neither of these sensors was designed with high pressure applications in mind, it soon became obvious that some modifications were needed. Despite the good results obtained by Kobayashi et. al, this system requires extensive hardware and very sophisticated electronics and software. In contrast, the Helmholtz resonator approach overcomes many of these problems by using a simpler method that can function without a microphone. However this system was not designed for pressurized tanks, and requires the back of the speaker to have access to the outside of the tank. In addition, this system is more sensitive to temperature variation since its readings depend on the instantaneous speed of sound.

REFERENCES

1. Nagy, George Jr., "Fuel Level Sensor Design from a System Perspective", SAE Trans. 971072, (1997).

2. Williamson, Cecil M.; Taylor, Carl A., "Conductive Thermoplastic Fuel Level Sensor Element", SAE Trans. 960970, (1996).

3. Riley, Richard E., "Linear Design Fluid Level Sensor Utilizing New Material Technology", SAE Trans. 900492, (1990).

4. Shiratsuchi, Toshiharu; Imaizumi, Motomu; Naito, Masaki, "High Accuracy Capacitance Type Fuel Sensing System", SAE Trans. 930359, (1993).

5. Geslot, Francis, "Capacitive Fuel Level Sensor: Performance and System Approach", SAE Trans. 910492, (1991).

6. Maier, Lawrence C., "Apparatus and Method for Determining Liquid Levels", *United States Patent Number 4,908,783*, March 13, 1990.

7. Hart, John R., "Capacitive Fluid Level Sensor", *United States Patent Number 5,103,368*, April 7, 1992.

8. Lawson, John C., "Smart Fuel Tank Module", *United States Patent Number 5,626,052*, May 6, 1997.

9. Buehler, William S., "Liquid Level Sender Technology", SAE Trans. 933014, (1993).

10. Zabler, Erich; Dukart, Anton; Grein, Nicolas; Heintz, Frieder, "A Universal and Cost-Effective Fuel Gauge Sensor Based on Wave Propagation Effects in Solid Metal Rods", SAE Trans. 940628, (1994).

11. Interview with J. Cockburn of General Motors of Canada (February 16, 1998).

12. Interview with Jeffery S. Moore of Kautex (March 12, 1998).

13. Meeting with General Motors Engineers, Detroit, MI (March 12, 1998).

14. Riley, Richard E., "Linear Design Fluid Level Sensor Utilizing New Material Technology", SAE Trans. 900492, (1990).

15. Interview with Shawn Yates of Chrysler Canada (March 19, 1998).

16. Murphy, Michael J., "Properties of Alternative Fuels", *Office of Technical Assistence & Safety Federal Administration*, Columbus, OH: Batelle, (1992)

17. Gyorki, John R., "Liquid-Level Sensors Flood the Marketplace", *Machine Design*, v. 68, pp. 92-98, (June 13, 1996).

18. Telephone interview with David Bennet of Bi-Phase (April 15, 1998).

19. Wasserstrom, Henry, "Thick Film Rheostat Position and Pressure Senders", SAE Trans. 932402, (1993).

20. Gaston, Robert D., "Fuel Sender Assembly Having Reduced Wear Including Low Wear Resistor Card", SAE Trans. 930458, (1993).

21. Gaston, Robert D., "Design Evolution of the Fuel Sender Requiring No Electrical Calibration", SAE Trans. 930459, (1993).

22. Company Brochure, Mannesmann VDO North America.

23. Meeting with General Motors Engineers, Toronto, ON (January 29, 1998).

24. Interview with William Ing, Durham Bus Lines (May 4, 1998).

25. Interview with John Amor of PCI Propane Conversions (April 23, 1998).

26. Interview with Rick Gorski of Brydon Fuel Technologies (April 23, 1998).

27. Company Brochure, Walbro.

28. Company Catalogue, PAVE Technology Co., Inc., p 10.

29. Toth, Ferry N.; Gerard, Meijer C.M.; van der Lee, Matthijs, "A Planar Capacitive Precision Gauge for Liquid-Level and Leakage Detection", *IEEE Transactions on Instrumentation and Measurement*, v. 46, n. 2, pp. 644-646, (April, 1997).

30. Baxter, Larry K., *Capacitive Sensors: Design and Applications*, New York: IEEE Press, pp. 140-144, (1997).

31. Interview with representatives of Walbro, SAE Conference, Detroit, MI (February 25, 1998).

32. Interview with Bob Schmidt of Mannesmann VDO North America, SAE Conference, Detroit, MI (February 25, 1998).

33. Interview with representatives of Magneti Marelli, SAE Conference, Detroit, MI (February 25, 1998).

34. Interview with representatives of Pierburg Instruments, SAE Conference, Detroit, MI (February 25, 1998).

35. Datcon Instrument Company Website, (www.omnimex.com/datcon/diagram.html).

36. Vargas, E.; Ceres, R.; Martin, J.M.; Calderon, L., "Ultrasonic Sensor for Liquid-Level Inspection in Bottles", *Sensors and Actuators A 61*, pp. 256-259, (1997).

37. Chern, E.J.; Djordjevic, B.B., "Nonintrusive Ultrasonic Low-Liquid-Level Sensor", *Materials Evaluation*, v. 48, pp. 481-485, (April, 1990).

38. Auger, Tim; Newton-Woof, Tony, "Ultrasonics Sound Good for Level Measurement", *Process Engineering*, v. 75, pp. 31-32, (July, 1994).

39. Asher, R.C.; Place, J.D., "Sonic Measurement of Liquid Levels in Fuel Cycle Plants", *Nuclear Engineering International*, v. 31, pp. 55-57, (October, 1986).

40. Hendrik, William, "Non-Contact Monitors Curb Tank Emissions", *Chemical Engineering*, v. 100, pp. 16-18, (Supp. October, 1993).

41. Asher, R.C., "Ultrasonic Sensors for Chemical and Process Plant", Philadelphia, PA: Institute of Physics, p. 262, (1997).

42. Asher, p. 273.

43. Asher, p. 286.

44. Asher, p. 265.

45. Asher, p. 150.

46. Betta, Giovanni; Ippolito, Lucio; Pietrosanto, Antonio; Scaglione, Antonio, "An Optical Fiber-Based Technique for Continuous-Level Sensing", *IEEE Transactions on Instrumentation and Measurement*, v. 44, n. 3, pp. 686-689, (June, 1995).

47. Iwamoto, Katsuharu; Kamata, Isao, "Liquid-Level Sensor with Optical Fibers", *Applied Optics*, v. 31, n. 1, pp. 51-54, (January, 1992).

48. Babchenko, Anatoly; Bodenheimer, Joseph S.; Nitzan, Meir, "Optical Sensor Based on Coated Light Guides", *Optical Engineering*, v. 34., n. 12., pp. 3587-3586, (December, 1995).

49. Waterbury, Robert C., "Level Sensing Tips Toward Basics", *INTECH*, v. 41, pp. 24-27, (May, 1994).

50. "Electro-Optic Level Sensor Has No Moving Parts", *Engineering*, pp. 573, (October, 1997).

51. Weiss, Jonathan D., "The Pressure Approach to Fiber Liquid-Level Sensors", *Photonics Spectra*, pp. 119-123, (Novemebr, 1990).

52. Morris, Henry M., "Tank Level Sensing - Not a 'One-Size Fits All' Market", *Control Engineering*, v. 41, pp. 60-63, (January, 1994).

53. Kobayashi, Hideaki; Watanabe, Kajiro; Kawa, Eiji; Chen, Yung S.; Ishizuka, Hiroyuki, "Gauging Fuel in Deformed Tanks by Pneumatic Methods - Application to Automobile Fuel Gauges", SAE Trans. 900467, (1990).

54. Watanabe, Kajiro; Takebayashi, Yasuhiro, "Volume Measurement of Liquid in a Deformed Tank - Application to the Fuel Meter of Automobiles", SAE Trans. 871964, (1987).

55. Watanabe, K.; Takebayashi, Y.; Himmelblau, D.M., "Volume Measurement of Deformed Materials in Tanks", *ISA Transactions*, v. 27, n. 4, pp. 9-19, (1988).

56. Bates, Kenn S.; Chang, David B., "Low Frequency Acoustic Fuel Sensor", *United States Patent Number 5,251,482*, October 12, 1993.

57. Sheng, Hwai-Ping; Garza, Cutberto; Winter, Dean C.; Deskins, William G., "Method and Apparatus for Acoustically Measuring the Volume of an Object", *United States Patent Number 4,640,130*, February 3, 1987.

58. Warnaka, Glenn E.; Warnaka, Mark E., "Phase Track System for Monitoring Fluid Material Within a Container", *United States Patent Number 4,991,433*, February 12, 1991.

59. Marciniak, Robert D.; Poole, Lynn A., "System for Monitoring Fluent Material Within a Container", *United States Patent Number 4,811,595*, March 14, 1989.

60. Doshi, Navin H., "Acoustical Volume/Pressure Measurement Device", *United States Patent Number 4,704,902*, November 10, 1987.

61. Kamen, Dean L.; Scale, Joseph B.; Briggs Joseph; Arnold, Finn, "Pump Controller Using Acoustic Spectral Analysis", *United States Patent Number 5,349,852*, September 27, 1994.

62. Kamen, Dean L.; Scale, Joseph B.; Briggs Joseph; Arnold, Finn, "Flow Control System", *United States Patent Number 5,526,844*, June 18, 1996.

63. Fudim Efrem V., "Liquid Volume Monitoring Apparatus and Method", *United States Patent Number 4,840,064*, June 20, 1989.

64. Denz, Helmut; Blumenstock, Andreas, "Method and Device for Detecting the Fluid Level in a Tank", *United States Patent Number 5,379,638*, January 10, 1995.

65. Kinsler, Lawrence E.; Frey, Austin R.; Coppens, Alan B.; Sanders, James V., "Fundamentals of Acoustics", Third Edition, Toronto: John Wiley & Sons, Inc., pp. 225-228, (1982).

66. Kinsler, Lawrence E.; Frey, Austin R., "Fundamentals of Acoustics", Second Edition, New York: john Wiley & Sons, Inc., pp. 186-216, (1962).

67. Boullosa, Ricardo R.; Orduna-Bustamante, Felipe; "The Reaction Force on a Helmholtz Resonator Driven at High Sound Pressure Amplitudes", *American Journal of Physics*, v. 60, n. 8, pp. 722-726, (1992).

68. Troke, Robert W., "Tube-Cavity Resonance", *The Journal of the Acoustical Society of America*, v. 44, n. 3, pp. 684-688, (1968).

69. Khosropour, Roset; Millet, Peter, "Excitation of a Helmholtz Resonator by an Air Jet", *Journal of the Acoustical Society of America*, v. 88, n. 3, pp. 1211-1221, (1990).

70. Ingard, Uno, "On the Theory and Design of Acoustic Resonators", *The Journal of the Acoustical Society of America*, v. 25, n. 6, pp. 1037-1061, (1953).

71. Product Data Sheets, Bruel & Kjaer.

72. Photiadis, Douglas M., "The effect of Wall Elasticity on the Properties of a Helmholtz Resonator", *Journal of the Acoustical Society of America*, v.90, n. 2, pp. 1188-1190, (1991).

73. Kleppe, J.A., *Engineering Applications of Acoustics*, Norwood, MA: Artech House Inc., p. 75, (1989).

74. Kinsler, (1982), p. 36.

75. Ingard, Uno, "The Near Field of a Helmholtz Resonator Exposed to a Plane Wave", *The Journal of the Acoustical Society of America*, v. 25, n. 6, pp. 1062-1067, (1953).

76. Ingard, Uno; Hartmut, Ising, "Acoustic Nonlinearity of an Orifice", *The Journal of the Acoustical Society of America*, v. 42, n. 1, pp. 6-17, (1967).

APPENDIX I: White Noise Generator Control Panel

Summary of inputs and outputs available to the user through this software.

Signal Generation	
Output Buffer Size	Defines the number of samples per wave period to be sent to the output buffer. This number can be used to control the resolution of the output. The buffer size must reflect the maximum output frequency of the board, which is given in the total number of samples that can be generated in a second.
Random Noise Seed	Provides the computer with a seed number used to generate a "random" waveform.
Output Channel	Refers to the label of the channel connected to the speaker.
Sweep Step Size	This value defines the spacing between adjacent frequencies during a sweep. A smaller step gives a better resolution, but also requires a larger data sample. Therefore, this number

	must reflect a balance between resolution and available processing power.
Amplitude	This control specifies the amplitude of the outgoing waveform. The amplitude must be large enough to cause a measurable response. However, very large amplitudes may cause very loud sounds that are uncomfortable or even painful for human observers.
Signal Acquisition	
Scan Rate	The scan rate defines the number of samples per second to be collected in each input channel. A higher rate is desirable in order to provide higher resolution and accuracy and in order to prevent aliasing. The scan rate used should reflect a balance between hardware capabilities and measurement requirements.
Delay	This delay specifies the amount of time that the system waits between exciting the speaker and collecting the data. This delay allows the system to settle so that the collected data corresponds to the steady state. The delay is usually given in terms of milliseconds.
Input Channels	Refers to the label of the input channel used. In this case, only one channel was used for the microphone.
Frequency Scan START	Refers to the start of the frequency range that is analyzed and displayed.
Frequency Scan END	Refers to the end of the frequency range that is analyzed and displayed.
Save to File?	If set to YES, it will prompt the user for a file name to save the collected data. This data is saved as plain text in one column corresponding to the microphone readings
Display	
Output Waveform	Displays one period of the outgoing waveform. This period is sent to the output channel once every second.
Acquired Data	Displays the FFT of the response acquired through the microphone.

APPENDIX II: Frequency Sweep Control Panel

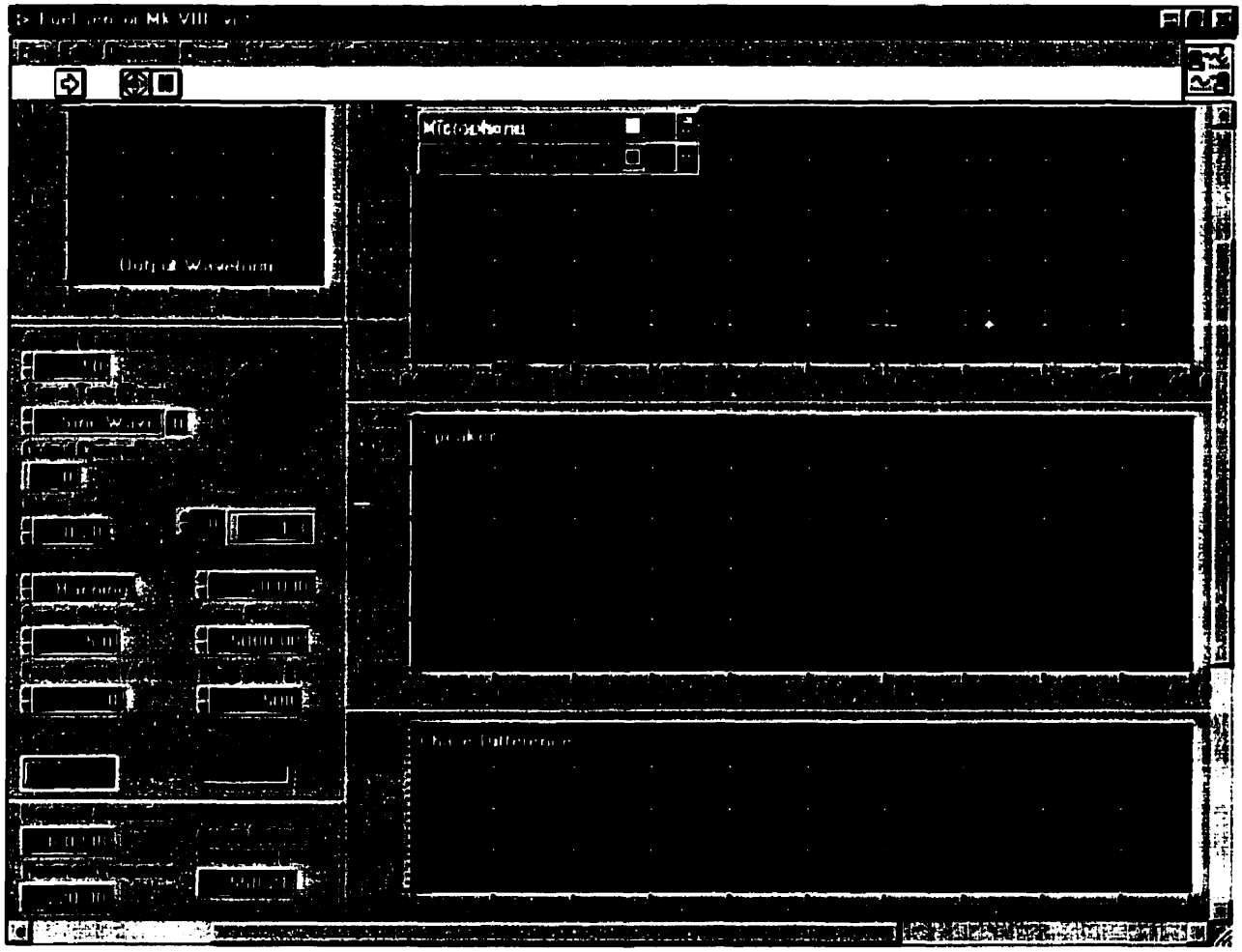

Summary of inputs and outputs available to the user through this software.

Signal Generation	
Output Buffer Size	Defines the number of samples per wave period to be sent to the output buffer. This number can be used to control the resolution of the output. The buffer size must reflect the maximum output frequency of the board, which is given in the total number of samples that can be generated in a second.
Signal Type	Specifies the type of waveform to be generated at the output. Typically, the waveform used is a sinusoid since it provides the simplest frequency output.
Output Channel	Refers to the label of the channel connected to the speaker.
Sweep Step Size	This value defines the spacing between adjacent frequencies

	during a sweep. A smaller step gives a better resolution, but also requires a larger data sample. Therefore, this number must reflect a balance between resolution and processing time.
Amplitude	This control specifies the amplitude of the outgoing waveform. The amplitude must be large enough to cause a measurable response. However, very large amplitudes may cause very loud sounds that are uncomfortable for human observers.
Signal Acquisition	
Scan Rate	The scan rate defines the number of samples per second to be collected in each input channel. A higher rate is desirable in order to provide higher resolution and accuracy and in order to prevent aliasing. The scan rate used should reflect a balance between hardware capabilities and measurement requirements.
Delay	This delay specifies the amount of time that the system waits between exciting the speaker and collecting the data. This delay allows the system to settle so that the collected data corresponds to the steady state. The delay is usually given in terms of milliseconds.
Input Channels	Refers to the label of the input channels used. In this case, three channels were used: one for the microphone, one for the shunt resistor in the speaker circuit, and one to measure the actual outgoing waveform generated by the board in channel 0.
Window	This control defines the type of window used to process the incoming signal in order to reduce spectral leakage. A Hanning window was used for all the experiments.
Peak Quality	This command specifies the minimum acceptable peak quality for the response collected through the microphone. The peak quality measures the sharpness of a peak and is defined as the ratio between the resonant frequency and the difference between its two half power points [61]. The software calculates the quality of all the peaks in the scan and marks the ones with a quality higher than the minimum using a white dot.
Frequency Scan START	Refers to the start of the frequency range that is analyzed and displayed.
Frequency Scan END	Refers to the end of the frequency range that is analyzed and displayed.
Save to File?	If set to YES, it will prompt the user for a file name to save the collected data. This data is saved as plain text in three

	columns. The first corresponds to the microphone readings, the second to the shunt resistor readings, and the third corresponds to the phase shift. This data is the same as is displayed on the control panel during run time.
Filter	When turned ON, it applies a low pass filter which is automatically set to prevent aliasing.
Display	
Output Waveform	The display shows what one period of the outgoing waveform looks like at the set resolution. Using a higher resolution results in a smoother outgoing signal, and therefore in a reduction of noise in the system.
Microphone	This plot shows two curves. The one in green is the FFT for the currently examined frequency. The one in red is a recollection of the amplitude of the response at each scanned frequency. In addition, a white dot is added at the top of any peak in the red curve that has a quality higher than the specified minimum.
Speaker	The speaker plot also has two curves, except that these correspond to the shunt resistance. The reason that an FFT is necessary in reading the voltage across the shunt is that this is an alternating current. Therefore the amplitude of the driving voltage is given by the amplitude of the peak in the FFT at the driving frequency.
Phase Difference	This plot shows the shift in phase between the signal sent out to the speaker and the signal received at the microphone.
Maximum Amplitude	Records the amplitude of the largest resonant peak recorded by the microphone.
Resonant Frequency	Records the frequency of the largest resonant peak recorded by the microphone.
Actual Output Frequency	Shows the current output frequency of the system. This frequency is not always the same as the specified output frequency because of hardware limitations.

APPENDIX III: Design Frequency Requirements of a Vehicle

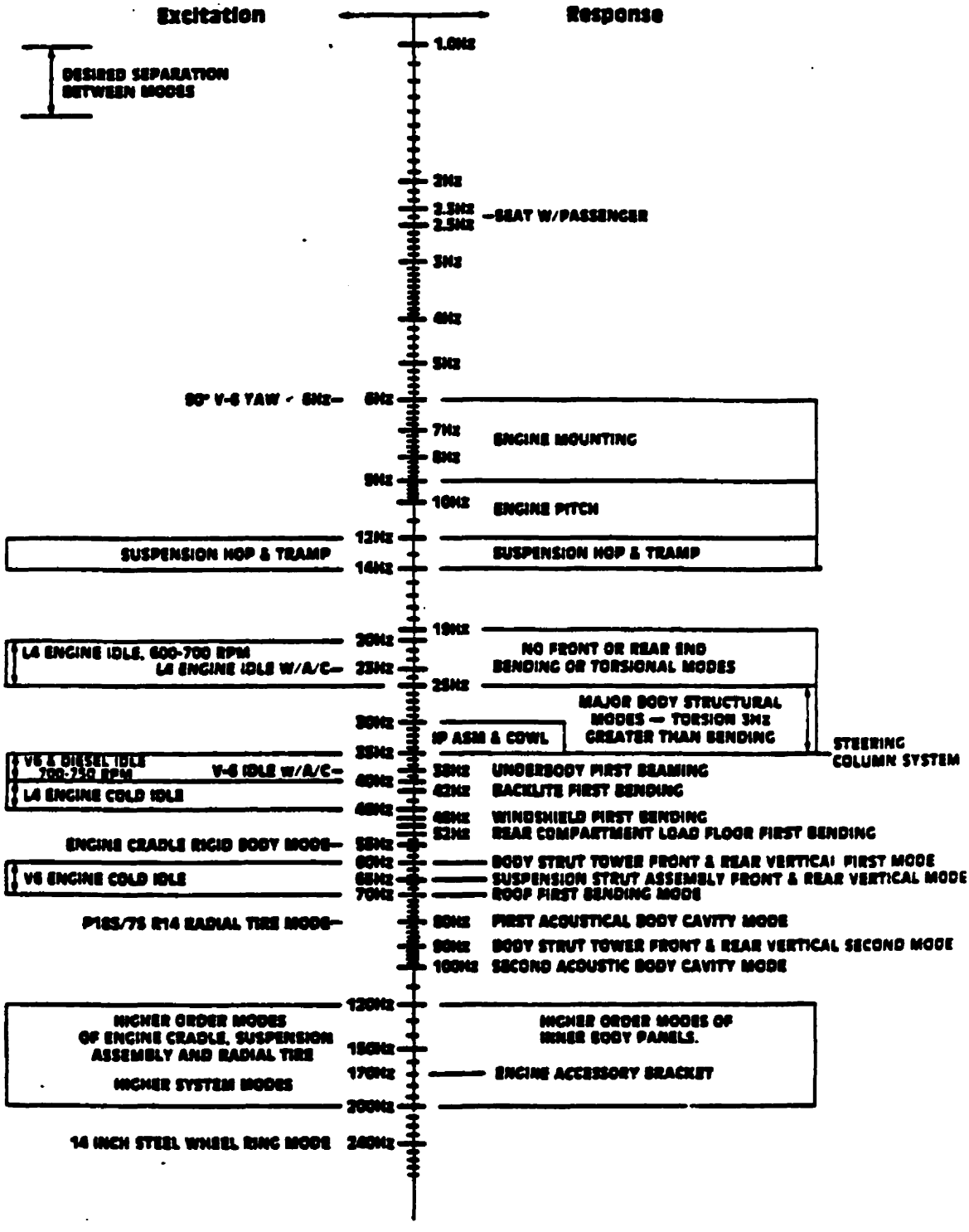

APPENDIX IV: Testing Fixture for Tilting and Sloshing Experiments